

DIFFERENTIAL EFFECTS OF REPEATED LOW-DOSE KETAMINE ON CROSS-  
FREQUENCY INTERACTIONS IN NAÏVE AND PRECLINICAL MODELS OF  
MOVEMENT DISORDERS

by

Tony Ye

---

Copyright © Tony Ye 2018

A Dissertation Submitted to the Faculty of the

DEPARTMENT OF PSYCHOLOGY

In Partial Fulfillment of the Requirements

For the Degree of

DOCTOR OF PHILOSOPHY

In the Graduate College

THE UNIVERSITY OF ARIZONA

2018

THE UNIVERSITY OF ARIZONA  
GRADUATE COLLEGE

As members of the Dissertation Committee, we certify that we have read the dissertation prepared by *Tony Ye*, titled *Differential Effects of Repeated Low-Dose Ketamine on Cross-Frequency Interactions in Naïve and Preclinical Models of Movement Disorders* and recommend that it be accepted as fulfilling the dissertation requirement for the Degree of Doctor of Philosophy.

  
\_\_\_\_\_  
*Stephen L. Cowen, Ph.D.* Date: *July 23, 2018*

  
\_\_\_\_\_  
*Torsten Falk, Ph.D.* Date: *July 23, 2018*

  
\_\_\_\_\_  
*Mary A. Peterson, Ph.D.* Date: *July 23, 2018*

Final approval and acceptance of this dissertation is contingent upon the candidate's submission of the final copies of the dissertation to the Graduate College.

I hereby certify that I have read this dissertation prepared under my direction and recommend that it be accepted as fulfilling the dissertation requirement.

  
\_\_\_\_\_  
Dissertation Director: *Stephen L. Cowen, Ph.D.* Date: *July 23, 2018*

## STATEMENT BY AUTHOR

This dissertation has been submitted in partial fulfillment of the requirements for an advanced degree at the University of Arizona and is deposited in the University Library to be made available to borrowers under rules of the Library.

Brief quotations from this dissertation are allowable without special permission, provided that an accurate acknowledgement of the source is made. Requests for permission for extended quotation from or reproduction of this manuscript in whole or in part may be granted by the head of the major department or the Dean of the Graduate College when in his or her judgment the proposed use of the material is in the interests of scholarship. In all other instances, however, permission must be obtained from the author.

SIGNED: Tony Ye

## Acknowledgements

My transition from film to science was the most challenging yet equally rewarding experience in my life to date. Never in my most farfetched fantasies did I think I would become a neuroscientist. My journey through the Ph.D. would not have been possible without the contribution of countless individuals along the way.

First and foremost, I am deeply indebted to my advisor, Stephen L. Cowen. Out of twelve Ph.D. programs, you were the only one that gave me a chance. I came into your lab with absolutely ZERO experience in surgeries, electrophysiology, and programming (among many other skills). Through your firm nudges and guidance, I emerged from your lab with an invaluable skillset that will carry me above and beyond in my career as a neuroscientist.

As my arsenal of science techniques evolved, so did my research direction thanks to my co-advisor, Torsten Falk. I began my Ph.D. with interests in learning and memory, through our collaboration you have successfully reeled me into the world of movement disorders – a field that I will continue to pursue in my career. A great deal of my gratitude also goes to Mitchell J. Bartlett for all those 5AM mornings and a seamless collaboration that resulted in my dissertation. This would not have been possible without your collaborative efforts.

A very special thanks to Mary A. Peterson for your inspirational transition from the arts to science. Our conversation during interview weekend served as a motivating foundation to complete the Ph.D. Although I wish we had opportunities to collaborate, I am very grateful that you served on my dissertation committee to send me off.

Aside from my dissertation, I would have graduated in a timely manner without our Graduate Program Coordinator (read: Den Mother), Beth Owens. I cannot overstate the number of times I have forgotten to sign up for units, overlooked [insert every program requirement here], and countlessly pestered Beth with questions that I should know the answer to. Thank you maintaining close tabs on me and for your unwavering patience.

Although not directly involved in my dissertation, my gratitude must be expressed to my master's advisor, Alicia Izquierdo. My path to becoming a scientist was only possible because she gave this former filmmaker - with ZERO science background, a chance 7 years ago.

Finally, I am profoundly grateful for Ana, who sparked my motivation to pursue my passion. Her support at every single step of this entire journey was vital to my success. I also would like to express my deepest gratitude to our dog, Millie, for staying up with me all those nights working on this dissertation.

# TABLE OF CONTENTS

|   |           |
|---|-----------|
| <b>LIST OF FIGURES .....</b>  | <b>10</b> |
| <b>LIST OF TABLES .....</b>   | <b>11</b> |
| <b>ABSTRACT .....</b>   | <b>12</b> |
| <b>CHAPTER 1: GENERAL INTRODUCTION.....</b>   | <b>15</b> |
| <b>1.1 PARKINSON’S DISEASE .....</b>  | <b>17</b> |
| <i>1.1.a Parkinson’s Disease: Diagnosis and Pathophysiology .....</i>   | <i>18</i> |
| <i>1.1.b Akinesia/Hypokinesia .....</i>   | <i>18</i> |
| <i>1.1.c Bradykinesia .....</i>   | <i>19</i> |
| <i>1.1.d Resting Tremors .....</i>  | <i>21</i> |
| <i>1.1.e Rigidity and Postural/Gait Instability .....</i>   | <i>22</i> |
| <b>1.2 ETIOLOGY OF PARKINSON’S DISEASE.....</b>   | <b>24</b> |
| <i>1.2.a Mitochondrial Dysfunction .....</i>  | <i>24</i> |
| <i>1.2.b Oxidative Stress.....</i>  | <i>25</i> |
| <b>1.3 THE 6-HYDROXYDOPAMINE ANIMAL MODEL OF PARKINSON’S DISEASE.....</b>   | <b>26</b> |
| <b>1.4 PATHOLOGICAL BETA OSCILLATIONS IN PARKINSON’S DISEASE.....</b>   | <b>29</b> |
| <b>1.5 L-DOPA-INDUCED DYSKINESIA .....</b>  | <b>31</b> |
| <i>1.5.a Mechanisms of L-DOPA-Induced Dyskinesia.....</i>   | <i>31</i> |
| <i>1.5.b The Animal Model of L-DOPA-Induced Dyskinesia.....</i>   | <i>33</i> |
| <i>1.5.c Pathological Oscillations of L-DOPA-Induced Dyskinesia.....</i>  | <i>34</i> |
| <i>1.5.d Gamma Networks .....</i>   | <i>35</i> |
| <b>1.6 KETAMINE .....</b>   | <b>37</b> |
| <i>1.6.a Ketamine Mechanisms and Oscillations .....</i>   | <i>37</i> |
| <i>1.6.b Ketamine and The Opioid System .....</i>   | <i>38</i> |
| <i>1.6.c Ketamine and The Dopamine System.....</i>  | <i>39</i> |
| <b>1.7 KETAMINE-INDUCED OSCILLATORY ACTIVITY .....</b>  | <b>40</b> |
| <i>1.7.a Delta.....</i>   | <i>41</i> |
| <i>1.7.b Theta.....</i>   | <i>41</i> |
| <i>1.7.c Beta.....</i>  | <i>41</i> |
| <i>1.7.d Gamma .....</i>  | <i>42</i> |
| <i>1.7.e High-Frequency Oscillations .....</i>  | <i>42</i> |
| <i>1.7.f A Summary of Ketamine’s Mechanisms.....</i>  | <i>43</i> |
| <b>1.8 POTENTIAL THERAPEUTIC APPLICATIONS FOR KETAMINE .....</b>  | <b>45</b> |
| <i>1.8.a Parkinson’s Disease.....</i>   | <i>45</i> |
| <i>1.8.b L-DOPA-Induced Dyskinesia.....</i>   | <i>46</i> |
| <b>CHAPTER 2 TEN-HOUR EXPOSURE TO LOW-DOSE KETAMINE ENHANCES<br/>CORTICOSTRIATAL CROSS-FREQUENCY COUPLING AND<br/>HIPPOCAMPAL BROAD-BAND GAMMA OSCILLATIONS .....</b> | <b>47</b> |
| <b>2.1 INTRODUCTION.....</b>  | <b>47</b> |
| <b>2.2 MATERIALS AND METHODS.....</b>   | <b>51</b> |
| <i>2.2.a Animals and Surgical Procedures.....</i>   | <i>51</i> |

|  |           |
|--|-----------|
| 2.2.b Drug Treatments .....  | 52        |
| 2.2.c Neurophysiological Recordings .....  | 53        |
| 2.2.d Histology .....  | 53        |
| 2.2.e Data Analysis.....   | 53        |
| 2.2.f References and Addressing Volume Conduction .....  | 54        |
| 2.2.g Spectral Power .....   | 55        |
| 2.2.h Cross-Frequency Coupling .....   | 58        |
| 2.2.i Statistical Analyses.....  | 58        |
| <b>2.3 RESULTS .....</b>   | <b>59</b> |
| 2.3.a A Single Injection of Sub-Anesthetic Ketamine Triggers<br>Gamma Oscillations in M1, HFOs in Striatum, and Broadband<br>Activity in Hippocampus ..... | 59        |
| 2.3.b Repeated Ketamine Injections Significantly Increased<br>High-Frequency Oscillatory Power in the Hippocampus.....                                     | 64        |
| 2.3.c Prior History of Extended Exposure to Ketamine<br>Does Not Alter Resting Oscillatory Activity.....   | 64        |
| 2.3.d Acute Ketamine Exposure Increases Locomotion,<br>but This Increase is Not Enhanced by Extended Exposure.....   | 67        |
| 2.3.e Ketamine-Induced Changes in Cross-Frequency Coupling.....  | 69        |
| 2.3.f Prolonged Exposure to Ketamine Enhances<br>Cross-Frequency Coupling in the Dorsal Striatum During<br>the 2-90 Minute Post-Injection Period.....      | 71        |
| 2.3.g Ketamine-Induced Gamma in M1 and Locomotion Are<br>Reduced by D1R Antagonist SCH-23390.....  | 75        |
| <b>2.4 DISCUSSION .....</b>  | <b>78</b> |
| 2.4.a Ketamine-Induced Gamma in Motor Cortex.....  | 79        |
| 2.4.b Cross-Frequency Coupling and HFOs in Corticostriatal Circuits.....   | 80        |
| 2.4.c Ketamine Induces Broad-Band Gamma and<br>Persistent Activity in the Hippocampus .....  | 81        |
| 2.4.d Ketamine's Effect on Oscillatory Power and Cross-Frequency<br>Coupling was Restricted to the 2-90 Minute Post-Injection Interval.....                | 83        |
| 2.4.e Conclusion.....  | 84        |
| <b>CHAPTER 3: EXPERIMENTAL AIMS FOR REPEATED<br/>KETAMINE EXPOSURE IN ANIMAL MODELS OF<br/>MOVEMENT DISORDERS.....</b>                                     | <b>85</b> |
| <b>3.1 AIM 1: DOES REPEATED KETAMINE REDUCE<br/>PATHOLOGICAL BETA OSCILLATIONS IN AN ANIMAL<br/>MODEL OF PARKINSON'S DISEASE? .....</b>                    | <b>85</b> |
| <b>3.2 AIM 2A: DOES REPEATED KETAMINE EXPOSURE REDUCE<br/>L-DOPA-TRIGGERED FOCAL 80 HZ HIGH-GAMMA? .....</b>   | <b>87</b> |
| <b>3.3 AIM 2B: DOES REPEATED KETAMINE EXPOSURE REDUCE<br/>L-DOPA-TRIGGERED WIDE-BAND GAMMA? .....</b>  | <b>88</b> |
| <b>3.4 AIM 2C: ARE OPIOID-, D1-, OR D2-RECEPTORS INVOLVED IN<br/>KETAMINE-INDUCED OSCILLATIONS IN LID ANIMALS? .....</b>                                   | <b>89</b> |

|   |            |
|---|------------|
| <b>CHAPTER 4: EXPERIMENT 1: INVESTIGATING THE EFFECTS OF KETAMINE-INDUCED OSCILLATORY ACTIVITY IN AN ANIMAL MODEL OF PARKINSON'S DISEASE AND L-DOPA-INDUCED DYSKINESIA.....</b> | <b>91</b>  |
| 4.1 <i>Animals</i> .....  | 91         |
| 4.2 <i>Surgery 1: Unilateral 6-OHDA Lesion</i> .....  | 92         |
| 4.3 <i>Amphetamine-Induced Rotations</i> .....  | 92         |
| 4.4 <i>Induction of L-DOPA-Induced Dyskinesia in Unilateral Lesioned Rats</i> .....   | 92         |
| 4.5 <i>Surgery 2: Electrode Implantation</i> .....  | 94         |
| 4.6 <i>Drug Treatments</i> .....  | 94         |
| 4.7 <i>Neurophysiological Recordings and Timeline</i> .....   | 95         |
| <b>CHAPTER 5: EXPERIMENT 2: INVESTIGATING THE CONTRIBUTION OF OPIOID-, DOPAMINE D1-, AND D2-RECEPTORS IN KETAMINE-INDUCED OSCILLATIONS.....</b>                                 | <b>97</b>  |
| 5.1 <i>Drug Treatments</i> .....  | 97         |
| 5.2 <i>Neurophysiological Recordings and Timeline</i> .....   | 97         |
| 5.3 <i>Histology: Nissl Staining</i> .....  | 98         |
| 5.4 <i>Immunohistochemistry: Tyrosine Hydroxylase Staining</i> .....  | 98         |
| <b>CHAPTER 6: DATA ANALYSIS.....</b>  | <b>99</b>  |
| 6.1 <i>Spectral Power</i> .....   | 99         |
| 6.2 <i>Cross-Frequency Coupling</i> .....   | 100        |
| 6.3 <i>Statistical Analyses</i> .....   | 100        |
| <b>CHAPTER 7: AIM 1: INCREASED BASELINE BETA POWER IN 6-OHDA-LESIONED AND LID ANIMALS COMPARED TO NAIVE.....</b>  | <b>103</b> |
| 7.1 <i>Ketamine Does Not Reduce Beta Oscillations in 6-OHDA-Lesioned Animals</i> .....  | 105        |
| 7.2 <i>Greater Ketamine-Induced Delta Oscillations in M1 of Naïve Animals</i> .....   | 107        |
| 7.3 <i>6-OHDA-Lesioned Animals Have Lower Ketamine-Induced Gamma and HFOs in the 92-110 Min Period</i> .....  | 107        |
| 7.4 <i>Ketamine Initially Triggers a Weaker Low-Gamma and HFO Response in 6-OHDA-Lesioned Animals</i> .....   | 109        |
| 7.5 <i>Ketamine-Induced HFO Power Was Not Statistically Different in the DMS Between Naïve and 6-OHDA Animals in the 2-90 Min Period</i> .....                                  | 109        |
| 7.6 <i>Suppression of Low- and High-Gamma, and HFOs in the 6-OHDA DMS (92-110 Min)</i> .....  | 110        |
| 7.7 <i>Ketamine Triggers Stronger HFOs in the NAc of the Naïve Group Compared to 6-OHDA Animals in the 2-90 Min Period</i> .....  | 111        |

|   |            |
|---|------------|
| 7.8 Suppression of Low- and High-Gamma, and HFOs in the 6-OHDA NAc (92-110 Min) .....   | 111        |
| 7.9 Ketamine-Induced Locomotor Activity is Significantly Lower in 6-OHDA-Lesioned Animals .....   | 112        |
| 7.10 Prior History of Ketamine Exposure Does Not Alter Resting Oscillatory Activity in 6-OHDA-Lesioned Animals. ....                    | 114        |
| 7.11 Ketamine Does Not Trigger Cross-Frequency Interactions in M1 of 6-OHDA Animals .....   | 116        |
| 7.12 Ketamine Does Not Trigger Cross-Frequency Interactions in DLS of 6-OHDA Animals.....   | 117        |
| <b>CHAPTER 8: AIM 2A: L-DOPA INJECTIONS IN LID ANIMALS</b>  |            |
| <b>TRIGGERS WIDE-BAND GAMMA .....</b>   | <b>120</b> |
| 8.1 Baseline AIMs Scores Are Not Correlated to L-DOPA-Induced Gamma .....   | 123        |
| 8.2 Increased Low-to-Wide-Band Gamma Immediately After L-DOPA Injection .....   | 125        |
| <b>CHAPTER 9: AIM 2B: REPEATED KETAMINE EXPOSURE DOES NOT REDUCE L-DOPA-TRIGGERED GAMMA IN LID ANIMALS.....</b>                         | <b>128</b> |
| 9.1 Cross-Frequency Coupling in LID Animals.....  | 132        |
| 9.2 Delta- and Theta-HFO CFC Was Not Present in M1 of LID Animals .....   | 133        |
| 9.3 Delta- and Theta-HFO CFC Was Not Present in DLS of LID Animals .....  | 133        |
| 9.4 Ketamine + L-DOPA Enhances Theta-HFO CFC in the DMS and Suppresses Theta-High-Gamma CFC in the NAc.....                             | 134        |
| 9.5 Repeated Ketamine Exposure Has No Long-Term Effect on L-DOPA-Induced Gamma .....  | 136        |
| <b>CHAPTER 10: AIM 2C: OPIOID-, D1-, AND D2-RECEPTOR ANTAGONISM DOES NOT AFFECT KETAMINE'S OSCILLATORY ACTIVITY DURING L-DOPA .....</b> | <b>138</b> |
| 10.1 Blocking Opioid-Receptors Does Not Affect Ketamine-Induced Locomotion in LID Animals .....   | 143        |
| 10.2 Blocking D1-Receptors Suppresses Ketamine and L-DOPA-Induced Locomotion in LID Animals.....  | 143        |
| 10.3 Blocking D2-Receptors Reduces Ketamine-Induced Locomotion But Not in the Presence of L-DOPA .....                                  | 144        |
| <b>CHAPTER 11: BETA OSCILLATIONS IN 6-OHDA-LESIONED ANIMALS ARE UNAFFECTED BY KETAMINE.....</b>   | <b>147</b> |
| 11.1 Suppression of Low- and High-Gamma, and HFOs in the 92-110 Min Period of 6-OHDA-Lesioned Animals .....                             | 148        |
| 11.2 Prior History of Extended Ketamine Exposure  |            |

|   |            |
|---|------------|
| <i>Does Not Alter Resting-State Oscillatory Activity<br/>in 6-OHDA-Lesioned Animals</i> .....   | 149        |
| 11.3 <i>Lack of Ketamine-Induced Cross-Frequency<br/>Interactions in 6-OHDA Animals</i> .....   | 150        |
| <b>CHAPTER 12: RESULTS OF AIM 2A: L-DOPA DID<br/>NOT TRIGGER FOCAL 80 HZ HIGH-GAMMA<br/>IN LID ANIMALS</b> .....  | <b>151</b> |
| 12.1 <i>Differences in L-DOPA Priming</i> .....   | 151        |
| 12.2 <i>L-DOPA-Induced Wide-Band Gamma Mechanism</i> .....  | 153        |
| 12.3 <i>Baseline AIMs Scores Were Not Significantly<br/>Correlated to L-DOPA-Induced Gamma</i> .....  | 154        |
| 12.4 <i>Gamma Response Immediately After<br/>L-DOPA Administration in LID Animals</i> .....   | 155        |
| 12.5 <i>Repeated Ketamine Exposure Does Not<br/>Acutely or Chronically Reduce L-DOPA-Induced Gamma</i> .....  | 155        |
| 12.6 <i>Differential Effects on Cross-Frequency<br/>Coupling During Ketamine + L-DOPA</i> .....   | 157        |
| <b>CHAPTER 13: AIM 2C: OPIOID-, D1-, D2-RECEPTOR<br/>ANTAGONISM DID NOT ALTER KETAMINE-INDUCED<br/>OSCILLATIONS DURING L-DOPA, BUT DIFFERENTIAL<br/>EFFECTS ON LOCOMOTION WERE OBSERVED</b> ..... | <b>160</b> |
| 13.1 <i>Blocking Opioid Receptors Did Not Alter<br/>Ketamine-Induced Oscillatory Activity During L-DOPA</i> .....   | 160        |
| 13.2 <i>Differential Effects of D1- And D2-Receptor<br/>Antagonism on Locomotor Activity Despite Lack of<br/>Impact On Ketamine-Induced Oscillatory Activity</i> .....                            | 161        |
| <b>CHAPTER 14: CONCLUSIONS</b> .....  | <b>163</b> |
| <b>APPENDICES</b> .....   | <b>166</b> |
| APPENDIX A: NISSL-STAINED TISSUE OF NAÏVE ANIMALS (N=8) .....   | 166        |
| APPENDIX B: NISSL- AND TH-STAINED TISSUE OF<br>6-OHDA-LESIONED ANIMALS (N=7) .....  | 167        |
| APPENDIX C: NISSL- AND TH- STAINED TISSUE OF LID ANIMALS (N=7) .....  | 168        |
| <b>REFERENCES</b> .....   | <b>169</b> |

## List of Figures

|  |     |
|--|-----|
| FIGURE 1: EXPERIMENTAL DESIGN AND NEURAL RECORDINGS .....                | 56  |
| FIGURE 2: KETAMINE-INDUCED OSCILLATORY ACTIVITY (SPECTROGRAM).....       | 61  |
| FIGURE 3: KETAMINE-INDUCED OSCILLATORY ACTIVITY (BAR GRAPHS) .....       | 63  |
| FIGURE 4: PRIOR HISTORY OF KETAMINE ON RESTING OSCILLATIONS (NAÏVE)..... | 64  |
| FIGURE 5: KETAMINE-INDUCED LOCOMOTION (NAÏVE) .....                      | 68  |
| FIGURE 6: EXAMPLES OF CFC IN NAIVE.....                                  | 70  |
| FIGURE 7: KETAMINE-INDUCED CFC COMPARISONS (NAÏVE) .....                 | 73  |
| FIGURE 8: KETAMINE-INDUCED OSCILLATIONS (D1R).....                       | 76  |
| FIGURE 9: EXPERIMENTAL DESIGN AND NEURAL RECORDINGS .....                | 101 |
| FIGURE 10: BASELINE BETA POWER .....                                     | 104 |
| FIGURE 11: KETAMINE-INDUCED OSCILLATIONS (6-OHDA SPECTROGRAM).....       | 106 |
| FIGURE 12: 6-OHDA VS. NAÏVE OSCILLATIONS.....                            | 113 |
| FIGURE 13: PRIOR HISTORY OF KETAMINE EXPOSURE IN 6-OHDA .....            | 115 |
| FIGURE 14: KETAMINE-INDUCED CFC IN 6-OHDA .....                          | 119 |
| FIGURE 15: L-DOPA WIDE-BAND GAMMA (SPECTROGRAM/PSD).....                 | 122 |
| FIGURE 16: BASELINE AIMS AND GAMMA CORRELATION .....                     | 124 |
| FIGURE 17: GAMMA IMMEDIATELY AFTER L-DOPA (PSD) .....                    | 127 |
| FIGURE 18: AVERAGE SPECTROGRAM OF KETAMINE SESSIONS (LID) .....          | 130 |
| FIGURE 19: KETAMINE VS. L-DOPA GAMMA .....                               | 131 |
| FIGURE 20: KETAMINE-INDUCED CFC COMPARISONS (LID) .....                  | 135 |
| FIGURE 21: PRIOR HISTORY OF KETAMINE EXPOSURE IN LID.....                | 137 |
| FIGURE 22: RECEPTOR ANTAGONISM (SPECTROGRAM).....                        | 141 |
| FIGURE 23: RECEPTOR ANTAGONISM (PSD) .....                               | 142 |
| FIGURE 24: M1 RECEPTOR ANTAGONISM AND MOVEMENT .....                     | 145 |

## List of Tables

|  |    |
|--|----|
| TABLE 1: AIMS AND ROTATION TEST SCORES ..... | 93 |
|--|----|

## ABSTRACT

Ketamine is a well-established anesthetic in high-doses that has been in use for over 50 years (Domino et al., 1965). At low sub-anesthetic doses, ketamine is therapeutically effective at treating a wide range of disorders such as treatment-resistant depression (Berman et al., 2000; Diamond et al., 2014), chronic pain (Hocking and Cousins, 2003; Niesters et al., 2014) and post-traumatic stress disorder (PTSD) (Feder et al., 2014). Recent retrospective case reports have identified sub-anesthetic ketamine as a novel treatment for L-DOPA-induced dyskinesia (LID). Infusions in human parkinsonian patients with LID lead to a reduction of dyskinesia for up to one month (Sherman et al., 2016), with similar findings in an animal model of LID using repeated injections to mimic patient infusions (Bartlett et al., 2016). Despite its therapeutic success, the oscillatory mechanisms underlying ketamine's anti-dyskinetic properties are unknown. These lasting effects may be due to ketamine's pervasive ability to modify oscillatory patterns throughout the brain (Hunt and Kasicki, 2013). Ketamine-induced oscillatory activity may contribute to the prolonged reduction of motor fluctuations as observed in previous work (Bartlett et al., 2016; Sherman, 2016).

Furthermore, ketamine may also have a therapeutic role in treating Parkinson's disease (PD). Hypersynchronous beta (15 – 30 Hz) is the pathological oscillatory signature of PD. Additionally, gamma oscillations are pro-kinetic and voluntary movement exhibits a decrease in beta with an increase in gamma (Muthukumaraswamy, 2010). Administration of low-dose ketamine in healthy patients reduced beta oscillations in the cortex (de la Salle et al., 2016; Ma et al., 2018) and increased gamma across regions (Shaw et al., 2015). Surgical treatments for PD such as Deep Brain Stimulation (DBS) triggers high-frequency stimulation (>140 Hz), DBS

reduces beta to restore motor function (Little and Brown, 2014). A potential secondary mechanism is the reduced beta-gamma cross-frequency coupling in motor cortex (de Hemptinne et al., 2015a). Given that ketamine induces both gamma oscillations and high-frequency oscillations (HFOs), it is conceivable that ketamine exposure in an animal model of PD may produce similar therapeutic benefits as DBS.

Using the experimental protocols of Bartlett and colleagues (2016) with the addition of measuring local-field potential activity, we show that the pathological oscillations associated with Parkinson's disease (e.g., beta (15 – 30 Hz)) in 6-hydroxydopamine (6-OHDA)-lesioned animals are not reduced after ketamine exposure. In LID animals, we observed that L-DOPA triggers region-dependent low-to-wide-band gamma oscillations. This contrasts with the existing literature where a strong focal 80 Hz gamma response was found after L-DOPA (Dupre et al., 2016; Halje et al., 2012a). These differences are likely due to our use of a clinically-relevant extended L-DOPA priming protocol. To our knowledge, we are the first to report a new L-DOPA-induced spectral response in a LID animal. We observed that repeated ketamine exposure does not provide acute or chronic reductions in the overall power of L-DOPA-induced gamma oscillations.

Ketamine does produce differential effects on cross-frequency interactions. Ketamine enhanced coordination between low and high frequencies in the striatum, but with the opposite effect in the hippocampus. In LID animals, ketamine reverses theta coupling triggered by L-DOPA in the DMS and NAc. Furthermore, antagonism of opioid-, D1-, and D2-receptors did not affect ketamine-induced oscillations during L-DOPA treatment. Taken together, our results suggest that ketamine-induced oscillations do not underlie its therapeutic benefits in LID, but may trigger the initiation of gradual synaptic reorganization (Phoumthippavong et al., 2016b)

and growth-factor production (Garcia et al., 2008; Yang et al., 2013) resulting in the long-term reduction of LID (Bartlett et al., 2016; Sherman, 2016) that may not necessarily be reflected in oscillatory activity.

## Chapter 1: General Introduction

Pharmacological dopamine replacement therapy for Parkinson's disease (PD) via L-3,4-dihydroxyphenylalanine, also known as Levodopa (L-DOPA) has been the gold standard treatment for several decades (Bastide et al., 2015). However, long-term administration of L-DOPA (up to 80% in patients after 10 years) results in additional motor complications often more debilitating than PD, deemed L-DOPA-induced dyskinesia (LID). This raises the urgency to find a treatment for the treatment.

Sub-anesthetic ketamine administration has been used successfully to treat a range of disorders such as treatment-resistant depression (Berman et al., 2000; Diamond et al., 2014), chronic pain (Hocking and Cousins, 2003; Niesters et al., 2014), and post-traumatic stress disorder (Feder et al., 2014). Recent reports suggest that LID may be a potential candidate for ketamine's therapeutic uses. Infusions of sub-anesthetic ketamine has been found to reduce dyskinesia for up to one month in both retrospective patient case studies and an animal model of LID (Bartlett et al., 2016; Sherman et al., 2016b). However, the mechanisms underlying ketamine's anti-dyskinetic effects are unknown.

Movement disorders treated with ketamine are associated with hypersynchronous oscillatory activity in the cortex and striatum. This suggests that ketamine may act to disrupt network-level oscillatory activity associated with the pathology. In PD, exaggerated beta-band oscillations (15 – 30 Hz) in the cortex and striatum may contribute to increased immobility (Brittain and Brown, 2014). In contrast, low-gamma oscillations (~50 Hz) in the motor cortex are pro-kinetic in healthy subjects and those exposed to low-dose ketamine. Evidence shows that

ketamine induces pro-kinetic gamma in the cortex and striatum, suggesting that ketamine may work to improve mobility in PD (de Hemptinne et al., 2015b; Muthukumaraswamy, 2010).

In LID, narrow-band high-gamma (~80 Hz) is correlated with the onset and duration of abnormal involuntary movements (AIMs), as dyskinesia is termed in animals) (Dupre et al., 2016; Halje et al., 2012b). This LID-associated high-gamma and the ketamine-associated low-gamma are likely generated by different local circuits (e.g., interneuron-interneuron vs. pyramidal-interneuron networks). Given the convincing behavioral evidence of ketamine's long-term reduction of LID (Bartlett et al., 2016; Sherman et al., 2016b), it is conceivable that co-activation of the two gamma-generating networks via co-administration of ketamine + L-DOPA may cause interference that ultimately reduces pathological high-gamma. This is a proposed mechanism by which sub-anesthetic ketamine may disrupt pathological oscillatory activity to reduce LID (Bartlett et al., 2016; Sherman et al., 2016b).

The present set of experiments will replicate the animal models and experimental protocol of Bartlett and colleagues (2016) with the addition of electrode implantation targeting the corticostriatal circuit to record local field potentials (LFPs). The aims of these experiments were to: **1)** explore ketamine's capacity to alter network-level oscillatory activity and cross-frequency coupling in PD and LID, and **2)** identify potential mechanisms via pharmacological manipulations (e.g., via D1-, D2-, and opioid-receptor antagonism).

Deep-brain stimulation (DBS) is an alternative treatment of PD that is often used when replacement therapy is no longer effective. Unfortunately, DBS requires an invasive surgical procedure. There are currently no adequate non-surgical treatments for PD patients suffering from LID. Therefore, there is a pressing need for new therapies to reduce these side effects to improve the quality of life for patients. The scope of this work is intended to fill this gap by

uncovering the oscillatory mechanisms of ketamine's capacity to ameliorate movement disorders as shown by previous work (Bartlett et al., 2016; Sherman et al., 2016b). Understanding the mechanisms will allow for ketamine's acceleration into controlled clinical trials and the identification of new drug targets for movement disorder therapies.

## **1.1 PARKINSON'S DISEASE**

Parkinson's disease is a slowly-progressing, long-term neurodegenerative disorder that affects 2-3% of the population  $\geq 65$  years of age (Poewe et al., 2017). Approximately 5 to 35 new cases of PD are estimated per 100,000 individuals annually (Twelves et al., 2003) and these numbers are expected to double between now and 2030 (Dorsey et al., 2007). First described by James Parkinson in 1817 as 'the shaking palsy' (Parkinson, 1817), the cardinal symptoms of this disorder are impairments in proper motor function such as bradykinesia, rigidity, and tremors (Olanow et al., 2009). These motor dysfunctions stem from the severe loss of dopaminergic neurons originating from the substantia nigra pars compacta (SNc) projecting to the striatum (STR) (Damier et al., 1999). The lack of dopamine (DA) afferents to the STR results in an imbalance in the corticostriatal motor circuit that regulate movement (Lang and Lozano, 1998). The overall impact of PD on one's quality of life is not only limited to motor symptoms. PD also shares numerous non-motor features such as sleep disorders, autonomic dysfunction, depression, chronic pain, and cognitive impairments (Poewe et al., 2017).

### *1.1.a Parkinson's Disease: Diagnosis and Pathophysiology*

The original clinical descriptions of the associated motor dysfunctions remain unchanged over the past decades, the pathophysiology of PD, however, is by no means unequivocal. A variety of proposed mechanisms are theorized to contribute to one or multiple akinetic (i.e., loss of voluntary movement) or hypokinetic (i.e., loss of muscle movement due to disturbed basal ganglia function) symptoms associated with this disorder. However, a widely accepted agreement in both the clinical and pre-clinical literature holds DA depletion as the basis for PD motor symptom pathophysiology (Bhatia and Joao, 2012; Gopalakrishna and Alexander, 2015). It is important to note that norepinephrine (NE) is involved in the non-motor features of PD and NE dysregulate even precedes DA depletion (Delaville et al., 2011). The following outlines the cardinal symptoms of PD and its possible underlying mechanisms.

### *1.1.b Akinesia/Hypokinesia*

The central theme of PD is the reduced voluntary control of movement (i.e., akinesia), which is highly regarded as the outcome of disrupted basal ganglia output similar to hypokinesia (i.e., diminished/abnormally slow movement) (Gopalakrishna and Alexander, 2015). The feature of decreased rhythmic movements in hypokinesia suggests that *timing* is crucial in its pathophysiology. Central pattern generators (CPGs) originating from the brainstem are thought to initiate repetitive rhythmic movements from small reflexive swings (e.g., during balance) to the large swing of both legs during walking. Additionally, DA has been found to play a crucial role in the function of CPGs and perception of time (Buhusi and Meck, 2005). Imaging and tracing studies from humans and animals agree that time perception involves the connectivity between the basal ganglia and substantia nigra, and their projections to the Premotor Cortex (PMA), Supplementary Motor Areas (SMA), and dorsolateral prefrontal cortex (Jahanshahi et

al., 2006; Meck, 2006). There is also evidence to show that PD patients have a distorted perception of time (Pastor et al., 1992a, 1992b). In conjunction with rodent models and non-human primate models of PD, this has been associated with increased dopamine D2-receptor (i.e., inhibitory in nature) expression in the basal ganglia (Buhusi and Meck, 2005; Leblois, 2006). Converging clinical and pre-clinical evidence suggests that CPGs and neurotransmission within the brain likely serve an integrative role in hypokinetic symptoms, such that impaired CPGs disturbs timing of rhythmic movement paired with increased inhibition of the basal ganglia to obstruct voluntary movement.

### *1.1.c Bradykinesia*

Bradykinesia is the slowness of movement with a progressive loss of speed during rapid movements regardless of body part. Given its generic set of observable descriptions, bradykinesia is often a major source of misdiagnosis as these symptoms overlap with general slowness of movement. However, bradykinesia does not involve paresis (i.e., decreased muscle power), reduced motivation, or spasticity. These motor symptoms are assessed clinically by having the patient execute rapid and repetitive movements ranging from opening/closing their hands to tapping their feet. The severity of bradykinesia can also bring these repetitive movements to a complete stop. Other clinically observable features include hypomimia (i.e., decreased facial expression/eye blink), hypophonia (i.e., lowered voice), and micrographia (i.e., small handwriting) (Gopalakrishna and Alexander, 2015).

Clinical assessment of bradykinesia show that PD patients can correctly identify and choose movement patterns but the speed and magnitude of the movement were inaccurate combined with slow reaction time (Espay et al., 2009). An abundance of evidence from the animal literature suggests that medium spiny neurons (MSNs) in the striatum may be a key

contributor. Copiously found across the striatum, a single MSN contains approximately 10,000 efferent synaptic contacts, of which approximately 100 contacts converge onto a single Globus Pallidus Internal Segment (GPi) neuron in the non-human primate (Yelnik et al., 1991). It is important to note that there are minor differences in the prevalence of MSNs across species. In rodents, MSNs account for approximately 95% of the cells in the striatum (Graveland et al., 1985) while non-human primates and humans contain approximately 70% (Graveland et al., 1985).

Several experiments in non-human primates suggest that the immense inhibitory input from striatal MSNs to the GPi results in an imbalance in the selection and execution movements (Boraud et al., 2001; Heimer et al., 2002). This is complemented by evidence from rodent microdialysis experiments that support striatal MSNs preferentially activating the indirect pathway (i.e., inhibiting movement) that ultimately results in increased GPi output in the corticostriatal circuitry for movement (Taverna et al., 2008). The increased GPi output is correlated with abnormal hypersynchrony in beta-band oscillations in the motor circuit regions (Dejean et al., 2008). Electrophysiology recordings in PD patients correspond to the hypersynchronous beta oscillations observed in animals (Brown, 2006; de Hemptinne et al., 2015a; Hammond et al., 2007). Additionally, PD patients who are on dopamine-replacement therapy (e.g., levodopa) show a reduction in beta oscillations similar to healthy patients (Brittain and Brown, 2014; Brown, 2003).

### 1.1.d Resting Tremors

The resting tremor is characterized by an involuntary rhythmic (~3-6 Hz) movement of a body part while at rest. The tremor vanishes when the affected limb is engaged in active movement. The amplitude of a resting tremor can range from 1/3” up to 4”. The most common form of resting tremor is known as *pill-rolling*, as the patient’s thumb and index fingers are constantly rubbing against each other. Resting tremors are best observed in the clinical setting by having patients focus on a mental task (e.g., counting from one to 50) to facilitate the resting state of muscles (Bhatia and Joao, 2012; Gopalakrishna and Alexander, 2015).

Synchrony of theta oscillations (4-8 Hz) in the STN and GPi may play a large role in these tremors as found in non-human primates and PD patients (Porras et al., 2012; Rivlin-Etzion et al., 2008; Rodriguez et al., 1998b) as the rhythm of these oscillations are highly correlated with the tremors themselves. Although the theory of DA loss is the most supported explanation of PD, it is not well understood how this plays into tremors. However, lesions to the Subthalamic Nucleus (STN) in both humans and non-human primates successfully reduces tremors (Rodriguez et al., 1998a), suggesting this localized region in an abnormally functioning basal ganglia plays a significant role.

Evidence suggests the thalamus is likely involved in resting tremors. Specifically, the Ventral Intermediate nucleus (VIM) of the thalamus. Initial findings show that lesioning the VIM in PD patients removed their tremors (Hirai et al., 1983). More recent evidence suggests that stimulating the VIM via high-frequency deep brain stimulation (DBS), rather than lesioning, is equally as effective (Barbe et al., 2011).

The VIM’s involvement is of significant interest given that this region is independent of the basal ganglia’s projections (Brown, 2003). The VIM receives input from proprioceptors (i.e., sensing limb position) from the muscles and projects to the Primary Motor Cortex (M1) and

Primary Somatosensory Cortex (S1) (Bosch-Bouju et al., 2013). Although more research is needed of the VIM's involvement in tremors, it is hypothesized that the VIM plays a constant role in suppressing tremors. Such that certain bands of oscillations (e.g., high-frequency DBS) or complete inactivation (e.g., lesioning) facilitates the suppression of tremors at rest. It is also possible that hypersynchrony of certain frequency bands contribute to tremors (Barbe et al., 2011). Furthermore, the VIM may work in tandem with other structures highly involved in fine motor movement (e.g., cerebellum) (Baradaran et al., 2013; Barbe et al., 2011). A disruption along this circuit may contribute tremors at rest.

### *1.1.e Rigidity and Postural/Gait Instability*

Rigidity is the third hallmark feature associated with PD in which muscle tone is increased. Rigidity often manifests in the neck and limbs and can be felt for the entire duration of a movement. These features overlap with spasticity, however, the defining feature is that the resistance in rigidity does not increase as a function of movement speed. Additionally, when rigidity is diagnosed alongside resting tremors in a patient, *cogwheel rigidity* can be found where a limb displays abrupt jerks throughout the duration of a movement (Cantello et al., 1996; Gopalakrishna and Alexander, 2015).

The final cardinal feature of PD is an abnormality in posture and/or gait. Similar to rigidity, this instability can be primarily attributed to the loss of certain reflexes. Reflexes play a crucial role in balance and posture as we unconsciously make small corrections in the sway of our body/limbs to prevent falling over. As such, a *pull test* is the best clinical assessment used to detect postural instability. In this exam, the practitioner tugs the patient's shoulders from behind and a healthy patient should easily step backwards to regain balance, whereas an affected patient would tumble backward and likely fall (Gopalakrishna and Alexander, 2015).

The clinical features of rigidity and abnormal posture/gait is indicative of complex pathophysiology. For example, muscle rigidity is only present during rest but not active movement (Baradaran et al., 2013; Delwaide et al., 1991). The physical sequelae of rigidity overlaps with abnormal posture and/or gait. As such, one hypothesis is that rigidity is exclusive to the motor neurons in the spinal cord and muscle fibers involved in reflexes rather than the areas above the brain stem. For example, pioneering studies in the 1960's suggest that the type I muscle fibers of PD patients - responsible for the tendon reflex, is unharmed (Baradaran et al., 2013). In conjunction, the inhibitory interneurons of complimentary muscle fibers projecting to the spinal cord (i.e., type II fibers) become hyperactive (i.e., increased inhibition) that may facilitate rigidity (Delwaide et al., 1991).

Given the nature of a tendon reflex facilitates natural movement that is contrast to rigidity, higher cortical areas that regulate muscle stretch may be involved as well. In PD patients, slowed muscle stretch is increased but the mechanisms are not entirely established (Rothwell et al., 1983). It is believed that this stretch reflex is mediated by the excitability of the motor areas, such that a hyperactive motor loop underlies clinical rigidity (Baradaran et al., 2013). Studies using Transcranial Magnetic Stimulation (TMS) have reduced the increase in M1 excitability in PD patients and PD non-human primates (Cantello et al., 1996; Goldberg et al., 2002). However, other evidence does not support this idea where electrical stimulation of the PMA had no effect on M1 excitability in PD patients who were off dopaminergic medication (Lefaucheur, 2005), whereas healthy controls and PD patients on dopaminergic medication did have increased M1 excitability after PMA stimulation (Mir et al., 2005). Overall, these findings suggest that multiple cortical regions may be dependent on dopaminergic input in PD-associated rigidity.

## 1.2 ETIOLOGY OF PARKINSON'S DISEASE

The pathological hallmark that precedes the motor impairments of PD is the severe degeneration of DA-producing neurons (~70 - 75%) in the SNc of the basal ganglia (Hornykiewicz, 1966). This type of PD is also known as 'idiopathic PD' as the precise cause of this degeneration is unclear. In contrast, the other 10% of PD cases are due to mutations of specific genes (e.g., alpha-synuclein, Leucine-rich repeat kinase 2 (LRRK2), etc.). Mounting evidence suggests that a combination of multiple factors likely contributes to the apoptosis of these DA cells (Poewe et al., 2017).

### *1.2.a Mitochondrial Dysfunction*

Mitochondria are clusters of organelles in the cytosol of a cell. The main function of mitochondria is to produce energy for cells in the form of adenosine triphosphate (ATP). Mitochondria also regulates the maintenance of a cell's growth cycle and evidence suggests that this process is a key factor in the pathogenesis of PD (Bose and Beal, 2016). The first report implicating mitochondrial dysfunction in PD came from accidental administration of 1-methyl-4-phenyl-1,2,3,6-tetrahydropyridine (MPTP), a neurotoxin that disrupts the mitochondrial electron transport chain to result in PD-like symptoms (Burns et al., 1984; Langston et al., 1983). Specifically, mitochondrial Complex 1 is an enzyme in this chain that transports electrons to drive ATP production, and MPTP was found to selectively inhibit this enzyme to result in energy failure and cell death (Chan et al., 1991). Further evidence is drawn from other complex 1 inhibitors such as rotenone, fenpyroximate, and pyridaben which produced similar PD-like symptoms in humans and rodents (Chaturvedi and Beal, 2008). MPTP is now widely accepted to induce SNc cell death in animal models of PD (Morin et al., 2014).

### *1.2.b Oxidative Stress*

Oxidative stress is usually the result of mitochondrial dysfunction and is common in the brain tissue of individuals with Parkinson's disease (Dias et al., 2013). Oxidation is a normal bodily function that combats pathogens using free radicals. A balance must be kept between the levels of free radicals and antioxidants. As this balance shifts towards more free radicals than antioxidants, free radicals will begin to attack fatty tissue and proteins. The dopaminergic neurons in the substantia nigra are thought to be particularly vulnerable to oxidative stress (Poewe et al., 2017) with evidence linking elevated iron levels in the substantia nigra of Parkinson's patients as a leading cause of oxidative stress (Hirsch and Faucheux, 1998).

### **1.3 THE 6-HYDROXYDOPAMINE ANIMAL MODEL OF PARKINSON'S DISEASE**

One of the pathological hallmarks of PD is the loss of dopaminergic neurons in the substantia nigra pars compacta. The motor symptoms of PD manifest when DA denervation reaches approximately 80% (Dauer and Przedborski, 2003). Animal models of PD can be divided into two categories: genetic and neurotoxic. Genetic models offer the advantage of identifying targets that are known to cause PD in humans (Bezard and Przedborski, 2011). However, the disadvantage is that these models do not exhibit neurodegeneration and behavioral phenotypes (Dawson et al., 2010). Thus, neurotoxic models offer the advantage of targeted lesions to the nigrostriatal pathway that parallels PD in humans.

One widely-accepted method to induce dopaminergic denervation is via 6-Hydroxydopamine (6-OHDA), a neurotoxin that targets catecholaminergic neurons such as dopaminergic and noradrenergic (Ungerstedt, 1968). Direct infusions of 6-OHDA into target regions such as the substantia nigra, striatum, and medial forebrain bundle (MFB) is standard procedure to target specific DA neurons and bypass the blood-brain barrier (Jonsson, 1980). It should be noted that infusions of 6-OHDA into the MFB or substantia nigra induces accelerated dopaminergic cell loss (>90%) within 2-3 days, whereas delivery into the striatum causes a slow retrograde damage to the substantia nigra across a 3-week period (Przedborski et al., 1995; Sauer and Oertel, 1994). The latter method is advantageous for investigating early stage PD and/or non-motor symptoms such as cognitive and gastrointestinal dysfunction (Branchi et al., 2008). Administration of desipramine (*i.p.*) is given prior to 6-OHDA infusion to prevent damage to noradrenergic neurons. Oxidation of 6-OHDA in the cytosol (i.e., the aqueous component of a cell's cytoplasm) causes an increase in reactive oxygen species and shifts the balance between

free radicals vs. antioxidants to result in oxidative stress-related cytotoxicity (Blum et al., 2001; Graham, 1978; Jonsson, 1980; Niedzielska et al., 2016). One limitation of this model is that infusions of 6-OHDA are generally applied to one hemisphere (i.e., unilateral 6-OHDA lesion). Bi-lateral lesions better mimic DA neurodegeneration in humans, however, this is less utilized as lesioning both DA production centers risks the survival of the animal.

Verification of 6-OHDA-induced DA cell loss can be accomplished in two ways in the animal model. Immunohistochemical methods are used to stain brain tissue for tyrosine hydroxylase (TH) – an enzyme that initiates DA synthesis. Expression of TH in the human striatum and SNc is indicated by the abundant presence of neuromelanin (i.e., dark pigmentation). Neuromelanin is also present in the rodent SNc and striatum but not enough to provide visual contrast to non-DAergic projections. To supplement this, contrast is enhanced via 3,3'-diaminobenzidine (DAB) staining to visualize the existence of DA terminals in the striatum and DA cell bodies in the SNc. In the whereas the absence of TH results in a light/opaque pigmentation. TH-staining is a post-mortem analysis of brain tissue, the second method of verification addresses this limitation. Behavioral quantification of the degree of lesion takes place approximately 2 weeks after the 6-OHDA surgery via amphetamine-induced rotation tests to assess the motor asymmetry of the unilateral lesioned rat (Dekundy et al., 2007). A dopamine agonist (e.g., amphetamine) is administered (*i.p.*) to induce rotational behavior and is measured by an experimentally blind investigator. The direction and frequency of the rotation is correlated to the magnitude of 6-OHDA lesion. For example, if the animal's right hemisphere was lesioned, administration of amphetamine induces DA release from the intact striatal terminals of the non-lesioned hemisphere (left). This influx of DA in the left hemisphere increases movement on the right-side of the animal's body, thereby rotation to the right-side (i.e., ipsilateral to the lesioned

hemisphere). The number of ipsiversive rotations are counted for a total of 60 min after injection, an average of  $\geq 5$  full ipsilateral rotations/min corresponds to a  $>90\%$  striatal lesion (Dekundy et al., 2007).

## **1.4 PATHOLOGICAL BETA OSCILLATIONS IN PARKINSON'S DISEASE**

A key physiological marker of pathological oscillatory activity in PD is the increase in beta-band oscillations (13 – 30 Hz) in M1 and basal ganglia (Brown, 2006). The enhancement in this band also correlates with increased bradykinesia and rigidity (Kühn et al., 2005). Treatment of PD via both L-DOPA and deep-brain stimulation has been shown to suppress the exaggerated beta-band (15 – 30 Hz), therefore ameliorating the associated motor impairments (de Hemptinne et al., 2015b). With extended L-DOPA treatment, increased lower frequencies such as theta-band (4 – 10 Hz) have been found in the STN along with higher gamma-band (~80 Hz) throughout M1 and STR (Dupre et al., 2016; Halje et al., 2012b). Although hypersynchronous (i.e., exaggerated/enhanced) beta is the fundamental oscillatory pattern of PD, its mechanism and region of origin remains debatable with numerous theories to posit an explanation. It is widely agreed that the excessive and increased inter-regional coherence of beta oscillations are due to the brain's DA-depleted state (Weinberger et al., 2006). However, the origin of hypersynchronous beta remains unclear.

One theory suggests that this pathological oscillation are the result of interactions between the motor cortex and extra-striatal regions of the basal ganglia via the hyperdirect pathway (Brittain and Brown, 2014). Direct glutamatergic projections from cortex to the Subthalamic Nucleus (STN) bypasses the striatum (i.e., direct/indirect pathways) and is thought to be critical for suppressing erroneous movement (Nambu and Tachibana, 2014). Mounting evidence suggests that such cortical input is the likely source of enhanced beta in PD (Burianova et al., 2010; Gradinaru et al., 2009; Hammond et al., 2007; Moran et al., 2011). The STN also has reciprocal connections with the globus pallidus external segment (GPe), such that GPe

suppresses STN via GABAergic input and STN excites GPe via glutamatergic input (Sigtermans et al., 2009). Evidence suggests that this GPe-STN circuit can oscillate independently (McCarthy et al., 2011) and maintain hypersynchronous beta coming from cortical input in PD (Brittain and Brown, 2014). Alternatively, other groups theorize that pathological beta oscillations are generated from the STR. Specifically, via striatal Medium Spiny Neurons (MSNs).

Approximately 70% (i.e., non-human primates) to 90% (i.e., rodents) of striatal neurons are GABAergic MSNs (Tepper et al., 2004) These MSNs are reciprocally connected via GABA<sub>A</sub> receptors and contain the cellular and network properties to support the generation of beta. For example, striatal MSNs are reciprocally connected via the M-current (i.e., non-activating potassium current) that is temporarily reduced by GABA<sub>A</sub> receptors that increases membrane excitability, increasing the likelihood of rebound spiking (e.g., counterintuitive cell firing after an inhibitory input) (McCarthy et al., 2011). This dynamic interaction between the slow time constants of decay of each current enables rebound spiking to occur with the lags that fit with beta oscillations (McCarthy et al., 2011).

## 1.5 L-DOPA-INDUCED DYSKINESIA

Currently, the most effective pharmacological treatment for alleviating the motor impairments of PD is via the DA precursor L-3,4-dihydroxyphenylalanine, also known as Levodopa (L-DOPA) (Bastide et al., 2015). When administered to patients with PD, L-DOPA acts to enhance synaptic DA transmission by restoring net DA concentrations in the striatum (Jenkinson and Brown, 2011; Picconi et al., 2003) and thereby reinstating proper motor function. L-DOPA is typically ingested daily via oral tablets in combination with a decarboxylase inhibitor (e.g., Carbidopa) to prevent metabolization of L-DOPA in the bloodstream. While the effects of L-DOPA on PD-induced motor impairments are astounding, prolonged exposure to L-DOPA (~5 years; (De Jong et al., 1987)) leads to the induction of a new set of motor dysfunction deemed L-DOPA-induced dyskinesia (LID) in ~80% of PD patients within the first 6 years (Jankovic, 2005), and renders the long-term use of DA replacement therapy for PD unsatisfactory. Contrary to PD symptoms, LID is characterized by abnormal involuntary movements (AIMs). The most commonly forms are chorea (i.e., rapid and irregular movements flowing from one limb to another), dystonia (i.e., sustained muscle contractions), and ballism (i.e., flailing high-amplitude movements).

### *1.5.a Mechanisms of L-DOPA-Induced Dyskinesia*

The classic view of LID suggests that overstimulation of both D1- and D2- receptors by L-DOPA results in decreased activity of the indirect pathway (D2-receptors) and hyperactivity of the direct pathway (D1-receptors) (Jenner, 2008). This imbalance of the striatal pathways leads to a reduction in the inhibitory output to the thalamus thereby increasing thalamic firing to result in AIMs. However this classic view of LID has been proven incorrect as evidence from non-

human primate models of dyskinesia show that indirect pathway activity is not reduced (Vila et al., 1997).

A combination of several factors likely contribute to the induction LID. The first requisite is dopamine depletion. In healthy human patients and non-human primates, acute or chronic administration of L-DOPA at clinical doses does not develop dyskinesia (Rajput et al., 1997). Second, the loss of dopamine presynaptic terminals in the striatum accelerates the development of dyskinesia. In the early stages of Parkinson's disease, L-DOPA is synthesized into DA via the L-Amino Acid Decarboxylase (AADC) enzyme and DA is then stored in the existing presynaptic terminals of DAergic neurons in the striatum. DA is gradually released to balance tonic dopamine levels to facilitate voluntary movement. This gradual controlled release of dopamine is regulated by D2 autoreceptors (i.e., inhibitory receptors located on the presynaptic terminal) and dopamine transporters (DAT) for reuptake. As the disease progresses and more dopamine terminals are denervated, dopamine synthesis and release now occurs in nearby serotonin (5-HT) neuron terminals due to the presence of the AADC enzyme for synthesis and Vesicular Monoamine Transporter (VMAT) for packaging (Bastide et al., 2015). However, dopamine release is now uncontrolled and aberrant as these 5-HT neurons do not contain D2 autoreceptors or DAT, resulting in excessive swings of dopamine release. Another factor is the delivery rate of dopamine. Administration of dopamine agonists that are long-lasting result in lower levels of dyskinesia (Oertel et al., 2006; Rascol et al., 2000). Subcutaneous injections of short-lasting dopamine agonists results in greater dyskinesia than infusions of the same agonist (Smith et al., 2005; Stocchi et al., 2005). Although LID can be delayed to a degree, dyskinesia will ultimately still manifest (Hauser et al., 2007). Once dyskinesia develops, any dopamine agonist will trigger symptoms (Dupre et al., 2016). Other proposed factors that may contribute to the expression of

dyskinesia are increased corticostriatal extracellular glutamate concentrations, glutamate receptor phosphorylation, and glutamate transporter expression after prolonged L-DOPA administration (Dupre et al., 2011; Sgambato-Faure and Cenci, 2012), along with enhanced sensitivity of striatal DA receptors (Cenci and Konradi, 2010) and amplified activity of the direct pathway (Mela et al., 2012).

### *1.5.b The Animal Model of L-DOPA-Induced Dyskinesia.*

Behavioral quantification is required to assess the degree of LID via the AIMs rating scale (Cenci et al., 1998). Administration of L-DOPA is required to induce AIMs for assessment; this is known as the L-DOPA priming period. Priming protocols may vary in dose and duration (Dekundy et al., 2007; Lundblad et al., 2002). There are 3 AIMs categories that assess specific symptoms of dyskinesia in the animal model. The first category is axial dyskinesia (i.e., dystonic posture), consisting of twisting movements toward the side contralateral to the 6-OHDA lesion and affects the neck and upper trunk of the animal. The second category is orolingual dyskinesia, this form involves tongue protrusions and repetitive opening/closing of the jaw. The final category is limb dyskinesia manifesting as rapid movements of the forelimbs contralateral to the 6-OHDA lesion. All 3 AIMs subtypes can be easily distinguished from normal behavior as AIMs only affect one side of the body (Cenci et al., 2002; Winkler et al., 2002). L-DOPA increases extracellular DA, the hypersensitive DA receptors on the DA-depleted striatum are stimulated, causing excess movement on the side of the body contralateral to the depleted hemisphere.

AIMs are scored by observation for 60 seconds every 10 minutes across a 160- to 200-minute period while rat is confined in a large clear cylinder. A 0 to 4 rating scale is utilized: 0 = no AIMs present, 1 = present <50% of the observation period, 2 = present for >50% of the

observation period, 3 = present for the entire observation period + interruption by loud stimulus (e.g., experimenter tapping on the cylinder), 4 = present for entire observation but not interrupted by loud stimulus. Scores for all 3 AIMs are then combined for a single ALO AIM score (Cenci et al., 1998).

### *1.5.c Pathological Oscillations of L-DOPA-Induced Dyskinesia*

Investigating the oscillatory activity of LID whether in human patients or animal models of LID is still in its infancy. Several reports have established that the key physiological signature of L-DOPA treatment in the dopamine-depleted basal ganglia and motor cortex is a reduction in exaggerated beta and increase in high gamma (>50 Hz) (Litvak et al., 2011). Specifically, the L-DOPA-induced gamma activity ranges from 60 to 90 Hz with a strong focal peak at 80 Hz, deemed “finely-tuned gamma” (FTG). Evidence from two different laboratories have provided compelling evidence that the onset and duration of LID symptoms are associated with this FTG at 80 Hz (Dupre et al., 2016; Halje et al., 2012b). This oscillatory response is triggered by L-DOPA and thought to coordinate the over-activation of principle cells in M1, resulting in further over-activation of downstream striatal targets that correlate with dyskinesia.

M1 and DLS are the only two regions that have been documented to exhibit this high-gamma oscillation at 80 Hz after L-DOPA administration in a LID animal. Its mechanism is still unclear but evidence suggests that the severity of DA lesion is a factor as partially-lesioned (~67%) and control rats did not exhibit the same response after L-DOPA administration (Dupre et al., 2016) as animals with lesions affecting >90% of DA neurons. D1-receptors in the cortex are linked to this high-gamma as application of the D1-receptor antagonist (SCH-23390) to the surface of cortex abolishes both dyskinesia and 80 Hz gamma (Halje et al., 2011). Additionally, D1- and D2- receptors are involved as administration of D1-receptor agonist (SKF81297) and

D2-receptor agonist (quinpirole) both induced the focal 80 Hz response and dyskinesia (Dupre et al., 2016). This adds further support to the claim that any DA agonist can induce dyskinesia once established. Finally, 5-HT is implicated in 80 Hz gamma generation as administration of 5-HT-receptor agonist (8-OH-DPAT) following L-DOPA eliminated the focal 80 Hz response and stopped dyskinesia, while a subsequent injection of 5-HT-receptor antagonist (WAY100635) resumed both L-DOPA-induced features (Dupre et al., 2016). These findings are consistent with the aberrant DA release mechanism of LID via 5-HT neurons (see 1.5.a).

#### *1.5.d Gamma Networks*

Interactions between within-region local circuits of pyramidal cells and interneurons that share recurrent connections are widely-agreed upon as one mechanism for generating gamma band oscillations. The basis for increased gamma power or frequency is due to increased neuronal excitability of these neurons. The first proposed gamma network is the interneuron-interneuron network (I-I) (Buzsáki and Wang, 2012). Circuits of interconnected inhibitory interneurons co-activate each other via fast-acting electrical gap junctions to result in synchronized firing. Modeling work suggests that I-I networks are better suited for sustaining the high-gamma frequencies, suggesting that I-I networks may be optimal for the L-DOPA-induced high-gamma in LID (Brunel and Wang, 2003).

The second mechanism of gamma generation involves the interactions between excitatory pyramidal neurons and inhibitory interneurons, deemed the pyramidal-interneuron network (P-I) (Buzsáki and Wang, 2012). Excitatory pyramidal cells send fast excitation to interneurons, which in turn causes interneurons to inhibit the same pyramidal neuron through recurrent connections. The inhibition of the pyramidal neurons causes a conduction delay before sending fast excitation again back to the interneuron. This delay results in a slow-/low-gamma oscillation (Brunel and

Wang, 2003). Recent evidence suggest that P-I interactions may even generate beta frequencies orchestrated by distinct inhibitory interneuron input to pyramidal cells (Chen et al., 2017).

Although I-I and P-I circuits are distinct gamma-generating networks, evidence suggests that they can cooperate or compete to produce or suppress gamma (Brunel and Wang, 2003).

## 1.6 KETAMINE

Ketamine is a FDA-approved anesthetic primarily used for surgical procedures at high doses (<2mg/kg, intravenous (IV)) (Rowland, 2005). At low, sub-anesthetic doses (>0.5 mg/kg, IV; (Kurdi et al., 2014)) ketamine encompasses a wide range of applications including but not limited to treatment-resistant depression (Berman et al., 2000; Diamond et al., 2014), chronic pain (Hocking and Cousins, 2003; Niesters et al., 2014) and post-traumatic stress disorder (PTSD) (Feder et al., 2014). Ketamine interacts with multiple receptor binding sites (e.g., cholinergic, glutamatergic, opioid) with a multitude of dose-dependent effects, which may explain its versatility in therapeutic applications. However, it is established that the primary mechanism of ketamine is NMDA-receptor antagonism. Nonetheless, ketamine's multiple binding sites complicate the understanding of its underlying mechanisms.

### *1.6.a Ketamine Mechanisms and Oscillations*

A host of receptor targets are part of ketamine's arsenal of neuropharmacological actions. These dose-dependent effects range from neuromodulatory (e.g., glutamate, dopamine, region-specific acetylcholine) to gene expression (e.g., brain-derived neurotrophic factor (BDNF), mechanistic target of rapamycin (mTOR)) (Sleigh et al., 2014b). The most-studied property of ketamine is its function as a non-competitive N-methyl-D-aspartate (NMDA) receptor antagonist. NMDA receptors are a sub-class of ionotropic channels that bind to the neurotransmitter glutamate. NMDA receptors are present on nearly all cells of the central nervous system (CNS) and glutamate is the most prevalent neurotransmitter (Mion and Villevieille, 2013). As a derivative of phencyclidine (PCP), ketamine blocks calcium influx in ion channels at the PCP binding site within the NMDA receptor. The effects of ketamine-induced NMDA receptor blockade are numerous. For example, ketamine at low-doses can cause

an efflux of glutamate release especially in the cortex (Krystal et al., 2013). Known as the disinhibition hypothesis (Hunt and Kasicki, 2013), this NMDA receptor antagonist-induced burst of glutamate release triggers a series of signaling cascades that leads to increased synthesis of proteins, synapses, and plasticity. This cascade begins with the tonic firing of GABAergic interneurons which is driven by NMDA receptors, antagonism of these receptors by ketamine results in the disinhibition of pyramidal cells releasing them from controlled firing. This in turn causes a surge of glutamate release and a signaling cascade of events that leads to increased activation of  $\alpha$ -amino-3-hydroxy-5-methyl-4-isoxazolepropionic acid (AMPA) receptors to depolarize voltage-dependent  $\text{Ca}^{2+}$  channels. Release of BDNF follows to stimulate mTOR – a kinase controlling protein translation, leading to increased protein synthesis for synaptogenesis and plasticity (Abdallah et al., 2016). This series of events ultimately leads to ketamine-facilitated synaptic reorganization as ketamine increases BDNF production (Garcia et al., 2008; Yang et al., 2013) and spine density in the cortex (Phoumthippavong et al., 2016b).

### *1.6.b Ketamine and the Opioid System*

Ketamine also serves as an opioid agonist by binding to  $\mu$ -,  $\delta$ -, and  $\kappa$ -opioid receptors with an affinity similar to NMDA receptors (Fink and Ngai, 1982; Gupta et al., 2011; Mion and Villeveille, 2013). Single administration of low-analgesic doses in humans have been found to induce acute (~10 min) and prolonged (~3 hours) reduction of ongoing neuropathic pain (Backonja et al., 1994). The analgesic properties of ketamine are believed to be the result of ketamine-opioid receptor interactions as ketamine modifies opioid receptor function to reduce opioid tolerance (Sarton et al., 2001; Shikanai et al., 2014). Furthermore, these anti-nociception features of ketamine are mediated by  $\mu$ - and  $\delta$ -opioid receptors as opioid receptor antagonists can

reverse this effect (Da Fonseca Pacheco et al., 2008). These observations support ketamine's role in treating chronic pain (Hocking and Cousins, 2003; Niesters et al., 2014).

### *1.6.c Ketamine and the dopamine system*

Despite ketamine's therapeutic benefits, there are some limitations and safety concerns that accompany this drug at non-clinical doses, such as inducing psychotomimetic effects (Cooper et al., 2017). The ketamine-induced psychotomimetic effects have been linked to the dopaminergic system, particularly as ketamine's action on DA may contribute to its rapid antidepressant effects (Kokkinou et al., 2018). Evidence shows that ketamine increases DA concentrations across the striatum (Li et al., 2015) and cortex, with twice as much release in the cortex and nucleus accumbens compared to the rest of the striatum (Kokkinou et al., 2018). In addition to stimulating DA release, ketamine also binds directly to D2-receptor sites (Kapur and Seeman, 2002; Li et al., 2015). Whether the amount of stimulated DA release is preferential or dose-dependent remains to be debated. A possible mechanism behind ketamine-induced DA release again relies on NMDA-receptor blockade of GABAergic interneurons that regulate the excitatory projections to the substantia nigra and ventral tegmental area (VTA). The decreased interneuron activity disinhibits pyramidal neuron firing to increase DA release (Olney et al., 1999). Increasing DA neuron firing and DA release is proposed to be one potential mechanism for ketamine's antidepressant effects. However, other mechanisms may also be implicated as ketamine metabolites (2S,6S;2R,6R – hydroxynorketamine) have also shown to contribute by sustaining AMPA receptor activation (Zanos et al., 2016a). Taken together, ketamine's interaction with the DA system may only be one of a combination of mechanisms that underly its therapeutic benefits.

## 1.7 KETAMINE-INDUCED OSCILLATORY ACTIVITY

### 1.7.a Delta

Ketamine's effect on oscillatory activity is just as widespread as its molecular mechanisms as distinct oscillatory signatures are triggered throughout the brain after exposure. Delta oscillations (0 – 4 Hz) are important for integrating functionally connected regions. These slower frequencies are commonly observed during basic processes such as autonomic regulation and sleep, to higher-order functions such as motivation and cognition. Low doses of ketamine (9 mg/kg) have been found to increase delta oscillations in the pre-frontal cortex (PFC) and primary somatosensory cortex (S1) with power increases in a dose-dependent manner. High doses (~50 mg/kg) increases delta power in the CA1 of the hippocampus (HC) and thalamus. Interestingly, lower doses (~20 mg/kg) did not elicit delta in these regions. However, NMDA receptor antagonists at high doses generally increases the amplitude of slow oscillations. Changes in ketamine-induced delta oscillations are thought to have origins in thalamic nuclei. The cortex and thalamus have strong reciprocal connections (Steriade et al., 1994) and can thus synchronize oscillatory activity across cortical networks to delta oscillations. For example, infusions of NMDA receptor antagonist MK-801 to the mediodorsal thalamus increases low-delta in the PFC, while infusions to the PFC does not affect delta (Kiss et al., 2011).

### 1.7.b Theta

Theta oscillations (4 – 12 Hz) are most observable during locomotion, sensorimotor integration, and memory formation/recall and can be recorded from many regions such as the striatum, anterior thalamus, brain stem nuclei, and the amygdala. One of the most important functional correlates is theta coupling in the HC serving as a mechanism for learning and memory. Ketamine has been found to reduce theta power and conversely increase gamma in the

HC (Lazarewicz et al., 2010). The ketamine-induced effects on theta in the cortex, however, increases theta power. Systemic injections of ketamine and other NMDA receptor antagonists such as PCP and MK-801 all increased theta oscillations and are not dose-dependent (Ehlers et al., 1992; Marquis and Paquette, 1989; Mattia and Moreton, 2008; Páleníček et al., 2011). Similar increases were also observed with larger doses but power was weaker due to the larger-amplitude neighboring delta oscillations (Sharma et al., 2010). This trend continued at the highest anesthetic dose (Fu et al., 2008). Not all studies have found theta increases after ketamine. Administration of ketamine did not significantly alter theta power in the motor and visual areas (Phillips et al., 2012). Many factors may account for these differential results such as dosage, electrode placement, and other methodological variances. Taken together, the opposing ketamine-induced alterations to theta oscillations in the HC and cortex suggests multiple independent theta generators with selective ketamine-induced effects.

### *1.7.c Beta*

Beta band oscillations (15 – 30 Hz) have been implicated in working memory processes (Kopell et al., 2011). The most-investigated function of beta oscillations, however, is their role in movement preparation and rest (Jenkinson and Brown, 2011) with emphasis on hypersynchronous activity as an oscillatory signature of PD (Brittain and Brown, 2014; Brown, 2006; Hammond et al., 2007; Mallet et al., 2008; Moran et al., 2011). Administration of low-dose ketamine in healthy patients reduced resting-state EEG beta oscillations in the posterior cingulate cortex (de la Salle et al., 2016). Similarly, opposing effects were observed in the lateral PFC after low-dose ketamine where beta power decreased and gamma power increased during task and non-task periods (Ma et al., 2018). Although more research is needed to thoroughly

explore ketamine-induced effects on beta oscillations, the available studies suggest beta power is reduced in the cortex.

#### *1.7.d Gamma*

Gamma oscillations (>30 Hz) have a fundamental role in binding information from anatomically distinct regions. For example, gamma coherence between the CA1 and CA3 regions of the HC increases during memory retrieval in a delayed spatial memory task. In terms of movement disorders, gamma oscillations are thought to be pro-kinetic in nature (Muthukumaraswamy, 2010). The frequency range of gamma oscillations can vary drastically from 30 – 80 to even upwards of 100 Hz (Crone et al., 2006). However, it is generally agreed that the established canonical gamma oscillation range is 30 – 90 Hz with distinctions between low and high (Buzsáki and Wang, 2012). Gamma oscillations are generally increased across regions after ketamine exposure. For example, dose-dependent increases were observed in the frontoparietal areas after low-doses of ketamine (2.5 mg/kg). Gamma power also exhibits significant increases in the cortex (Shaw et al., 2015) and HC after ketamine (Hunt et al., 2011; Lazarewicz et al., 2010). Topical application of ketamine or NMDA receptor antagonist MK-801 increases gamma in the supragranular and infragranular layers of the parietal cortex, suggesting that NMDA receptor antagonists may act directly on cortical pyramidal neurons to influence gamma generation.

#### *1.7.e High-Frequency Oscillations*

High-frequency oscillations (130 – 180 Hz, HFOs), like gamma, are thought to be involved in the temporal binding of information in distinct structures and may reflect a dynamic mechanism that enables neuronal synchronization. HFOs are naturally occurring in regions such

as the HC (e.g., sharp-wave ripples of 180 – 200 Hz), cortex, striatum, and basolateral amygdala. Ketamine-induced HFOs are dose-dependent such that they are only triggered by doses less than 100 mg/kg (Hunt et al., 2006a). HFOs have been recorded in many regions after ketamine exposure such as M1, striatum, subthalamic nucleus, substantia nigra, hippocampus, thalamus, parietal cortex, and visual cortices (Hunt et al., 2011; Kulikova et al., 2012; Nicolás et al., 2011; Phillips et al., 2012). The mechanisms of ketamine-induced HFOs are not well understood. However, evidence suggests that one generator of HFO activity may originate in the NAc as neurotoxic lesions to this region abolishes ketamine-induced HFOs (Olszewski et al., 2013).

#### *1.7.f A Summary of Ketamine's Mechanisms*

Ketamine also produces distinct oscillatory signatures throughout the brain. For example, sub-anesthetic infusions in patients increases low-gamma (40-60 Hz) in the cortex and striatum, and decreases beta (20 Hz) and delta (1-5 Hz) (Blain-Moraes et al., 2014; Hong et al., 2010; Muthukumaraswamy et al., 2015a). Comparable doses in rodents also generates similar increases in low-gamma in the cortex, striatum, and hippocampus (Caixeta et al., 2013; Nicolás et al., 2011). These findings have also been replicated by our group (Ye et al., 2018). Ketamine's oscillatory mechanisms are not well understood, but mounting evidence suggests that HFOs and gamma generated by ketamine likely involves NMDA receptor antagonism since other selective NMDA receptor antagonists (e.g., MK-801) also produce the same effect (Hunt et al., 2015; Olszewski et al., 2013; Pinault, 2008b). Others have shown that ketamine also acts on metabotropic glutamate receptors (mGluR1) in the cortex to regulate gamma (Hiyoshi et al., 2014a). These cortical gamma oscillations are thought to strengthen the communication of neuron assemblies, bind multiple sensory properties, and facilitate spike-timing dependent plasticity. Both types of gamma oscillations (naturally occurring and ketamine-induced) in the

motor cortex are associated with voluntary movement initiation. This suggests that ketamine may facilitate long-term structural changes to ameliorate movement disorders. Furthermore, along with ketamine's actions on glutamate receptors, low-dose ketamine is thought to increase glutamate neurotransmission by both increasing glutamate release and increase AMPA receptor expression in the synapse (Duman et al., 2012). This in turn causes a signaling cascade to increase brain-derived neurotrophic factor (BDNF) and stimulation of the mechanistic target of rapamycin (mTOR) to increase synaptic protein expression (GluR1). The overall effect would lead to long-term structural changes in neuron connectivity.

## **1.8 POTENTIAL THERAPEUTIC APPLICATIONS FOR KETAMINE**

### *1.8.a Parkinson's Disease*

Although ketamine-induced effects on beta oscillations are relatively unexplored, several clues from available evidence may suggest a therapeutic role in PD involving beta, ketamine-induced gamma and HFOs. Suppression/decreased beta oscillations play an important role during voluntary movement (Muthukumaraswamy, 2010). Hypersynchronous beta has been established as the pathological oscillatory signature of PD in both patients and animal models.

Administration of low-dose ketamine in healthy patients was found to reduce beta oscillations in the cortex (de la Salle et al., 2016; Ma et al., 2018). Gamma oscillations are pro-kinetic and voluntary movement exhibits a decrease in beta while increase in gamma (Muthukumaraswamy, 2010). Ketamine is known to induce gamma across regions after ketamine exposure (Shaw et al., 2015). Currently surgical treatment is offered to PD patients taking DA-replacement therapy

Although the exact mechanism is unknown, DBS stimulates the target area at high-frequencies (>140 Hz) to decrease beta thereby restoring proper motor function (Little and Brown, 2014).

Several working hypothesis attempt to explain the DBS mechanism. For example, the neural jamming hypothesis suggests that DBS regulates and corrects pathological neural firing of the basal ganglia (Lee et al., 2018) A potential secondary mechanism is the reduced beta-gamma cross-frequency coupling (de Hemptinne et al., 2015a). Given that ketamine induces both gamma oscillations and HFOs, it is conceivable that ketamine exposure in an animal model of PD may produce similar results as DBS. Unpublished results from our group suggests that ketamine produces an acute anti-parkinsonian effect (Bartlett et al., SfN Abstract, 2017)

### *1.8.b L-DOPA-Induced Dyskinesia*

A recent retrospective case-study from our collaborators extends support of ketamine's efficacy in treating movement disorders such as LID. Patients receiving slow infusions (up to 96 hrs) of sub-anesthetic doses of ketamine (<0.15 mg/kg, IV) alleviated dyskinesias for up to one month (Sherman, 2016). Similarly, an animal model of LID was used to mimic patient ketamine infusions (5 x intravenous (*i.p.*) injections every two hours) and found a long-term reduction of dyskinesias, whereas single acute injections did not (Bartlett et al., 2016). Furthermore, unpublished results from our group show a suppression of LID development after weekly ketamine treatment during LID priming (Bartlett et al., SfN Abstracts, 2017). These lasting effects may be due to ketamine's pervasive ability to modify oscillatory patterns throughout the brain (Hunt and Kasicki, 2013). Specifically, ketamine induces significant region-wide dose-dependent increases in high-frequency oscillations (HFO, >100 Hz) and wide-band gamma (40 – 80 Hz) in naïve rats (Caixeta et al., 2013; Nicolás et al., 2011; Olszewski et al., 2013). Alterations in these frequency bands may contribute to the prolonged reduction of motor fluctuations as observed in previous work (Bartlett et al., 2016; Sherman, 2016).

# **Chapter 2: Ten-Hour Exposure to Low-Dose Ketamine Enhances Corticostriatal Cross-Frequency Coupling and Hippocampal Broad-Band Gamma Oscillations.**

(Original research published in *Frontiers in Neural Circuits*, Ye et al., 2018.)

Permission was obtained from the authors to include this published work as a chapter in this dissertation.

## **2.1 INTRODUCTION**

Ketamine is a widely available FDA-approved drug that was developed in the 1960s as an anesthetic (Domino et al., 1965). In the last decade, the potential therapeutic applications of ketamine have expanded considerably. For example, hour to days-long exposure to sub-anesthetic ketamine can provide weeks-to-month management of treatment-resistant depression (Andrade, 2017; Berman et al., 2000; Diamond et al., 2014), post-traumatic stress disorder (PTSD) (Feder et al., 2014), chronic pain (Niesters et al., 2014), and L-DOPA-induced dyskinesias (LID) (Bartlett et al., 2016; Sherman et al., 2016a). Although the mechanisms underlying ketamine's clinical effectiveness are not well understood, progress has been made towards understanding the action of ketamine and its metabolites upon N-Methyl-D-aspartate (NMDA),  $\alpha$ -amino-3-hydroxy-5-methyl-4-isoxazolepropionic acid (AMPA), opioid, and dopamine receptors (Sleigh et al., 2014; Zanos et al., 2016), and ketamine's capacity to trigger profound changes in oscillatory activity throughout the brain (Caixeta et al., 2013; Hunt et al., 2006b; Lazarewicz et al., 2010; Muthukumaraswamy et al., 2015b; Nicolás et al., 2011; Shaw et al., 2015).

The optimal duration of ketamine exposure for the treatment of neurological diseases has not been established, and the effects of extended exposure on neural activity is not understood. In the clinic, exposure duration can vary considerably. For example, while the majority of initial human studies investigating the anti-depressant effects of ketamine used a single 40-minute infusion, later publications report improved outcomes using 3-6 repeated 40-minute infusions over days to weeks (Murrough et al., 2013; Shiroma et al., 2014; Singh et al., 2016; Vande Voort et al., 2016), or longer 100-minute exposure sessions (Rasmussen et al., 2013). Far longer exposures are used for treating chronic pain where continuous ketamine exposure can last 72 to 96 hours (Noppers et al., 2010). Our original inspiration for the present study was preclinical (Bartlett et al., 2016) and clinical case-study data (Sherman et al., 2016a) that showed that extended ketamine exposure results in weeks-long reductions in LID. In these cases, exposure was 72 to 96 hours in humans (Sherman et al., 2016a) and 10-hours in rats (Bartlett et al., 2016). These infusion times were based on ketamine protocols used to treat pain states, such as intractable migraines (Niesters et al., 2014), where extended exposure durations can reduce pain for 2-3 months (Sigtermans et al., 2009). It is conceivable that extended ketamine exposure could also improve the treatment of treatment-resistant depression as the typical 40-minute infusions for depression improve symptoms for only ~2 weeks on average. Longer exposure times may improve outcomes (Rasmussen et al., 2013). Recently, a small feasibility clinical trial using 96-hour ketamine infusions to treat treatment-resistant depression supports the tolerability of extended exposure in this patient population (Lenze et al., 2016).

Almost all investigations of the neural responses to ketamine exposure have investigated the effects following a single injection. Thus, little is known about the effects of longer exposure

durations on neural activity and neural systems. A second outstanding question is how extended clinical exposure to ketamine during a 5- to 10-hour infusion session provides long-term relief, despite ketamine itself being metabolized within hours (Páleníček et al., 2011). It is therefore conceivable that extended periods of exposure further enhance ketamine's capacity to reorganize neural circuitry (Duman et al., 2012) and alter glutamatergic signaling (Li et al., 2016). This is suggested by a number of observations. For example, low-dose ketamine exposure enhances synchrony between neurons in multiple brain regions at low (1-7 Hz) and high (~140 Hz) frequencies (reviewed in Hunt and Kasicki, 2013). Such synchronization at low doses may support spike-timing dependent plasticity (Bi and Poo, 1998; Masquelier et al., 2009), which may contribute to ketamine's capacity to alter synaptic morphology (Phoumthippavong et al., 2016b). Thus, identifying changes in neural activity that emerge during extended ketamine exposure could identify circuit-level mechanisms involved in ketamine's therapeutic effectiveness at low doses.

Sub-anesthetic ketamine exerts diverse effects on neural synchrony (Hunt and Kasicki, 2013). For example, a single low-dose injection triggers a rapid increase in gamma (40-80 Hz) and high-frequency oscillations (HFOs, 120-160 Hz) in the striatum (Olszewski et al., 2013), cortex (Hakami et al., 2009; Nicolás et al., 2011; Shaw et al., 2015), and hippocampus (Caixeta et al., 2013). Low-dose ketamine also enhances cross-frequency coupling (CFC) which measures the degree to which the timing of high-frequency oscillations are organized by the phase of low-frequency oscillations. Increased CFC may support neural plasticity by organizing the precise timing of action potentials (Canolty and Knight, 2010; Lisman and Jensen, 2013b). Injection of sub-anesthetic doses of ketamine increases theta (5-10 Hz)-gamma and theta-HFO CFC in the

hippocampus (Caixeta et al., 2013) and delta (1-4 Hz)-HFO CFC in the cortex and striatum (Cordon et al., 2015). Some of these effects are likely due to ketamine's antagonism of NMDARs as injection of the selective non-competitive NMDAR antagonist MK-801 also triggers HFOs and gamma in the cortex (Hakami et al., 2009; Pinault, 2008) and HFOs in the ventral striatum (Hunt et al., 2006b; Olszewski et al., 2013).

Ketamine induces strong oscillatory activity and produces behavioral and therapeutic effects that last long after ketamine-induced NMDAR blockade subsides. Consequently, we hypothesized that 10-hour exposure to ketamine, as opposed to a single acute exposure, will entrain activity within corticostriatal circuits such that ketamine-induced oscillations become progressively enhanced over the course of exposure. To test this, we measured oscillatory activity during a 10-hour exposure to low-dose ketamine using the rodent prolonged infusion protocol described in Bartlett et al. (2016), and recorded local-field potentials (LFPs) from motor cortex (M1), ventral striatum (vSTR), dorsal striatum (dSTR), and hippocampus (HC) of awake and behaving rats. Corticostriatal regions (dSTR and M1) were chosen given their involvement in motor pathophysiology (Dupre et al., 2016), and vSTR and HC were selected given their involvement in depression and PTSD (Sailer et al., 2008; Dunkley et al., 2014). Our data suggest that sub-anesthetic ketamine's lasting effect on neural synchrony may not reside in its capacity to produce sustained HFOs, but, instead, in its capacity to increase CFC in corticostriatal circuits and to trigger broad-band high-frequency (> 30 Hz) neural activity in the hippocampus.

## 2.2 MATERIALS AND METHODS

### 2.2.a Animals and Surgical Procedures

Eight male Sprague-Dawley rats (~350 g at surgery, Envigo, Indianapolis, IN) were housed individually in a 12-hour reverse light/dark cycle (i.e., lights off from 9AM-9PM) room with food and water available *ad libitum*. Rats were anesthetized with isoflurane and implanted with two electrode arrays, each array composed of 16 stereotrodes (California Fine Wire Co., Grover Beach, CA). A skull screw over cerebellum was reference and ground. The first electrode array was centered at AP: +1.3, ML: +2.7, right hemisphere, with stereotrodes targeting M1 (DV: -1.4), dorsolateral striatum (DLS, DV: -3.8), dorsomedial striatum (DMS, DV: -4.6), and nucleus accumbens (DV: -6.8, **Figure 1B**). The second array targeted left HC and cortex (centered at AP: -3.0, ML: +2.2) with electrodes lowered near the fissure (DV: -3.2), CA1 (DV: -2.3), dentate gyrus (DV: -3.8), and S1 (DV: -1.4). Rats recovered for 1 week post-surgery. Animals were provided with post-operative analgesia. Carprofen (Zoetis, Parsippany, NJ) was delivered (5 mg/kg, *s.c.*) for 48 hours following surgery. Topical anti-biotic ointment (Water-Jel Technologies, Carlstadt, NJ) was applied to the incisional site for up to 5 days as needed. Sulfamethoxazol and Trimethoprim (Hi-tech Pharmacal Co., Inc., Amityville, NY) was administered orally (15 mg/kg) daily until conclusion of experiments.

Procedures were in accordance with NIH guidelines for the Care and Use of Laboratory Animals and approved IACUC protocols at the University of Arizona. One animal was eliminated from the study due to excessive recording artifacts.

### 2.2.b Drug Treatments

On a given experimental session during Experiment 1, animals received a total of five injections of ketamine (20 mg/kg, *i.p.*) or saline injections with injections occurring every 2 hours as described in (Bartlett et al., 2016) and summarized in **Figure 1A**. This paradigm is identical to that used by Bartlett and colleagues (2016) to model clinical infusions in rodents, and it was chosen as it has been shown to reduce levodopa-induced dyskinesia (LID) (Bartlett et al., 2016). Multiple injections ensured that serum concentrations of ketamine remained high throughout exposure. The 2-hour spacing between injections was important given the faster metabolism of ketamine in rodents (~ 1 hour, (Páleníček et al., 2011; Veilleux-Lemieux et al., 2013)) relative to humans (~3 hours (Clements et al., 1982)). Recording sessions involved injections of either ketamine hydrochloride (20 mg/kg, Clipper Distributing, St. Joseph, MO) or 0.9% saline. Each animal underwent one saline injection session and three ketamine sessions. These sessions were each separated by 1 week (**Figure 1A**).

After the completion of Experiment 1, the same animals were used for a second experiment (Experiment 2) in which the involvement of dopamine D1 receptors in ketamine-induced oscillatory activity was investigated. In this experiment rats received injections of a D1-antagonist (SCH-23390, Tocris Bioscience, Minneapolis, MN) and ketamine (20 mg/kg). Each session began with a 1-hr baseline. A single injection of SCH-23390 (1 mg/kg, *i.p.*) was administered followed by a single injection of ketamine 15 min after the injection. This procedure was repeated again after 2 hrs. After another 2 hrs rats received a single injection of SCH-23390.

### *2.2.c Neurophysiological Recordings*

Data was acquired from a multi-channel data acquisition system (KJE-1001, Amplipex Ltd.).

The digitizing headstage was connected to the animal, and the signal was sent to the recording system through a lightweight tether and commutator. A light-emitting diode (LED) was attached to the rat's implant for video tracking (Camera: Manta G-033C, Allied Vision, Exton, PA).

Recording sessions were conducted once per week for each animal (as in **Figure 1A**) with experiments starting at 5AM. The animals and their home cage were transported to the recording room, and remained in their home cage during recordings sessions with food and water available *ad libitum*.

### *2.2.d Histology*

At the conclusion of the experiment, rats were deeply anesthetized and electrolytic lesions were produced at recording sites via direct current stimulation (20 mA, 20 seconds). Rats were sacrificed 3 days later with Euthasol (0.35 mg/kg, *i.p.*; Virbac, Fort Worth, TX) and brains were extracted through transcardial perfusion with phosphate buffered saline (PBS) followed by 4% paraformaldehyde in PBS. Prepared 40- $\mu$ M thick coronal sections were cut using a frozen microtome and Nissl stained for verification of electrode placement (**Figure 1B**).

### *2.2.e Data Analysis*

Analysis was performed via custom-written code (MATLAB: MathWorks Inc., Natick, MA and R: R Core Team (2017)). Local-field signals were acquired at 20,000 Hz and down sampled to 500 Hz. Local-field traces were analyzed for artifacts through visual inspection and automatic artifact detection. Artifacts can come from multiple sources such as cable artifact and electromyographic (EMG) signal. The 2-min periods before and after each injection were

excluded from analysis to avoid potential artifacts created by the experimenter entering the room and picking up and injecting the animal. Candidate artifacts in the LFP signal were identified as periods where the absolute value of local-field traces exceeded 1.5 mV or when summed cross-band power (2-160 Hz) exceeded the 99.98<sup>th</sup> percentile.

### *2.2.f References and Addressing Volume Conduction*

Interpreting LFP signals as being local to a target region is complicated by contamination from volume-conducted signals from other regions or from EMG artifacts. One approach to address this is to reference signals from one electrode to a second within-region electrode. The capacity of re-referencing to localize region-specific and ketamine-induced oscillations has been previously reported (Hunt et al., 2011). Thus, to be confident that the measured signal was local, we followed the following procedure: **M1:** M1 electrode was referenced to a second M1 electrode 0.7 mm away and at the same depth (1.4 mm). **HC:** To ensure the signal was local to the HC and integrated the diverse oscillatory activity in the HC, the signal from the HC fissure electrode was referenced to the CA1 electrode (1-mm distance). **Striatum:** The geometry of the array allowed segregation of dorsal and ventral striatum, but the array did not have an arrangement allowing segregation of responses within subregions such as the nucleus accumbens core/shell. Consequently, we conservatively divided striatal recordings into dorsal and ventral components. This was accomplished by referencing the dorsolateral striatum electrode against the dorsomedial electrode to yield a dSTR signal, and referencing the nucleus accumbens (NAc) electrode against the dorsomedial electrode to yield a vSTR signal (see **Figure 1B**). **Figure 1C** presents the power-spectral density measured before (cerebellar reference) and after (local M1 reference) re-referencing, suggesting that HFOs in M1 are volume conducted.

### *2.2.g Spectral Power*

Spectral power across frequency bands was determined using a fast Fourier transform spectrogram (frequency bin = 0.5 Hz, 10-second Hanning window, spectrogram() in Matlab). A complex wavelet convolution spectrogram (Morlet family, cycles = 5, cwt() in Matlab) was only used to visualize spectral power for the analysis of cross-frequency coupling (see next section) given the high temporal resolution of the wavelet convolution. Statistical analysis of oscillatory power was restricted to the following frequency bands: delta (1-4 Hz), theta (5-10 Hz), beta (15-30 Hz), gamma (35-55 Hz), and HFO (120-160 Hz). Normalization: To address the issue of power-law 1/f scaling, data was normalized using the Z-transform method as described in Cohen (2014). This was accomplished by first subtracting the baseline mean from the spectral power and then dividing this value by the standard deviation to yield a z score. The baseline period was defined as the -32 to -2 minute interval preceding the first injection.

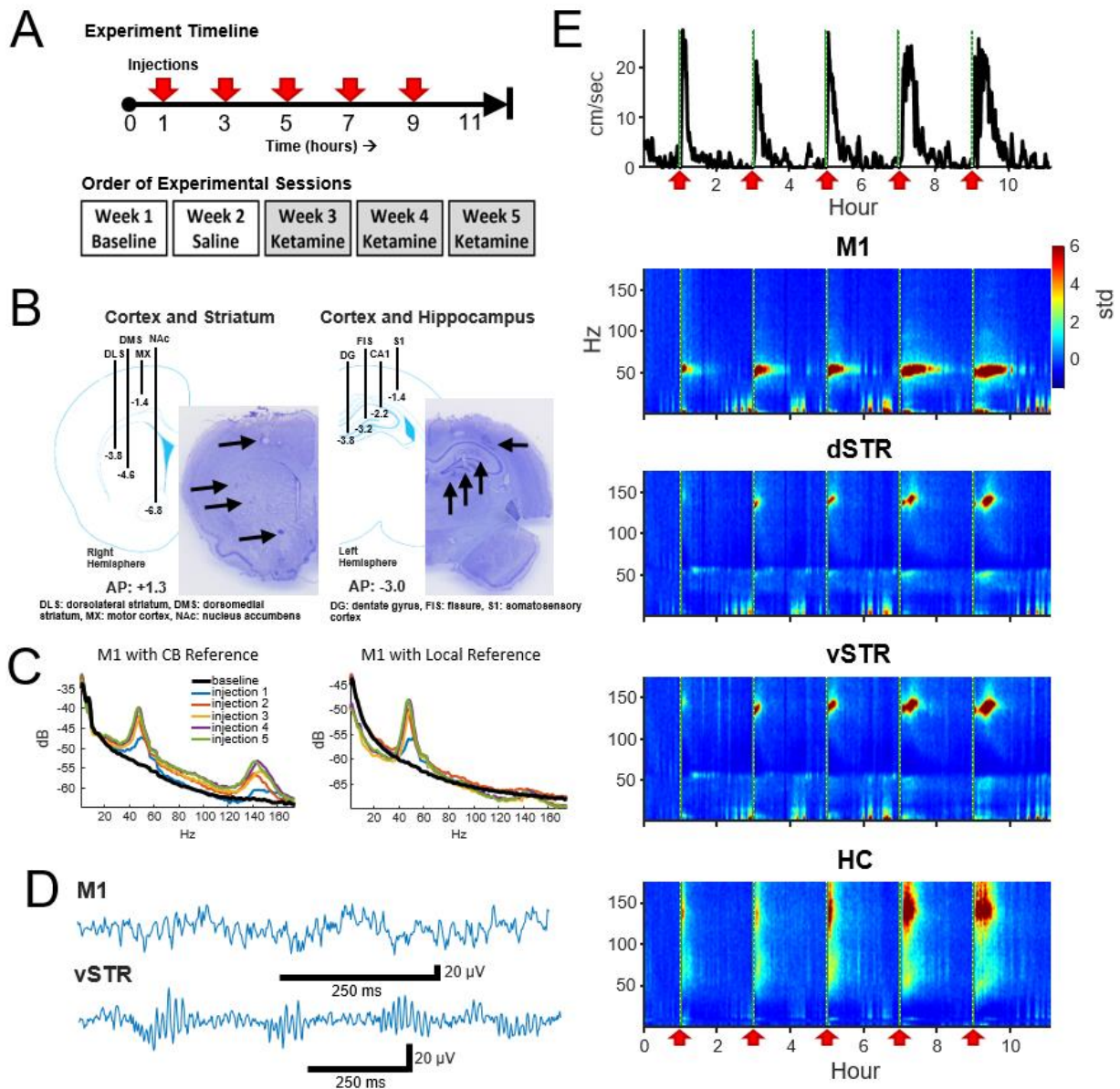


**Figure 1. Experiment design and neural recordings.** (A) TOP: Timeline of an individual experimental session. Five sub-anesthetic doses of ketamine (20 mg/kg, *i.p.*) or saline were injected throughout each 11+ hour recording session. One hour of pre-injection baseline was recorded prior to the first injection. BOTTOM: Timeline for experimental sessions. Each animal received a single ketamine or saline injection recording session each week. (B) Schematic of electrode array placement in the right-hemisphere (AP: +1.3, ML: +2.7 centered, DV: -6.8 deepest electrode) and the left-hemisphere (AP: -3.0, ML: -2.2 centered, DV: -3.8 deepest electrode) and exemplar histological sections. (C) Local-field electrodes were referenced to within-region electrodes to reduce contamination from volume conduction. To illustrate the effects of re-referencing, the power-spectral density (PSD) from an M1 electrode referenced to the cerebellar ground screw (left) or to a second within-region (M1) electrode (right) are presented. Recordings were acquired 10-minutes prior to ketamine injection (black) and 15

minutes following each ketamine injection (colored traces). Note the reduction in HFO power when using a local reference indicating that HFO activity was volume conducted. **(D)** Exemplar local-field traces of ketamine-induced gamma (M1) and HFOs (vSTR) recorded 15 minutes after injection. **(E)** Animal movement (top trace) and power spectrograms acquired from electrodes in M1, dSTR, vSTR, and HC. Ketamine injection times are indicated as vertical dashed lines and red arrows. Values are in standard deviations above the mean measured during the 30 minute period preceding the first injection.

### *2.2.h Cross-Frequency Coupling*

Phase-amplitude cross-frequency coupling (PAC) was measured as described in Cohen (2014).

First, LFP signals were filtered in the target low- and high-frequency bands using a Butterworth infinite impulse response (IIR) filter (fs = 500 Hz, order = 6). Phase was extracted using a

Hilbert transform, and power was extracted as the envelope of the absolute value of the filtered

signal. CFC was computed as  $PAC = |n^{-1} \sum_{t=0}^n a_t e^{i\varphi_t}|$  where  $a$  is high-frequency power and

$\varphi$  is the phase of the low-frequency signal. This value was compared to values computed using a

randomized shuffle control where the original low-frequency signal was randomly shifted in time

on each permutation ( $n = 200$  permutations). The mean and standard deviation of this null

hypothesis distribution were used to convert the measured PAC score into a z score (PACz).

### *2.2.i Statistical Analyses*

Statistical significance was assessed using ANOVA or Student's  $t$ -test (alpha = 0.05). Tukey's

honest significance test or Holm-Bonferroni method were used to adjust p values for post-hoc

comparisons unless otherwise stated. The Shapiro-Wilk test of normality (shapiro.test() in R)

was used to determine if the data was normally distributed, and the data used for ANOVA

satisfied this criterion (Shapiro-Wilk  $p > 0.05$ ).

## 2.3 RESULTS

### *2.3.a A Single Injection of Sub-Anesthetic Ketamine Triggers Gamma Oscillations in M1, Hfos in Striatum, and Broadband Activity in Hippocampus*

In rodents and humans, administration of sub-anesthetic ketamine triggers robust high-frequency activity throughout the brain (Caixeta et al., 2013; Cordon et al., 2015; Muthukumaraswamy et al., 2015; Nicolás et al., 2011). Our data support these observations as ketamine injections (20 mg/kg) induced powerful and region-specific gamma oscillations and HFOs. Spectrograms recorded from all 4 regions during a single experimental session are presented in **Figures 1E**. The mean spectral responses following each ketamine injection are shown in **Figure 2A** (average shown for  $n = 19$  sessions from 8 rats). Inspection of these figures indicates strong gamma-band activity induced in M1 and HFO activity in dorsal and ventral striatum. In contrast, hippocampal responses appeared decidedly broadband for frequencies  $> 30$  Hz. The time-course of the mean response ( $n = 8$  rats) in each canonical frequency band is presented in **Figure 2B**.

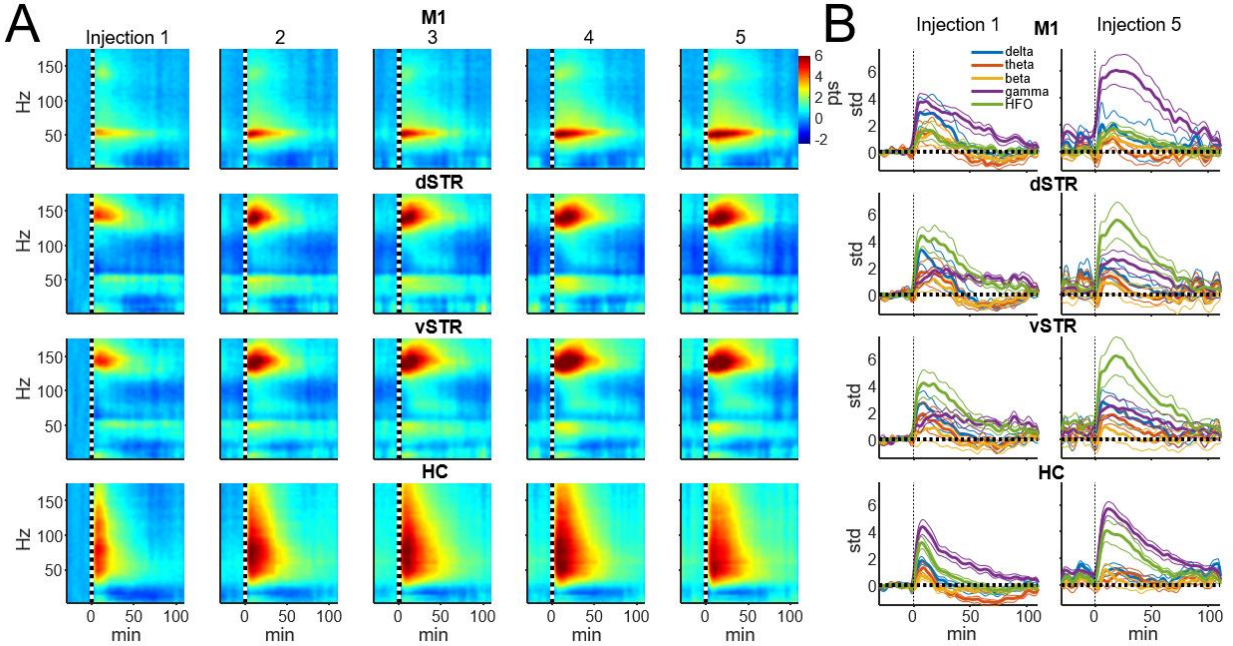


**Figure 2. Ketamine-induced oscillatory activity.** (A) Spectral responses aligned to the time of each of the 5 successive ketamine injections. Spectra for each recording session were averaged ( $n = 19$  sessions from 8 rats). Each row indicates the response for each brain region and each column indicates the injection number. Units are in standard deviations above or below the mean spectral power measured during the -32 to -2 minute period preceding the first injection. Spectral power was smoothed in time with a 5-minute Hanning window prior to averaging. (B) Time course of spectral responses following ketamine injections 1 and 5 by frequency band. Lines indicate mean  $\pm$ SEM ( $n = 8$  rats).

Spectral responses at canonical frequency bands were analyzed, and comparisons were made between the effects of ketamine and saline injection. Spectral power was measured in units of standard deviations (Z scores) above or below baseline spectral power (see Materials and Methods). Statistical comparisons for ketamine-triggered oscillatory power measured during control and ketamine sessions are summarized in **Figures 3A** and **3B** for the 2-90 and 92-110 minute post-injection intervals. These two intervals were chosen given previous work indicating that ketamine is metabolized ~1 hour post-injection (Páleníček et al., 2011). Thus, these intervals represent conservative estimates for periods when ketamine was (2-90 minutes) or was not (92-110 minutes) metabolically active. Black bold lines indicate significant comparisons between ketamine (orange and blue bars) and control saline (gray bars) sessions (*t*-test,  $p < 0.05$ , Holm-Bonferroni correction), and significant paired comparisons between ketamine injection 1 (orange) and injection 5 (blue, paired *t*-test,  $p < 0.05$ , Holm-Bonferroni correction).

A main effect of ketamine was observed during the 2-90 minute post-injection interval in all brain regions (**Figure 3A**, Two-way ANOVA (drug, frequency),  $p < 0.05$  following Holm-Bonferroni correction for 8 comparisons, F and p values are in **Supplementary Table 1A**). During the 92-110 minute interval, however, a strong main effect of ketamine was only observed in the hippocampus (**Figure 3B**,  $F(1,55)$ ,  $p = 0.0006$ ,  $\eta^2 = 0.25$ ), indicating that the lasting impact of extended exposure is in this brain region. Post-hoc analysis also indicated that delta (*t*-test,  $p < 0.004$ , Holm-Bonferroni correction) and HFO power ( $p < 0.031$ ) increased relative to the baseline period during the 92-110 minute interval.

Post-hoc comparisons revealed that during the 2-90 minute interval, ketamine increased gamma power in M1 and HFO power in dSTR and vSTR relative to saline control (**Figure 3A**, *t*-tests,  $p < 0.05$  following Holm-Bonferroni correction). Gamma power also increased in the dSTR and vSTR following the 1<sup>st</sup> and 5<sup>th</sup> injection, and delta power increased in M1 after the 1<sup>st</sup> but not the 5<sup>th</sup> injection. In the hippocampus, ketamine injections increased gamma and HFO power; however, inspecting the spectral responses in **Figure 2A** suggests that this reflects increased broadband power for most frequencies  $> 30$  Hz. This differs from the discrete narrowband increases in HFO and gamma power observed within M1 and the striatum. Thus, ketamine-induced oscillatory activity in the hippocampus is “noisier” and less focal relative to corticostriatal HFOs and gamma oscillations and lasts longer (into the 92-110 minute interval).

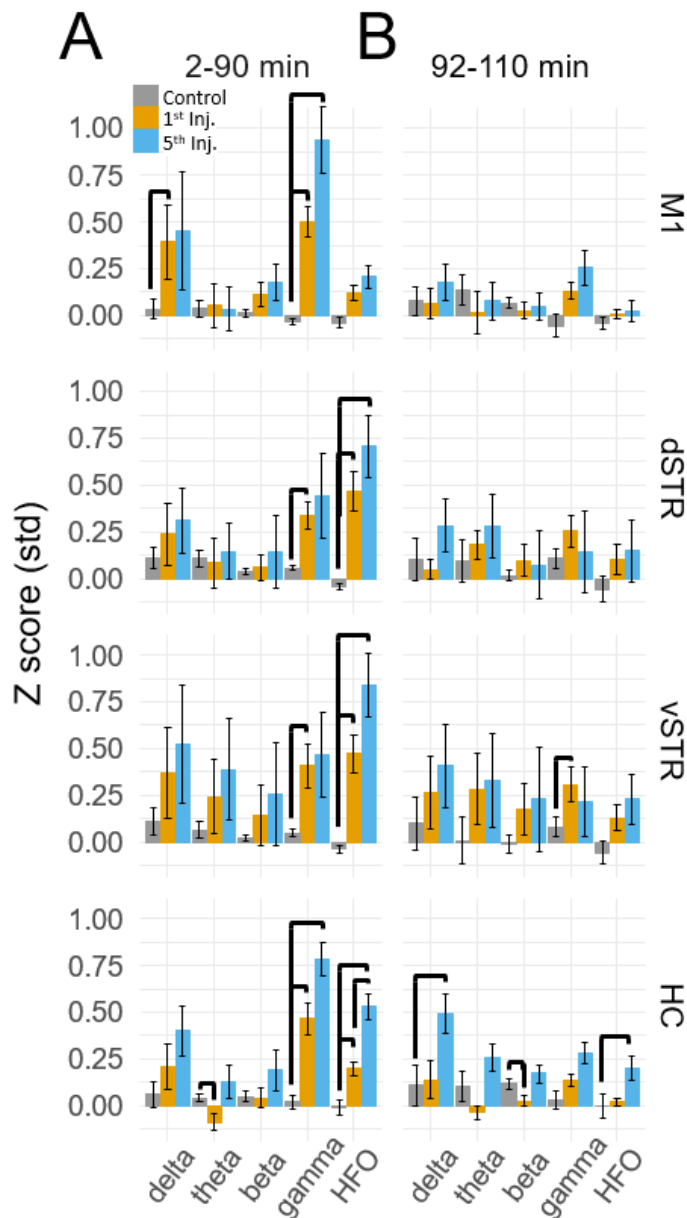


**Figure 3. Ketamine-induced oscillatory activity.** (A) Mean ( $\pm$ SEM) spectral power ( $n = 8$  rats) following ketamine and saline injections during the 2-90 minute post-injection period following the first (orange) and fifth (blue) injections. Bold bars indicate significant between-subject differences vs. controls and significant within-subject differences in either the 1<sup>st</sup> or 5<sup>th</sup> ketamine injections (paired  $t$ -test, Holm-Bonferroni correction, horizontal bars indicate significant effects at  $p < 0.05$ ). (B) As in A but for the 92-110 minute post-injection period. Significant increase in delta, beta, and HFO bands were observed in the hippocampus

### *2.3.b Repeated Ketamine Injections Significantly Increased High-Frequency Oscillatory Power in the Hippocampus*

A main objective of this study was to determine if extended exposure to ketamine produced a lasting change in oscillatory activity. This was investigated by determining if oscillatory power changed from the first to the fifth injection. As described in the previous section, ketamine increased gamma in M1, HFO's in striatum, and broadband (> 30 Hz) activity in the hippocampus, and these effects were observed during the 2-90 minute interval following injections 1 and 5 (**Figure 3A**). Although the mean power in all of these bands appeared to increase from injection 1 to 5, the increase was only significant for the HFO band in the hippocampus (post-hoc paired *t*-test,  $p_{\text{HFO}} = 0.007$ , Holm-Bonferroni correction). No significant differences between injections 1 and 5 were observed during the 92-110 minute post-injection interval (**Figure 3B**), although, as described in the previous section, oscillatory power in the delta and HFO bands in the hippocampus were larger relative to pre-injection baseline.

### *2.3.c Prior History of Extended Exposure to Ketamine Does Not Alter Resting Oscillatory Activity*

Because exposure to ketamine can produce weeks-long improvement in symptoms of chronic pain and treatment-resistant depression, we explored the hypothesis that 10-hr exposure to ketamine can produce measurable changes in oscillatory power that lasts for at least one week. This was assessed by comparing oscillatory power during the pre-injection period (-32 to -2 minutes prior to injection 1) for sessions in which rats had either no prior ketamine exposure sessions to sessions when the rats had at least one 10-hour ketamine exposure (**Figure 4**). Comparisons were made for each canonical frequency band (column) and brain region (row). A within-subject analysis (within subject = number of ketamine sessions, between subject = animal) identified no significant relationships between the number of previous ketamine exposure sessions and oscillatory power in any frequency band (paired *t*-test,  $p > 0.05$ ,  $n = 7$ ).



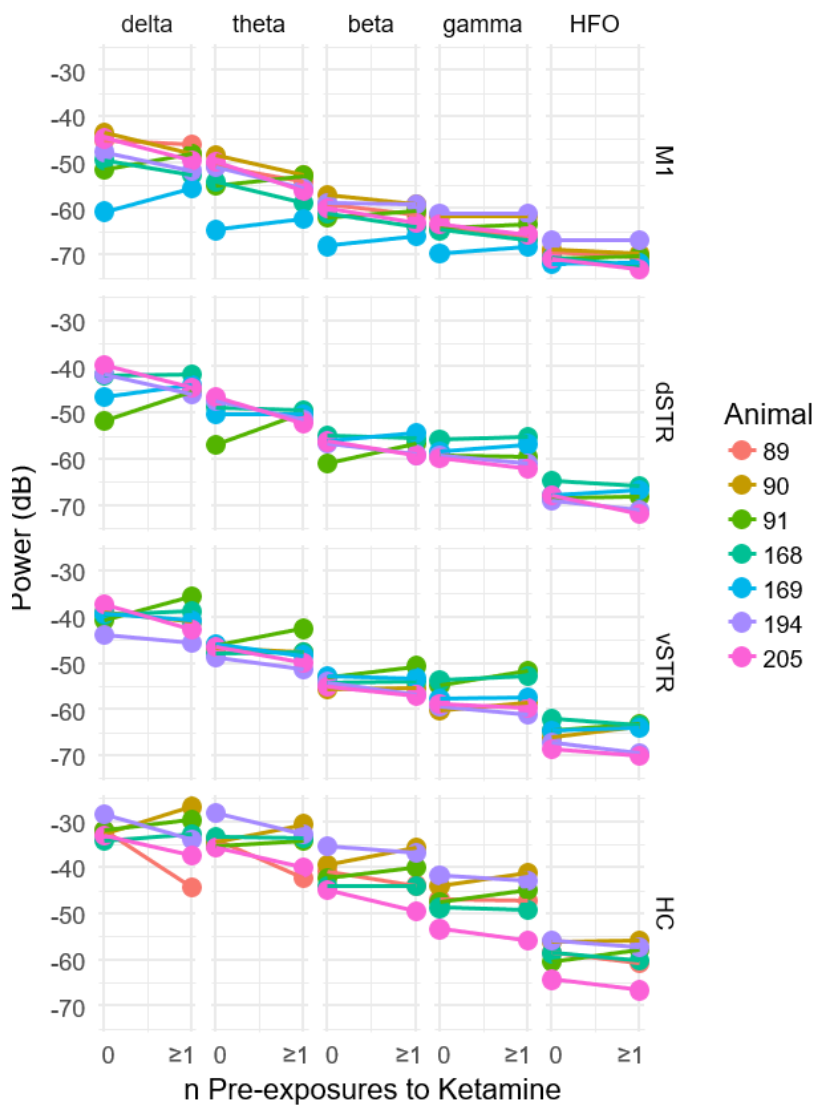


**Figure 4. Prior history of extended exposure to ketamine does not alter resting oscillatory activity.** The effect of the previous history of ketamine exposure on baseline oscillatory activity was investigated by comparing the oscillatory power during the -32 to -2 minute interval preceding the first injection on each recording session. Sessions were separated by at least 1 week. The x axis of each plot indicates the number of previous ketamine exposure sessions (0 indicates days that the rat had no prior ketamine exposure session). A significant difference between the number of ketamine sessions received and oscillatory power (y axis) would suggest that prior ketamine exposures produces persistent changes in oscillatory activity that last at least 1 week, which was the time between ketamine sessions. Individual plots are organized by region (row) and frequency band (column). A within-subject analysis (within subject = number of ketamine sessions, between subject = animal) identified no significant relationships between the number of previous ketamine exposure sessions and oscillatory power at any frequency band (paired t-test,  $p > 0.05$ ,  $n = 7$ ).

### *2.3.d Acute Ketamine Exposure Increases Locomotion, but This Increase is Not Enhanced by Extended Exposure*

Low-dose ketamine exposure increases locomotion and ataxic behaviors in rodents (Nicolás et al., 2011); however, motor activity is likely not causing the observed increase in HFO and gamma power as changes in locomotion lag behind ketamine-induced changes in HFO power (Caixeta et al., 2013). We also observed that ketamine increased locomotion relative to saline injection ( $t$ -test,  $p = 0.0015$ ,  $d = 4.0$ ,  $n = 8$  rats), and this increase was manifest as an initial bout of ataxic behaviors (e.g., rearing and falling over) followed by increased locomotor activity and circling in the home cage.

It was conceivable that the motor-activating effects of ketamine are enhanced by repeated ketamine exposures during an experimental session. Such increased locomotor activity could contribute to the rise in high-frequency broadband hippocampal power from injections 1 to 5 (**Figure 3**). To investigate this possibility, a within-subject analysis was performed that compared mean locomotion during the 2-20 minute interval following injections 1 and 5 (**Figure 5**). Locomotion was quantified as the absolute value of the first derivative of the x and y position of the rat (cm/sec). This analysis indicated that ketamine-induced locomotion did not increase from injection 1 to 5 (**Figure 5B**, paired  $t$ -test  $p = 0.59$ ,  $n = 8$  animals).

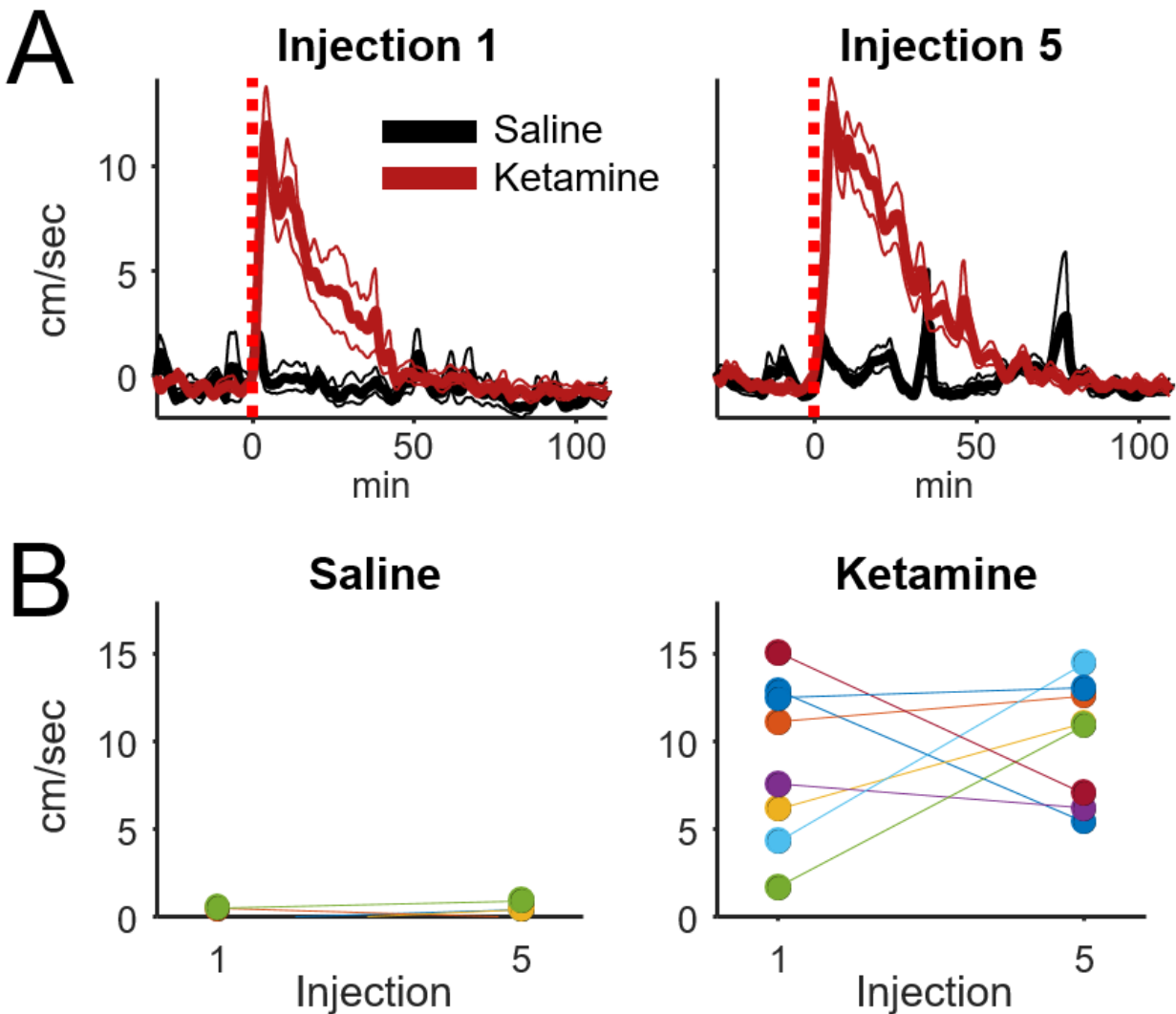


**Figure 5. Ketamine-induced locomotion on the 1<sup>st</sup> and 5<sup>th</sup> injection.** (A) Movement speed during each recording session was measured for periods surrounding ketamine or saline injection (bin size = 8 s, convolved with a 80 s Hanning window). This figure displays the mean and  $\pm$ SEM across sessions (ketamine:  $n = 19$ , saline:  $n = 11$  sessions from 8 rats) for the first and fifth injection. (B) To determine if movement speed was affected by multiple ketamine injections, average speed during the 2-20 minute post-injection interval was analyzed and averaged for each rat. A strong effect of drug (ketamine vs. saline) was observed following injections 1 ( $t$ -test,  $p = 0.0015$ ,  $n = 8$  rats) and 5 ( $p = 0.00006$ ,  $n = 8$  rats). The effect of multiple injections was determined by comparing within-subject responses on the 1<sup>st</sup> and 5<sup>th</sup> injection using paired  $t$ -tests. Neither saline nor ketamine groups exhibited a significant difference in mean movement speed between injections 1 and 5 (paired  $t$ -test, saline:  $p = 0.50$ ,  $n = 7$  rats; ketamine:  $p = 0.59$ ,  $n = 8$  rats).

### *2.3.e Ketamine-Induced Changes in Cross-Frequency Coupling*

Phase-amplitude CFC measures the degree to which the phase of a low-frequency oscillation modulates the amplitude of a high-frequency oscillation. Such cross-band modulation may impact information processing and plasticity by organizing the timing of ensembles of neurons (Canolty and Knight, 2010; Lisman and Jensen, 2013b). We investigated the effects of acute and extended low-dose ketamine exposure on within-region CFC. Representative examples of CFC measured during individual recording sessions are presented in **Figure 6**. The example in **Figure 6A** indicates strong ketamine-induced delta-HFO CFC in vSTR. **Figures 6B** and **C** present the average wavelet spectrogram aligned to the time of the trough of delta oscillations (1-4 Hz) in the vSTR and M1. These examples suggest a progressive increase in delta-HFO CFC from injection 1 to injection 5. The averaged time-course of ketamine-induced CFC following the first and fifth injection in all regions is presented in **Figure 7A**. Inspection of these responses indicates that ketamine induced a rapid increase in delta-HFO and theta-HFO CFC in corticostriatal regions, and these effects lasted from 20 to 90 minutes. Furthermore, the duration of ketamine-induced delta-HFO increased from injection 1 to injection 5, suggesting that prolonged exposure enhanced ketamine's capacity to induce delta-HFO CFC. Ketamine did not induce CFC in the hippocampus, a result that is consistent with the observation that ketamine induced a non-specific wide-band signal on the hippocampal electrodes (**Figure 2**).

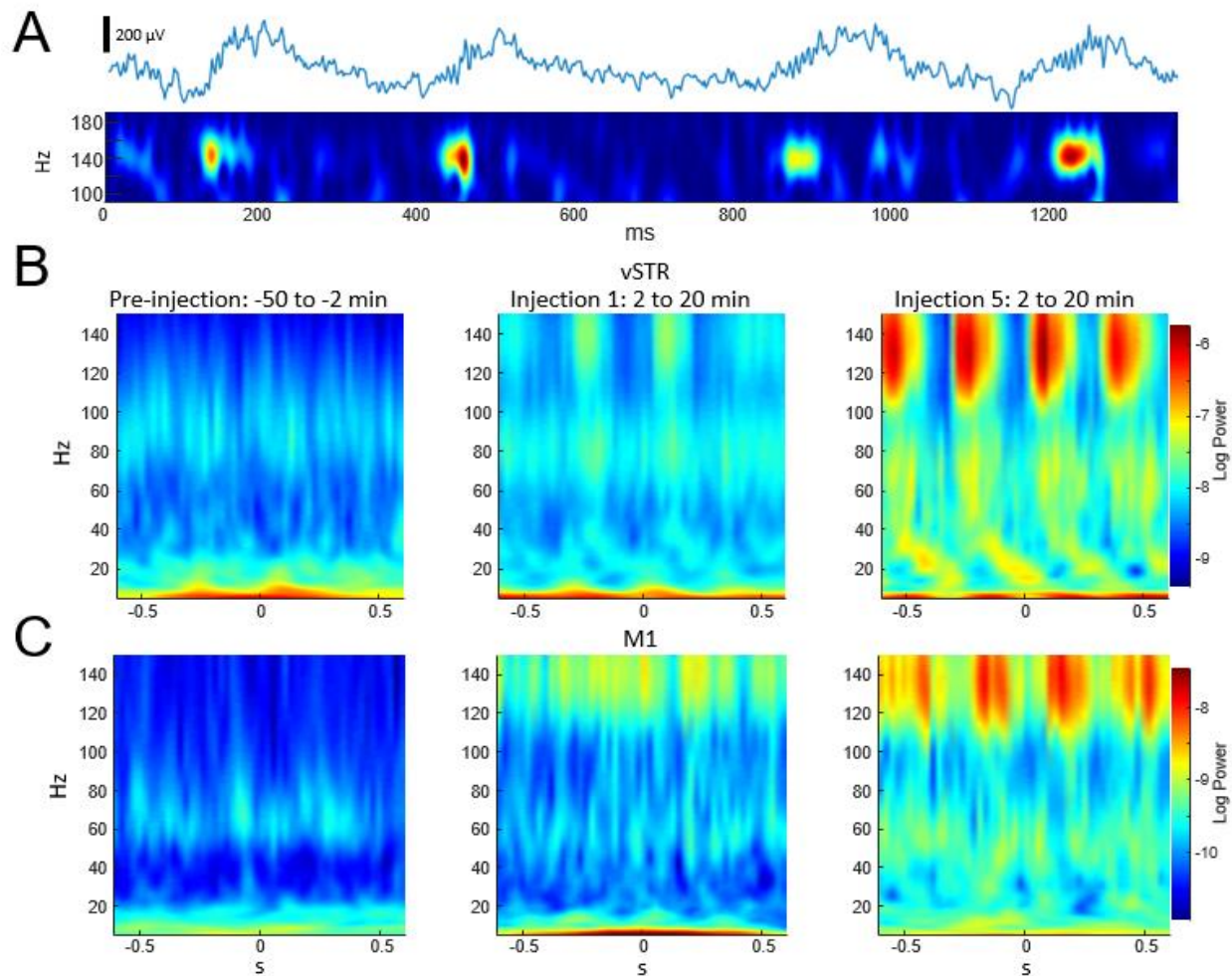


**Figure 6. Examples of cross-frequency coupling following ketamine injections.** (A) The top trace is an unfiltered 2 s representative local-field recording acquired from the vSTR during the 2-20 minute post-injection interval following injection #5. The bottom trace is a wavelet spectrogram of the same signal. The spectrogram highlights the high-frequency (140 Hz) oscillations nested in a slower (~3 Hz) oscillation. (B) Average wavelet spectrogram acquired from the vSTR aligned on the time of the troughs of the slower (1-4 Hz) oscillation for the pre-injection baseline period (first column) and for the 2-20 minute intervals following the first and fifth injections. This example illustrates the capacity of ketamine to enhance CFC. (C) As in B, but for average wavelet spectrogram of M1.

Statistical analyses of the effect of acute and prolonged exposure (from injection 1 to 5) on CFC are summarized in **Figures 7B**. Thick black lines indicate significant differences between saline (gray) and ketamine injection conditions or significant differences between injections 1 (orange) and 5 (blue). ANOVA (drug, frequency) was used to identify main effects and interactions, and result from the ANOVA are presented in **Supplementary Table 1B**. To summarize, main effects and interactions between drug and frequency were observed in M1, dSTR, and vSTR, but not the hippocampus. Post-hoc tests indicated that sub-anesthetic ketamine produced a significant increase in delta-HFO CFC in dSTR and vSTR during the 2-90 minute post-injection interval relative to saline (**Figure 7B**).

### *2.3.f Prolonged Exposure to Ketamine Enhances Cross-Frequency Coupling in the Dorsal Striatum During the 2-90 Minute Post-Injection Period*

Paired comparisons between injections 1 and 5 were performed to determine if extended exposure to ketamine enhanced CFC. Paired comparisons were performed using a within-subject ANOVA (drug, frequency) followed by paired *t*-tests (see **Supplementary Table 1B** for all *F* and *p* values). This analysis revealed that ketamine-induced delta-HFO CFC in dSTR increased from injection 1 to 5 (**Figure 7B**, post-hoc paired *t*-tests  $p = 0.02$ ,  $d = 1.4$ , Holm-Bonferroni corrected). In addition, theta-gamma CFC in dSTR decreased following the first injection ( $p = 0.003$ ); however, this effect was not significant following the 5<sup>th</sup> injection ( $p = 1.0$ , Holm-Bonferroni correction). Paired-comparison plots for delta-HFO CFC for each region are provided in **Supplementary Figure 2**.

These data indicate that prolonged exposure enhances the capacity of ketamine to increase delta-HFO CFC in dSTR; however, analysis of responses during the 92-110 minute post-injection interval did not identify any significant effects (**Figure 7C**). Consequently, the increase in delta-

HFO CFC is likely mediated by ketamine's direct action on corticostriatal receptor systems and not through ketamine's metabolites or through entrained persistent activity.

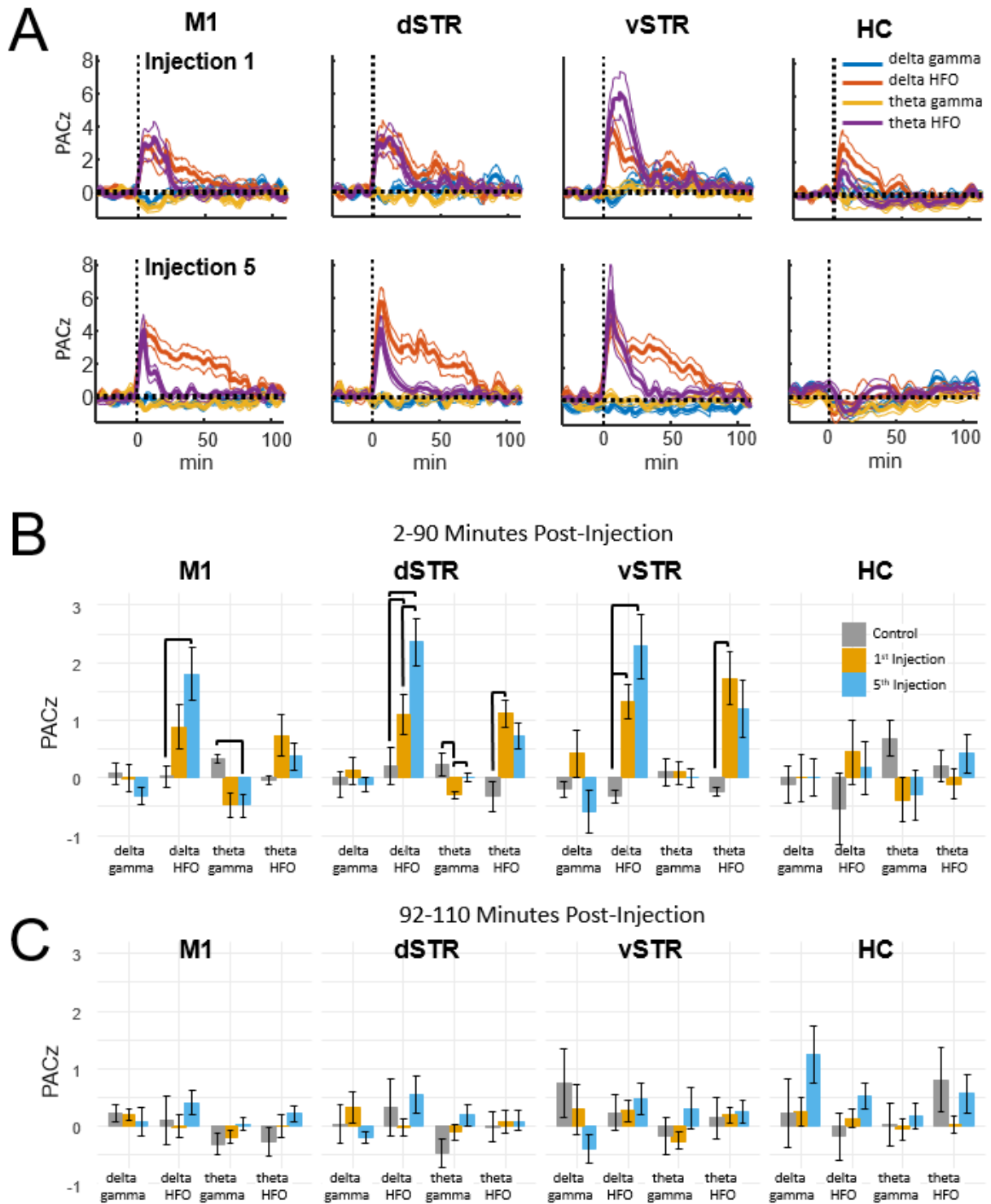


**Figure 7. Ketamine-induced cross-frequency coupling.** (A) The time course of CFC following the first (top row) and fifth (bottom row) ketamine injection (mean,  $\pm$ SEM,  $n = 8$  rats). Ketamine

increased delta-HFO and theta-HFO CFC. Inspection of these responses indicated no delta-gamma and theta-gamma CFC despite strong ketamine-associated gamma oscillations in M1. The duration of delta-HFO CFC appeared to increase from injection 1 to injection 5 in M1, dSTR, and vSTR. **(B)** Comparison of CFC following injections 1 and 5. Mean and  $\pm$ SEM CFC following ketamine and saline injections during the 2-90 minute post-injection period following the first (orange) and fifth (blue) injections. Bold bars indicate significant between-subject differences vs. controls and significant within-subject differences in either the 1<sup>st</sup> or 5<sup>th</sup> ketamine injections (paired *t*-test, Holm-Bonferroni correction). Paired-comparison plots are provided in Supplementary Figure 2. **(C)** As in B, but for the 92-110 minute post-injection period.

### *2.3.g Ketamine-Induced Gamma in M1 and Locomotion Are Reduced by D1R Antagonist SCH-23390*

Experiment 2 investigated whether oscillatory or locomotor activity induced by ketamine was produced by activation of D1 receptors. To test this, ketamine (20 mg/kg, *i.p.*) was administered 15 minutes after the injection of D1R antagonist SCH-23390 (1.0 mg/kg, *i.p.*). The 15-minute interval allowed the D1R antagonist to reach peak blocked of its targets. Spectral responses in **Figure 8A** and **B** show oscillatory responses to ketamine injection when ketamine was delivered either alone or after SCH-23390 injection. We tested the hypothesis that D1R antagonism would reduce ketamine-induced gamma or HFO activity (e.g., **Figure 2A**). Comparison of ketamine to the ketamine + SCH-23390 conditions indicated that SCH-23390 reduced ketamine-induced gamma in M1 ( $p = 0.03$ ,  $n = 6$ , Student's *t*-test with Holm-Bonferroni correction), but SCH-23390 did not alter gamma or HFOs in dSTR, vSTR, or HC (**Figure 8B**). Furthermore, administration of SCH-23390 eliminated ketamine-induced locomotion (**Figure 8D**, Student's *t*-test,  $p = 0.0002$ ). Thus, while M1 gamma produced by ketamine may involve activation of D1 receptors, ketamine's capacity to induce HFOs and gamma in the striatum and hippocampus does not appear to be D1R mediated or the product of locomotion (**Figure 8D**).

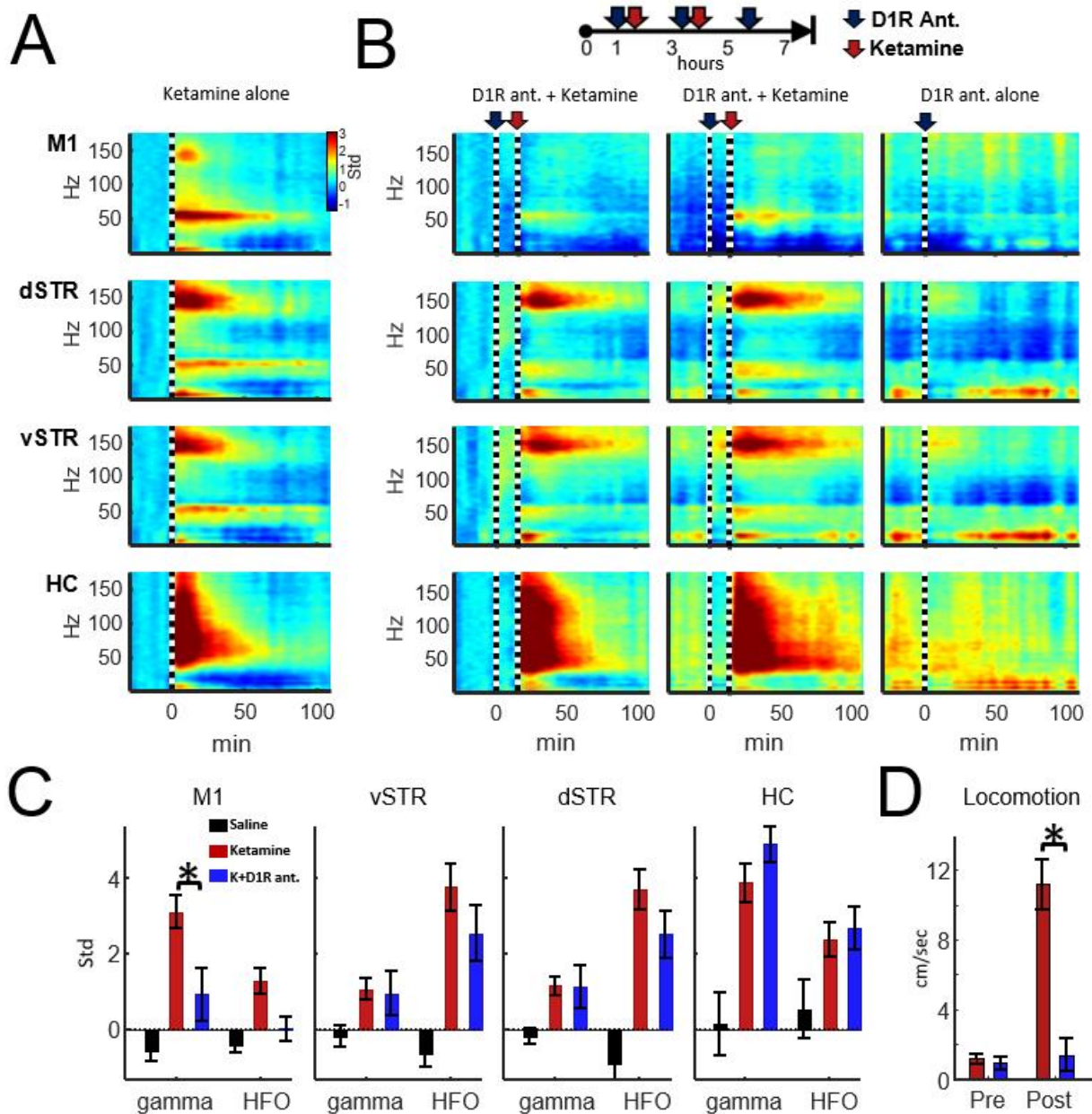


**Figure 8. Ketamine-induced oscillations and movement following D1R antagonism. (A)** Average power spectral responses to a single ketamine injection (20 mg/kg, *i.p.*,  $n = 16$  sessions and 6 rats). **(B) TOP:** Schematic timeline of the injection procedure for pharmacological evaluation of the effects of D1R antagonist SCH-23390 (1.0 mg/kg). **BOTTOM:** The leftmost 2 columns indicate power spectral responses aligned to ketamine injection (20 mg/kg, vertical dashed line) administered 15 minutes after injection of SCH-23390. The last column indicates responses to D1R antagonist delivered alone (no ketamine injection). **(C)** Ketamine-induced gamma oscillations in M1 were reduced when D1Rs were blocked. Ketamine-evoked oscillatory power was measured during the 2-20 minute post-injection period when ketamine was administered alone (red), after SCH-23390 (blue) or after saline injection. Comparisons between ketamine and ketamine + SCH-23390 conditions indicated that SCH-23390 significantly reduced

ketamine-induced gamma and HFOs in M1 ( $p = 0.03$ ,  $n = 6$  rats, Student's  $t$ -test with Holm-Bonferroni correction). **(D)** SCH-23390 eliminated ketamine-induced locomotion during the 2-20 minute post-injection period (Student's  $t$ -test,  $p = 0.0002$ ). Error bars indicate SEM.

## 2.4 DISCUSSION

Although sub-anesthetic infusions of ketamine are increasingly being used to treat chronic pain and treatment-resistant depression, the effects of prolonged exposure on neural synchrony are not understood. Using a spaced-injection procedure, we show that 10-hour exposure enhances ketamine-induced broad-band gamma power in the hippocampus and increases ketamine-associated delta-HFO CFC in the dorsal striatum. These changes were strongest during the 2-90 minute post-injection intervals that followed each of the five successive injections. In motor cortex and striatum, oscillatory activity was indistinguishable from baseline during the 92-110 minute post-injection interval, suggesting that prolonged ketamine exposure potentiates acute responses to ketamine, but does not induce a novel or long-lasting pattern of synchrony that persists beyond ketamine's period of metabolic action in these regions. Furthermore, and contrary to our original hypothesis, prolonged exposure did not increase the strength or extend the duration of ketamine-evoked HFOs in the striatum. In contrast, oscillatory responses in the hippocampus extended to the 92-110 minute post-injection interval. This suggests that processes lasting longer than ketamine's acute action on receptors, such as the activity of ketamine's metabolites (Sleigh et al., 2014; Zanos et al., 2016), could have a stronger impact on hippocampal activity.

Moreover, these data indicate that ketamine's acute effects on neuronal synchrony differ considerably in the cortex, striatum, and hippocampus. For example, where ketamine produced wide-band desynchronized activity in the hippocampus, responses in motor cortex and striatum were more narrow-band. Specifically, ketamine enhanced delta-HFO CFC, narrow-band gamma, and HFO power in motor cortex and striatum. It is therefore conceivable that ketamine exerts

region-specific effects on oscillatory activity that impact the timing of action potentials in cortical, striatal, and limbic circuits involved in motivation and episodic memory formation.

#### *2.4.a Ketamine-Induced Gamma in Motor Cortex*

Injections of ketamine increased gamma power in M1, and this increase lasted for 40-60 minutes following each injection. Gamma oscillations may organize the timing of action potentials (Buzsáki and Wang, 2012; van der Meer and Redish, 2009), which can impact neural plasticity and information transmission between brain regions (Colgin et al., 2009). Although circuit-level mechanisms underlying cortical gamma generation are debated, it is generally believed that interactions between parvalbumin-(PV) expressing GABAergic neurons or interactions between PV neurons and principal cells are involved (Buzsáki and Wang, 2012). Although the mechanisms underlying ketamine-triggered gamma are not well understood, there is evidence that ketamine's action on NMDARs plays a role in gamma generation as administration of selective NMDAR antagonists increase cortical gamma (Pinault, 2008a), and ablation of NMDARs on PV neurons increases gamma (Korotkova et al., 2010). Inactivation of NMDARs by ketamine may preferentially reduce excitation of GABAergic neurons, resulting in the disinhibition of principal cells (Homayoun and Moghaddam, 2007) and consequently increase extracellular glutamate release from principal neurons (Moghaddam et al., 1997). Increased principal neuron activity and glutamate may increase gamma through the activation of metabotropic glutamate receptors (Whittington et al., 1995). Finally, dopamine may be involved in gamma generation in M1 as ketamine-induced locomotion and gamma in M1, but not NAc or HC, were eliminated when ketamine was delivered after administration of a D1R antagonist (**Figure 8**). The absence of an effect of D1R antagonist on ketamine-induced oscillatory activity in NAc is also consistent with a previous investigation of the effects of D1R and D2R antagonists on ketamine-induced oscillatory activity in NAc (Matulewicz et al., 2010).

Ketamine's capacity to enhance M1 gamma suggests that ketamine treatment could impact disorders affecting motor cortex. In this regard, there is evidence that ketamine reduces LID in Parkinson's patients and in animal models of Parkinson's disease (Bartlett et al., 2016; Sherman et al., 2016a), with LID being associated with high-frequency cortical gamma (~80 Hz) (Dupre et al., 2016; Halje et al., 2012b; Swann et al., 2016). This is interesting as ketamine-induced gamma is about 30 Hz slower than the high gamma associated with LID. This large difference in frequencies suggests that in ketamine-induced and LID-associated gamma are produced by distinct circuits. Conceivably, these circuits could interfere with each other when simultaneously activated resulting in reduced LID. Future single-unit studies using animal models of LID could investigate whether cortical circuits generating low and high gamma are distinct and interfere with each other in LID. Patients with PTSD also experience increased high-gamma activity in resting-state networks (Dunkley et al., 2014), and PTSD patients can respond positively to ketamine treatment (Feder et al., 2014). Consequently, it is conceivable that interactions between distinct gamma circuits could mediate ketamine's impact on these conditions.

#### *2.4.b Cross-Frequency Coupling and Hfos in Corticostriatal Circuits*

Cross-frequency coupling may facilitate memory encoding and retrieval, and the transfer of information between brain regions (Canolty and Knight, 2010). Aberrant CFC is also implicated in schizophrenia (Allen et al., 2011) and Parkinson's disease (Belić et al., 2016). Consistent with other reports, we observed that sub-anesthetic ketamine triggers HFOs in the striatum and delta-HFO and theta-HFO CFC in dSTR and vSTR (Cordon et al., 2015). Furthermore, prolonged exposure enhances the duration of delta-HFO CFC in dSTR (**Figure 7**). The mechanisms that produce striatal HFOs and delta-HFO coupling are not understood; however, the generator of HFOs may originate in the NAc as inactivation of the NAc with

tetrodotoxin abolishes ketamine-induced HFOs (Olszewski et al., 2013). The locus and mechanism of striatal delta oscillations are less well understood. Delta is typically associated with slow-wave sleep and is thought to be generated by cortical and thalamic circuits (Amzica and Steriade, 1995; Lőrincz et al., 2015). Delta during sleep organizes the timing of thalamocortical sleep spindles (8-15 Hz) and hippocampal sharp-wave ripples (~150 Hz), two oscillations that are associated with memory consolidation (Reviewed in Mölle and Born, 2011). In contrast to sleep-associated delta, the delta-HFO activity that was observed in the present study occurred during waking locomotion, indicating that this form of delta differs from slow-wave sleep-associated delta. Delta in waking rats has been observed in the ventral tegmental area (VTA) and the prefrontal cortex, and this delta activity emerged when rats performed a spatial working-memory task (Fujisawa and Buzsáki, 2011). Future studies involving inactivation of VTA or prefrontal cortex following ketamine administration could determine if ketamine-induced delta-HFO CFC is produced by the prefrontal cortex or the VTA.

#### *2.4.c Ketamine Induces Broad-Band Gamma and Persistent Activity in the Hippocampus*

The hippocampus plays a central role in the consolidation of episodic memory and in the processing of configurations of items in space and in time. Hippocampal dysfunction is also associated with major depression (Schmaal et al., 2016) and PTSD (Dunkley et al., 2014). Notably, these two disorders can be treated with low-dose ketamine infusion (Berman et al., 2000; Diamond et al., 2014; Feder et al., 2014). There is evidence that narrow band low- and high-gamma can differentially direct the flow of signals through intra-hippocampal pathways in order to support memory recall and encoding (Colgin et al., 2009). We observed that ketamine injections produced wide-band gamma (> 30 Hz, **Figure 2**) during the 2-90 minute post-injection interval. Such a response could interfere with the low- and high-gamma oscillations associated

with memory storage and retrieval. This wide-band signal could also contribute to the observed reduction in CFC (**Figure 7**) in the hippocampus, a result that is in accord with predictions from computational modelling (Neymotin et al., 2011). The observed reduction in hippocampal CFC following ketamine injection is also consistent with experimental work where NMDAR ablation in CA1 reduces theta-gamma CFC in behaving mice (Korotkova et al., 2010).

The effects of acute low-dose ketamine exposure on neuronal synchrony suggest that ketamine exposure would reduce memory performance. Indeed, low-dose ketamine injections do impair spatial memory in an 8-arm maze during encoding and retrieval phases (Chrobak et al., 2008). Such impairment could result from the absence of a distinct gamma oscillation to organize the timing of action potentials. Reduced precision of action-potential timing along with ketamine-mediated NMDAR blockade could ultimately disrupt plasticity. It is interesting to consider that disorganized broad-band activity could have a beneficial effect by potentially “resetting” aberrant synaptic connectivity within the hippocampus that contributes to depression and PTSD.

Although our data did not identify CFC in the hippocampus, experimental work by Caixeta et al., (2013) indicates that moderate-to-high doses of ketamine (25-75 mg/kg) do increase hippocampal theta-HFO and theta-gamma CFC. Potential reasons for this difference include the larger ketamine doses used in the Caixeta study, and the use of high-density linear electrode arrays that allowed identification of layer-specific gamma generators. In contrast, our paired-electrode recordings measured signals from a larger hippocampal volume. Consequently, it is conceivable that the broad-band activity observed in our study reflects the integrated activity of

multiple distinct hippocampal gamma generators. Future experiments using high-density electrode arrays would resolve this issue.

A final interesting feature of the hippocampal response to ketamine was that, unlike motor cortex and striatum, some ketamine-induced oscillations in the hippocampus (e.g., delta and HFO) persisted into the 92-110 minute post-injection interval (**Figure 3B**). This suggests that ketamine's effect on memory consolidation and spatial information processing may last longer than its effects on motor and reinforcement-driven behaviors.

#### *2.4.d Ketamine's Effect on Oscillatory Power and Cross-Frequency Coupling was Restricted to the 2-90 Minute Post-Injection Interval*

Although low-dose ketamine significantly affected corticostriatal synchrony and CFC during the 2-90 minute post-injection period, these effects were largely indistinguishable from baseline during the 92-110 minute post-injection intervals (**Figures 3B, 7C**). This was surprising as ketamine infusions in human patients can produce week-to-month long reduction in depressive symptoms in patients with treatment-resistant depression (Berman et al., 2000; Diamond et al., 2014). One explanation for the time-limited response is that ketamine initiates the gradual synaptic reorganization of circuits involved in the pathology (Phoumthippavong et al., 2016b). Such reorganization may be facilitated by ketamine-induced gamma synchrony as gamma can enhance neuronal plasticity by synchronizing the timing of action potentials in pre- and post-synaptic neurons (Hasenstaub et al., 2016). Synaptic reorganization may be further facilitated by ketamine's capacity to increase BDNF production (Yang et al., 2013) and spine density in the medial frontal cortex (Phoumthippavong et al., 2016b).

#### *2.4.e Conclusion*

Our data demonstrate that 10-hour ketamine exposure produces desynchronized broadband gamma in the hippocampus and increases delta-HFO CFC in the dorsal striatum. Although single injections triggered strong HFOs and gamma in the striatum, these responses were not enhanced by prolonged ketamine exposure. The observation that prolonged exposure increased delta-HFO CFC in dorsal striatum indicates that extended exposure enhances coordination between striatal neurons and possibly facilitates spike-timing dependent plasticity and inter-regional communication. In contrast, we observed that ketamine-induced oscillations in the hippocampus were decidedly broadband, a result that suggests widespread desynchronization. Such broadband “noise” in the hippocampus could negatively affect coordination between neurons and reduce the strength of associative networks within the hippocampus. However, such disruptive effects could have positive implications if these associative networks contribute to pathologies such as depression and PTSD. An important next step is to determine if ketamine differentially alters coordination between neurons in cortical, striatal, and hippocampal circuits through single-unit ensemble recordings. Furthermore, combining ensemble recordings with animal models of PTSD, chronic pain, depression, and LID could identify circuit-level changes that underlie ketamine’s therapeutic effectiveness.

## **Chapter 3: Experimental Aims for Repeated Ketamine Exposure in Animal Models of Movement Disorders**

Our report naïve animals (Chapter 2) was the first set of published findings on the effects of prolonged ketamine in naïve animals. We observed that repeated low-dose ketamine exposure does not enhance HFOs in corticostriatal circuits, instead, enhances coordination between low and high frequencies in the striatum. This increased striatal CFC may facilitate spike-timing dependent plasticity, resulting in lasting changes in motor activity. In contrast, the observed wide-band high-frequency “noise” in the hippocampus suggests that ketamine disrupts action-potential timing and reorganizes connectivity in this region. Differential restructuring of corticostriatal and limbic circuits may contribute to ketamine’s clinical benefits. These findings provided new questions on the effects of repeated low-dose ketamine on neural oscillations in the diseased brain. The following are a set of specific aims guiding the next series of experiments using an animal model of Parkinson’s disease and LID.

### **3.1 Aim 1: Does Repeated Ketamine Reduce Pathological Beta Oscillations in an Animal Model of Parkinson’s Disease?**

Currently the most effective non-pharmacological treatment for PD is deep-brain stimulation (DBS). The STN is stimulated at ~140 Hz resulting in decreased beta and replaced by gamma-theta synchronization (Brittain and Brown, 2014), suggesting that DBS alters the relationship between pathological beta and pro-kinetic gamma in the motor cortex of PD patients (de Hemptinne et al., 2015b). Reports using single-dose ketamine administration in healthy rats show that ketamine triggers HFOs (>100 Hz) and low-gamma (~50 Hz) in the STR and cortex (Nicolás et al., 2011). Similarly, sub-anesthetic doses of ketamine in healthy human subjects also increased gamma (~50 Hz) in the cortical motor areas (Muthukumaraswamy et al., 2015a).

Therefore, **Aim 1** will assess ketamine's capacity to reduce hypersynchronous beta oscillations across the STR (e.g., dorsolateral (DLS), dorsomedial (DMS), nucleus accumbens (NAc)) and M1 using an animal model of PD.

Cross-frequency coupling (CFC) is another metric of coordinated activity. CFC measures how the amplitude of a high-frequency oscillation occurs at a particular phase of a low-frequency oscillation. Recently, our lab has shown ketamine-induced increases in low-gamma across multiple cortical, striatal, and hippocampal regions but no gamma CFC with other frequency bands (manuscript under review). This suggests that increases in oscillatory power does not necessarily imply an increase in synchronous activity. **Aim 1** will further assess ketamine's impact on CFC in PD.

Using the identical injection protocol to mimic clinical infusions as Bartlett and colleagues (2016), LFP activity will be simultaneously recorded in the corticostriatal circuit of the lesioned (i.e., dopamine-depleted) hemisphere during repeated exposure to sub-anesthetic ketamine across an 11-hr period. *I hypothesize that repeated sub-anesthetic ketamine will reduce hypersynchronous beta in the 6-OHDA-lesioned animal.* Given the similar oscillatory effects of DBS and ketamine on these cortical and subcortical regions, it is conceivable that ketamine may also alter inter-region communication and reducing hypersynchronous activity associated with PD. This may serve as a possible mechanism for ketamine's long-term structural changes and leading to gradual synaptic reorganization (Phoumthippavong et al., 2016b).

### **3.2 Aim 2a: Does Repeated Ketamine Exposure Reduce L-DOPA-Triggered Focal 80 Hz High-Gamma?**

Clinical retrospective case-reports and pre-clinical evidence suggest sub-anesthetic ketamine may reduce LID. However, the specific mechanism underlying its therapeutic efficacy remains unknown. Forming a clear understanding at the cellular- and systems-level is important in order to progress ketamine into controlled clinical trials and facilitate specific drug subtypes to further its efficacy.

Several groups have demonstrated that the oscillatory signature of LID to be a focal high-gamma oscillation (~80 Hz) in the motor cortex and in the DLS (Dupre et al., 2016; Halje et al., 2012b). Evidence from our collaborators convincingly show that repeated exposure to sub-anesthetic ketamine leads to a long-term reduction of LID symptoms (Bartlett et al., 2016; Sherman, 2016). However, the oscillatory actions during such ketamine exposure is unclear. Therefore, **Aim 2a** will examine ketamine's capacity to alter LID-associated high-gamma (80 Hz) in M1 and DLS. I hypothesize that chronic exposure to sub-anesthetic ketamine will reduce this specific range of high-gamma. It is conceivable that this interaction leads to the reduction of dyskinesia (i.e., AIMs) (Bartlett et al., 2016). Evidence supports NMDA receptor antagonism (e.g., dextrorphan, dextromethorphan) to suppress AIMs (Jenner, 2008). Such NMDA antagonists act selectively and effectively on the NR2B subunits of the receptor, and these subunits are abundant in the cortex and striatum (Goebel and Poosch, 1999; Jenner, 2008; Mutel et al., 1998). Given that ketamine acts on the NR2B subunit (among others), this may be a potential mechanism of dyskinesia suppression. Furthermore, ketamine-induced gamma is slower (~50 Hz peak) than LID-associated gamma (80 Hz), suggesting a difference in circuitry of gamma generators (e.g., interneuron-interneuron vs pyramidal-interneuron networks). It is

therefore conceivable that these distinct circuits may interfere with each other to result in reduced LID. As in Aim 1, the repeated injections protocol will be used with the identical dose of sub-anesthetic ketamine (20 mg/kg).

### **3.3 Aim 2b: Does Repeated Ketamine Exposure Reduce L-DOPA-Triggered Wide-Band Gamma?**

Preliminary evidence from the current experiments has rejected Aim 2a (above). Our hypothesis that ketamine would reduce LID-associated 80 Hz gamma was untestable as we failed to replicate this oscillatory response in our LID animals. *However, we did observe a novel finding that these animals displayed a wide-band gamma (40 - 85 Hz) response after L-DOPA, instead of a focal 80 Hz.* To our knowledge, there is no published data to in the LID literature that deviates from the focal 80 Hz gamma. Given that the published behavioral evidence from our colleagues (Bartlett et al., 2016) showing this identical experimental protocol reduces dyskinesia, our preliminary results warrants further investigation. Therefore, **Aim 2b** will explore ketamine's capacity to alter L-DOPA-induced hypersynchronous broad-band gamma that may underlie the reduction of dyskinesia (Bartlett et al., 2016).

LID is thought to be the result of abnormal plasticity in the striatum (Cenci and Konradi, 2010). To our knowledge, there is only one published report that investigated CFC in LID animals and unexpectedly found decreased coupling between LID-induced high-gamma (80 Hz) and low frequencies (up to 10 Hz) (Belić et al., 2016). Given our novel finding of LID-induced broad-band gamma, CFC analysis may also reveal changes in network-level communication between neural ensembles in the corticostriatal circuit of LID during co-administration of ketamine + L-DOPA.

*Therefore, I hypothesize that sub-anesthetic doses of ketamine will reduce LID-associated broad-band gamma and CFC in the corticostriatal circuit.* The reduction in broad-band gamma CFC may underlie ketamine's long-term structural changes and gradual synaptic reorganization (Phoumthippavong et al., 2016b) that leads to the long-term reduction of LID (Bartlett et al., 2016; Sherman et al., 2016b).

### **3.4 Aim 2c: Are Opioid-, D1-, or D2-Receptors Involved in Ketamine-Induced Oscillations in LID Animals?**

LID-induced high-gamma is thought to be generated by stimulating dopamine D1 and D2 receptor activation. Ketamine-induced low-gamma is not affected by D1 receptor blockage in healthy rats (manuscript under review) and is thought to be due to NMDA receptor antagonism (Hakami et al., 2009). However, ketamine is also a partial agonist for D2 receptors, suggesting potential involvement in gamma generation. Thus, **Aim 2c** will use dopaminergic pharmacological manipulations (e.g., D1-receptor antagonist SCH23390, D2-receptor antagonist Eticlopride) to investigate the mechanisms of ketamine-induced oscillatory activity in LID animals.

Other non-dopaminergic systems, such as the opioid system, are also thought to contribute to LID. The basal ganglia is rich in endogenous opioid peptides and receptors (Hadjiconstantinou and Neff, 2011) and abnormal increases in opioid signaling have been found in patients with LID (Aubert et al., 2007; Calon et al., 2002). The enkephalin family of endogenous opioid peptides are expressed in striatal medium spiny neurons (MSNs) (i.e., inhibitory interneurons) and act as co-transmitters for these GABAergic cells (Gerfen, 1992). This suggests that opioids may play a role in regulating interneuron-network gamma oscillations.

Ketamine is also an opioid receptor agonist with a high affinity akin to NMDA receptors (Finck and Ngai, 1982; Gupta et al., 2011). Stimulating opioid receptors on these MSNs effectively inhibits interneuron activity and in turn may regulate the broad-band gamma observed in LID.

Given that ketamine is an opioid agonist and opioid agonism may potentially be anti-dyskinetic, this suggests that one of ketamine's mechanisms in reducing LID and its associated broad-band gamma may be its action on opioid receptors. Therefore, **Aim 2c** will also use an opioid pharmacological manipulation (e.g., a multi-opioid receptor antagonist Naloxone) to probe this potential mechanism. *I hypothesize that blocking ketamine's action on opioid receptors in LID will increase LID-associated high-gamma, suggesting that opioid receptors play a role in regulating striatal MSN gamma generation.*

# **Chapter 4: Experiment 1: Investigating The Effects of Ketamine-Induced Oscillatory Activity in an Animal Model of Parkinson's Disease and L-DOPA-Induced Dyskinesia**

## **4.1 Animals**

Sprague-Dawley rats (250g upon arrival; Envigo, Indianapolis, IN) were used. Upon arrival to the facility, animals were housed individually in a climate controlled 12-hour reverse light/dark cycle. Lights off from 9AM-9PM. Food and water were available *ad libitum*. Multiple stages are involved for each rat prior to neural data collection. Briefly, rats are subjected to the first surgical procedure to induce the animal model of Parkinson's disease via 6-hydroxydopamine lesions. Quantification of lesion (i.e., amphetamine rotation tests) commenced after 1-week recovery from surgery. Lesioned animals are then primed with L-DOPA (7 mg/kg) daily for 21 days followed by behavioral quantification for degree of AIMs to qualify animals in the LID group. Maintenance injections of L-DOPA (7 mg/kg) are administered to these animals every 2-3 days to preserve dyskinesia. LID animals are then subjected to a second surgical procedure (i.e., electrode implantation) followed by 1-week recovery before data collection begins. All procedures are in accordance with the Institution for Animal Care and Use Committee at The University of Arizona.

## 4.2 Surgery 1: Unilateral 6-OHDA Lesion

Rats were anesthetized with isoflurane and intracranially injected with 6-hydroxydopamine hydrochloride (5.0  $\mu\text{g}/\mu\text{l}$  in 0.9% sterile saline with 0.02% ascorbic acid; Sigma-Aldrich, St. Louis, MO, USA) in the medial forebrain bundle (right hemisphere). Rats were pretreated with desipramine hydrochloride (12.5 mg/kg; Sigma-Aldrich) intraperitoneally (*i.p.*) prior to 6-OHDA injection to protect noradrenergic neurons.

## 4.3 Amphetamine-Induced Rotations

After 1-week recovery, the degree of the lesion was behaviorally quantified via amphetamine rotation tests. 6-OHDA-lesioned rats were injected with amphetamine (5.0 mg/kg, *i.p.*) to induce asymmetrical dopamine release. The number of ipsiversive rotations were counted for a total of 60 min after injection. Two weeks after surgery, rats that exhibited  $\geq 5$  full turns/min ipsilateral to the lesioned hemisphere were selected for the next stages of the experiment. These rats either advanced directly to Surgery 2 (i.e., 6-OHDA group) or to L-DOPA priming to induce LID (i.e., LID group). The number of rotations corresponds to the degree of dopamine depletion in the striatum  $>90\%$  (DeKundy et al., 2007).

## 4.4 Induction of L-DOPA-Induced Dyskinesia in Unilateral Lesioned Rats

6-OHDA-lesioned rats in the LID group were treated daily with L-DOPA (7 mg/kg + 14 mg/kg benserazide) for 21 days (*i.p.*). LID symptoms manifest as Abnormal Involuntary Movements (AIMs). The degree of Limb, Axial, and Orolingual (LAO) AIMs were scored by an

experimentally blinded investigator on a scale of 0 (absent) to 4 (most severe) (Dekundy et al., 2007). Rats with an average cumulative LAO scores of  $33.6 \pm 6.6$  (mean  $\pm$  S.D.) are considered mild to moderately dyskinetic (Bartlett et al., 2016) and advanced to Surgery 2 for electrode array implantation (**Table 1**).

**Table 1**  
Amphetamine-induced rotation and AIMs scores.

|                       | Ipsiversive Rotations<br>(Mean $\pm$ S.D.) | AIMs Scores<br>(Mean $\pm$ S.D.) |
|-----------------------|--|----------------------------------|
| 6-OHDA-lesioned Group | $7.88 \pm 1.01$                            | N/A                              |
| LID Group             | $7.10 \pm 3.02$                            | $33.6 \pm 6.6$                   |

**Table 1. Scores for amphetamine-induced rotation and AIMs tests.** All 6-OHDA-lesioned animals ( $N=14$ ) underwent amphetamine-induced rotation tests, while only the animals treated with L-DOPA (LID group,  $n=7$ ) were tested for AIMs. Mean ipsiversive rotations and standard deviation are shown.

## 4.5 Surgery 2: Electrode Implantation

Rats were be anesthetized with isoflurane and underwent stereotactic implantation of a custom-made 32-channel electrode array that housed 16 stereotrodes (California Fine Wire Co., Grover Beach, CA). A skull screw over cerebellum was reference and ground. The electrode array was centered at AP: +1.3, ML: +2.7, right hemisphere, with stereotrodes targeting M1 (DV: -1.4), dorsolateral striatum (DLS, DV: -3.8), dorsomedial striatum (DMS, DV: -4.6), and nucleus accumbens (NAc, DV: -6.8, **Figure 9B, center**).

Electrodes were secured into position using cyanoacrylate (Slo-Zap) and the entire implant will be cemented in dental acrylic. The naïve control group of animals began with surgical procedure 1-week after arrival as 6-OHDA lesioning and LID induction are not required.

Rats recovered for 1 week post-surgery. Animals were provided with post-operative analgesia. Carprofen (Zoetis, Parsippany, NJ) was delivered (5 mg/kg, *s.c.*) for 48 hours following surgery. Topical anti-biotic ointment (Water-Jel Technologies, Carlstadt, NJ) was applied to the incisional site for up to 5 days as needed. Sulfamethoxazol and Trimethoprim (Hi-tech Pharmacal Co., Inc., Amityville, NY) was administered orally (15 mg/kg) daily until conclusion of experiments.

## 4.6 Drug Treatments

On a given experimental session during Experiment 1, animals received a total of five injections of ketamine (20 mg/kg, *i.p.*) or saline injections with injections occurring every 2 hours as described in (Bartlett et al., 2016) and summarized in **Figure 9A**. This paradigm is identical to that used by Bartlett and colleagues (2016) to model clinical infusions in rodents, and it was chosen as it has been shown to reduce levodopa-induced dyskinesia (LID) (Bartlett et al.,

2016). Multiple injections ensured that serum concentrations of ketamine remained high throughout exposure. The 2-hour spacing between injections was important given the faster metabolism of ketamine in rodents (~ 1 hour, (Páleníček et al., 2011; Veilleux-Lemieux et al., 2013)) relative to humans (~3 hours (Clements et al., 1982)). Recording sessions involved injections of either ketamine hydrochloride (20 mg/kg, Clipper Distributing, St. Joseph, MO) or 0.9% saline. Each animal underwent one saline injection session and three ketamine sessions. These sessions were each separated by 1 week.

## 4.7 Neurophysiological Recordings and Timeline

Recordings (KJE-1001, Amplipex Ltd) were conducted with rats in a polycarbonate home cage (45cm x 23cm). A light-emitting diode (LED) light affixed to the rat's implant was used for motion tracking from an overhead USB camera (Manta G-033C, Allied Vision, Exton, PA). A digitizing headstage was connected to the animal with the signal sent to the recording system via a lightweight custom-made tether and commutator. Recording sessions were conducted once per week for each animal beginning at 5AM (as in **Figure 9A**). Animals and their home cage were transported to the recording room and remained in the home cage during neural recordings with food and water available *ad libitum*.

Each recording session began with a 1-hr baseline. At the second hour, a single injection of sub-anesthetic ketamine (20 mg/kg, *i.p.*) was administered, followed by another injection every two hours for a total of five injections over an 11-hr recording session (**Figure 9A**). This injection protocol is identical to Bartlett and colleagues (2016) to model clinical infusions in rats. Each rat undergoes one recording session on the same day each week beginning at 5AM. A total

of three ketamine sessions and one saline (SAL) session (counterbalanced) will be completed for each rat before advancing to Experiment 2.

# **Chapter 5: Experiment 2: Investigating the Contribution of Opioid-, Dopamine D1- and D2-Receptors in Ketamine-Induced Oscillations**

## **5.1 Drug Treatments**

After the completion of Experiment 1, LID animals were used for a second experiment (Experiment 2). Administration of a receptor antagonist in ketamine-induced oscillatory activity in LID was investigated. In this experiment rats received injections of a L-DOPA (7 mg/kg), ketamine (20 mg/kg), along with a co-injection of either an opioid antagonist (Naloxone, 0.9 mg/kg, Tocris Bioscience, Minneapolis, MN), D1-antagonist (SCH-23390, 1 mg/kg, Tocris Bioscience, Minneapolis, MN), or D2-antagonist (Eticlopride, 0.1 mg/kg, Tocris Bioscience, Minneapolis, MN). Each session began with a 1-hr baseline. A single injection of drug antagonist was administered followed by a co-injection of L-DOPA + ketamine 15 min after. This procedure was repeated again after 2 hrs minus the L-DOPA injection.

## **5.2 Neurophysiological Recordings and Timeline**

Recording equipment and apparatus for Experiment 2 are identical to Experiment 1. Each recording session began with a 1-hr baseline. At the second hour, a single injection (*i.p.*) of an antagonist drug (e.g., SCH-23390, 1.0 mg/kg; Eticlopride, 0.1 mg/kg; or Naloxone, 0.9 mg/kg) was administered along with a single injection of sub-anesthetic ketamine (20 mg/kg, *i.p.*) after 15 min. This antagonist + ketamine injection pair was repeated after two hours. And after another two hours, a single injection of the same antagonist drug was given. The 15 min spacing

between antagonist and ketamine was chosen to ensure onset of antagonist action upon ketamine administration (Andersen and Gronvald, 1986; Martelle and Nader, 2008).

### **5.3 Histology: Nissl Staining**

Upon completion of Experiment 2, electrolytic lesions were produced at the electrode's recording sites via direct current stimulation (20mA for 2 seconds). After 72 hours rats were deeply anesthetized with Euthasol (0.35 mg/kg, *i.p.*; Virbac, Fort Worth, TX) and sacrificed with Euthasol (0.35 mg/kg, *i.p.*; Virbac, Fort Worth, TX). Brains were immediately extracted via transcardial perfusion using phosphate buffered saline (PBS) and 4% paraformaldehyde. Tissue was prepared into 40- $\mu$ M thick coronal sections using a frozen microtome. Tissue sections were then Nissl stained for verification of electrode placement (**Figure 9B, center**). This procedure was performed for all three animal groups.

### **5.4 Immunohistochemistry: Tyrosine Hydroxylase Staining**

For the 6-OHDA-lesioned and LID groups, additional verification of dopaminergic cell loss was required. Tyrosine hydroxylase (TH) is an enzyme that initiates a series of downstream enzymatic reactions that ultimately converts L-tyrosine to the neurotransmitter DA. Staining for TH is a standard biomarker for the identification of DA neurons. Therefore, approximately 30% of the 6-OHDA and LID group's tissue samples were immunostained for TH. A representative example of an intact vs. DA-depleted striatum from this experiment is shown in **Figure 9B (right)**.

## Chapter 6: Data Analysis

Analysis was performed using custom-written code (MATLAB: MathWorks Inc., Natick, MA). Neurophysiological signals were acquired at 20,000 Hz and down-sampled to 500 Hz. Periods where the signal either exceeds 1.5 mV or when summed cross-band power (2-160 Hz) exceeds 99.98<sup>th</sup> percentile will be considered artifact and excluded from analysis. Volume conduction occurs when an LFP signal from one region is contaminated by signals from other regions, and raises concerns for interpreting LFP data. To address this issue, the measured signal from a particular region was referenced to a second electrode 0.7 mm away in the identical region and depth. The effects of re-referencing signals varied by region, a representative example on power-spectral responses is presented in **Figure 9C**.

### 6.1 Spectral Power

Spectral power across frequency bands was determined using a fast Fourier transform spectrogram (frequency bin = 0.5 Hz, 10-second Hanning window, spectrogram() in Matlab). Statistical analysis of oscillatory power was restricted to the following frequency bands: theta (4 - 10 Hz), beta (15 - 30 Hz), low-gamma (35 - 58 Hz), high-gamma (70 - 85 Hz), wide-band gamma (40 - 85 Hz) and HFO (120 - 160 Hz). All data were normalized to baseline unless otherwise noted. The baseline period was defined as the -32 to -2 minute interval preceding the first injection of each recording session.

## **6.2 Cross-Frequency Coupling**

Phase-amplitude cross-frequency coupling (PAC) was measured as described in Cohen (2014). The chosen low- and high- frequency bands were filtered using a Butterworth infinite impulse response (IIR) filter ( $fs=500$  Hz, filter order = 6). A Hilbert transform was used to extract the phase of the low frequency and the envelope of the absolute value of the filtered signal was used to extract the power of the high frequency. A randomized shuffle control was then used to compare these values such that the original low-frequency signal was randomly shifted in time on 200 permutations. The mean and standard deviation of this null hypothesis were used to convert the measured PAC score into a Z-score (PAC-Z).

## **6.3 Statistical Analyses**

All statistical analyses were performed using custom-written code on Matlab. Statistical significance was assessed using ANOVA or Student's *t*-test ( $\alpha = 0.05$ ). The Tukey-Kramer correction method was used to adjust p values for post-hoc comparisons unless otherwise noted.

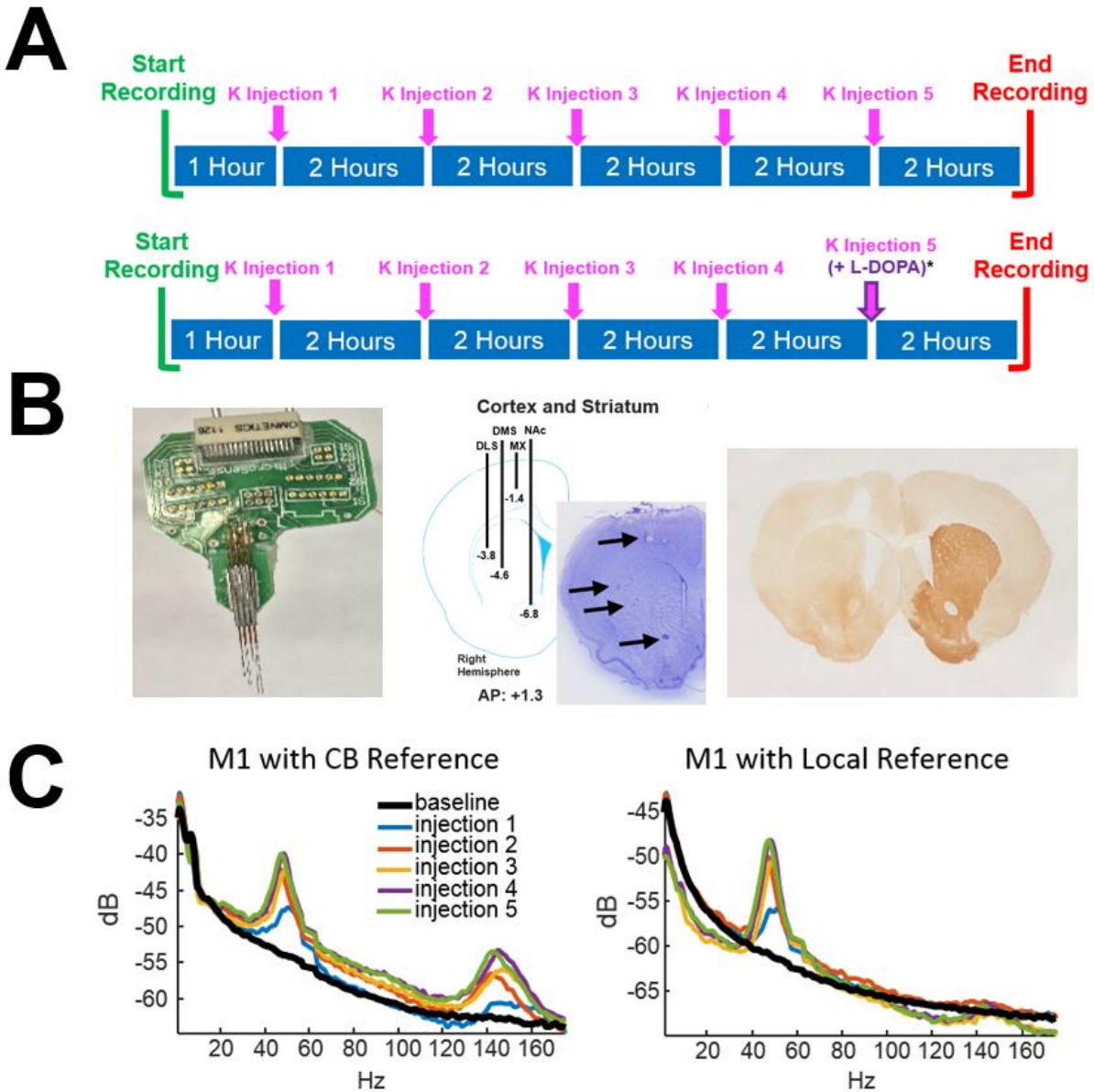


**Figure 9. Experimental design and neural recordings.** (A) TOP: Timeline of a single experimental session for naïve and 6-OHDA-lesioned animals. Each session began with one hour of pre-injection baseline. At the 2<sup>nd</sup> hour, a single injection of sub-anesthetic ketamine (20 mg/kg, *i.p.*) or saline was administered and repeated every 2 hours for a total of 5 injections across each 11+ hour session. BOTTOM: Timeline of a single experimental session for animals with L-DOPA-induced dyskinesia (LID). This experimental protocol is identical to the naïve/6-OHDA groups with the exception of a co-injection of L-DOPA (7 mg/kg, *i.p.*) with ketamine on the 5<sup>th</sup> injection. Each animal received a single ketamine or saline injection recording session each week. (B) LEFT: A custom-made 32-channel electrode surgically implanted into the right

hemisphere of all experimental animals. CENTER: Schematic of electrode array placement (AP: +1.3, ML: +2.7 centered, DV: -6.8 deepest electrode) and representative example of histological verification of targets. RIGHT: Verification of 6-OHDA lesioning in 6-OHDA and LID animals via tyrosine-hydroxylase staining. Expression of tyrosine-hydroxylase (dark pigmentation; left hemisphere) is a marker of functioning dopaminergic neurons. Validation of a successful (>90%) 6-OHDA lesion results in a light pigmentation of the striatum (right hemisphere). (C) Local-field electrodes were re-referenced to electrodes within-region electrodes to reduce signal contamination from volume conduction. LEFT: A representative LFP signal from the motor cortex originally referenced to the cerebellum (CB) shows ketamine-induced gamma and HFO activity. RIGHT: HFO activity was eliminated when referencing to another motor cortex electrode (~700uM apart), suggesting the HFOs were volume conducted.

## Chapter 7: AIM 1: Increased Baseline Beta Power in 6-OHDA-Lesioned and LID Animals Compared to Naïve

Increased beta oscillations (15 – 30 Hz) in M1 is a signature of Parkinson's disease in both human patients and animals models. In addition to amphetamine rotation tests and post-mortem histological verification of a DA-lesioned striatum, we examined baseline oscillatory activity in M1 of our 6-OHDA, LID, and naïve control animals (**Figure 10A**). As expected, we observed significant differences in beta power (ANOVA,  $F(2,18)=7.71$ ,  $p=0.004$ ). Post-hoc comparisons (Tukey-Kramer corrected t-tests) revealed both the 6-OHDA ( $p=0.002$ ,  $n=7$ ) and LID groups ( $p=0.04$ ,  $n=7$ ) had significantly greater mean beta power compared to naïve controls (**Figure 10D**). This frequency range was not statistically different between 6-OHDA and LID animals ( $p=0.11$ ). In the DLS, beta power was not statistically different between any of the groups (ANOVA,  $F(2,18)=1.21$ ,  $p=0.13$ ) (**Figure 10C**), suggesting increased beta of lesioned animals are only present in M1 rather than the DLS. The results from M1 validate our animal models of Parkinson's disease and L-Dopa-induced dyskinesia.

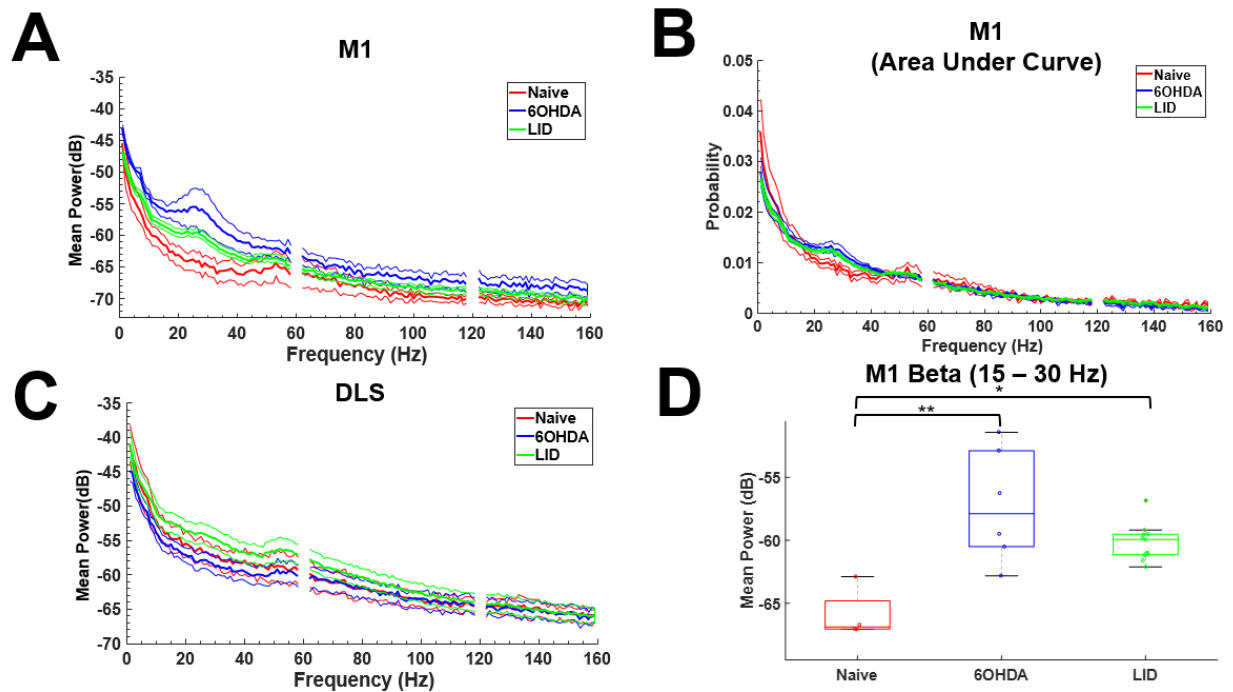


**Figure 10. Validation of increased beta (15-30 Hz) power in Motor Cortex (M1) of 6OHDA and L-DOPA-induced dyskinesia (LID) animals.** (A) Average baseline power of Naïve, 6OHDA, and LID animals up to 160 Hz. (B) Average spectral power up to 160 Hz of the three animal groups after computing Area Under the Curve (AUC). The increased beta power in 6OHDA and LID animals remain. (C) Average spectral power of baseline activity in the dorsolateral striatum (DLS). No significant differences across the power spectrum between animal groups ( $p=0.13$ ). (D) Box plot of average beta (15-30 Hz) power from (A). 6-OHDA-lesioned rats ( $n=7$ ) had significantly greater mean beta power [ $(F_{2,18})=7.71$ ,  $p=0.004$ ] compared to Naïve ( $p=0.002$ ,  $n=7$ ), but not vs. LID animals ( $p=0.11$ ,  $n=7$ ). LID rats also had significantly greater mean beta power than Naïve rats ( $p=0.04$ ). All post-hoc tests were Tukey-corrected.

## 7.1 Ketamine Does Not Reduce Beta Oscillations in 6-OHDA-Lesioned Animals

After confirming the beta signature of Parkinson's disease in M1 of our 6-OHDA lesioned rats, our first aim was to answer the question of whether repeated injections of low-dose ketamine would reduce this pathological oscillation. Increased beta oscillations are thought to be anti-kinetic and associated with parkinsonian symptoms (Little and Brown, 2014). In contrast, gamma oscillations are pro-kinetic in nature and most prominent during voluntary movement. A common treatment for patients with Parkinson's disease is DBS, whereby high-frequency stimulation (>140 Hz) reduces beta oscillations to regain voluntary motor control. Yet the DBS mechanism remains unknown. Given that evidence from the literature (Caixeta et al., 2013; Cordon et al., 2015; Muthukumaraswamy et al., 2015a) as well as our own published report (Ye et al., 2018) supporting the observation of ketamine (20 mg/kg) induces strong gamma and HFOs, it is conceivable that ketamine exposure produces similar therapeutic outcomes. Therefore, we hypothesized that repeated injections of low-dose ketamine will reduce pathological beta oscillations in 6-OHDA-lesioned animals.

Average spectrograms of ketamine sessions ( $n=7$ ) for all regions and locomotor activity are presented in **Figure 11**. The average spectral responses for injections 1 and 5 were compared between the 6-OHDA-lesioned and naïve animal **Figure 12**. Contrary to our original hypothesis, an ANOVA revealed that repeated injections of low-dose ketamine did not reduce beta oscillations 2-90 min post-injection in M1 ( $p=0.92$ ,  $\eta^2=0.02$ ), DLS ( $p=0.05$ ,  $\eta^2=0.34$ ), DMS ( $p=0.18$ ,  $\eta^2=0.23$ ), or NAc ( $p=0.75$ ,  $\eta^2=0.06$ ) (**12A**). Beta was not statistically different in the 92-110 min post-injection period in M1 ( $p=0.20$ ,  $\eta^2=0.21$ ), DLS ( $p=0.22$ ,  $\eta^2=0.20$ ), DMS ( $p=0.32$ ,  $\eta^2=0.17$ ), or NAc ( $p=0.05$ ,  $\eta^2=0.34$ ) (**12B**).

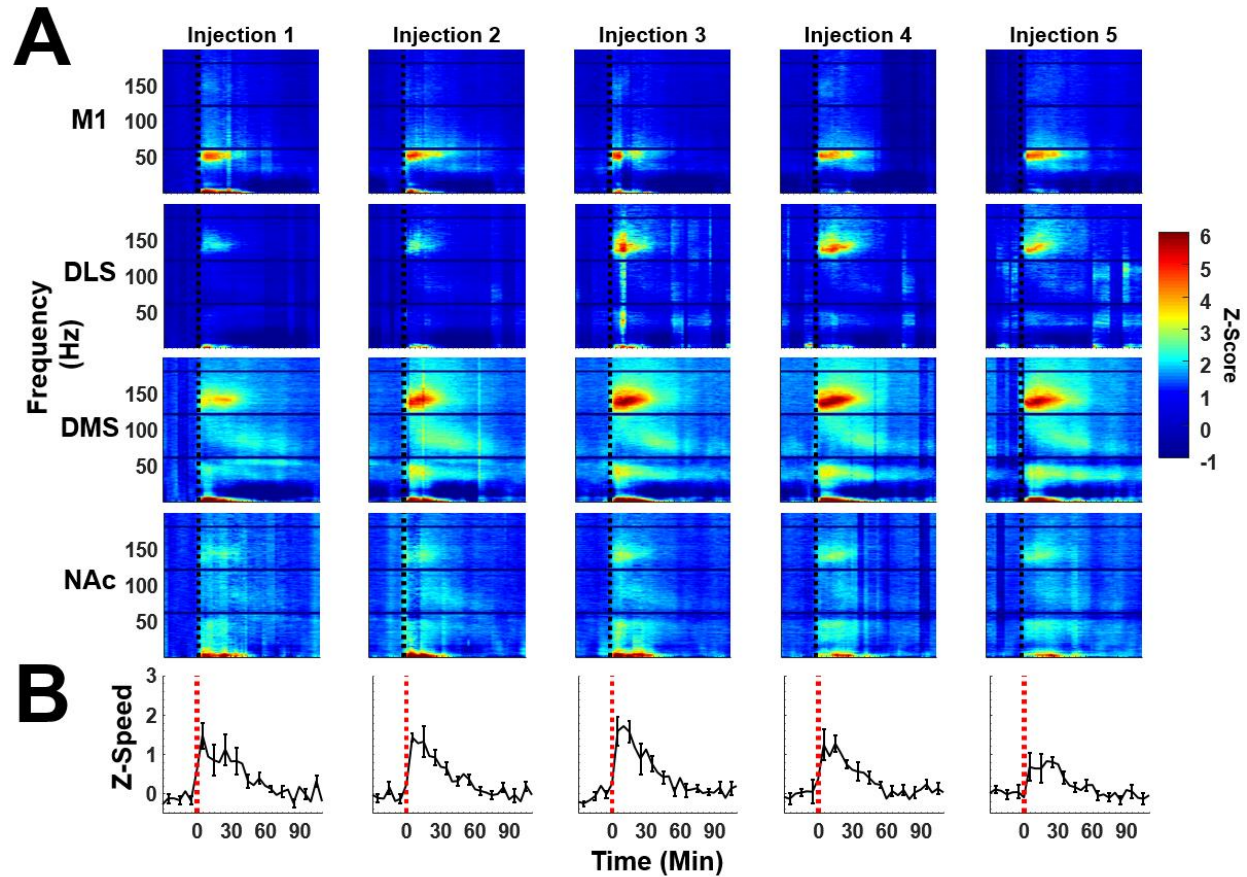


**Figure 11. Ketamine-induced oscillatory activity in 6-OHDA-lesioned animals. (A)** Average spectral responses ( $n=7$ ) for each successive ketamine injections (columns) in each region (rows). Spectra were aligned to each ketamine injection of a neural recording session at time=0 and all data were normalized to the -32 to -2 pre-injection 1 baseline (units in standard deviation). **(B)** Average ketamine-induced locomotion for each successive injection ( $n=7$ ). Locomotor activity were normalized to the pre-injection 1 (-32 to -2 min) baseline in units of standard deviation.

## **7.2 Greater Ketamine-Induced Delta Oscillations in M1 of Naïve Animals**

A significant increase in ketamine-induced delta (1 – 4 Hz) oscillations were observed only for the 2-90 min post-injection period in M1 (ANOVA,  $F(3,21)=3.93$ ,  $p=0.02$ ,  $\eta^2=0.39$ ) (12A). Specifically, ketamine injection 5 in naïve animals triggered significantly greater delta than injection 5 in 6-OHDA-lesioned animals ( $p=0.02$ ,  $d=1.5$ ). This suggests that repeated injections of ketamine have a stronger effect on increasing delta oscillations in a normal brain. Conversely in the 92-110 min period, a significant difference was observed for injection 1 (ANOVA,  $F(3,21)=3.39$ ,  $p=0.04$ ,  $\eta^2=0.36$ ). Post-hoc Tukey-Kramer-corrected multiple comparisons revealed Naïve animals had significantly greater delta oscillations than the 6-OHDA-lesioned group ( $p=0.04$ ,  $d=0.36$ ) after ketamine's metabolically active period. This effect was not statistically significant by the 5<sup>th</sup> injection ( $p=0.52$ ), suggesting no lasting effect of ketamine-induced delta oscillations in the 92-110 min period. Taken together, the DA-lesioned hemisphere of 6-OHDA-lesioned animals may explain the decreased ketamine-induced delta compared to naïve animals.

## **7.3 6-OHDA-Lesioned Animals Have Lower Ketamine-Induced Gamma and HFOs in the 92-110 Min Period**

Despite the lack of statistically different ketamine-induced gamma and HFOs between the naïve and 6-OHDA groups in the 2-90 min period, we observed significant differences for low-gamma (35 – 58 Hz) (ANOVA,  $F(3,21)=8.06$   $p=0.001$ ,  $\eta^2=0.57$ ), high-gamma (70 – 85 Hz)

(ANOVA,  $F(3,21)=12.6$ ,  $p=0.0001$ ,  $\eta^2=0.67$ ), and HFOs (120 – 160 Hz) (ANOVA,  $F(3,21)=10.33$ ,  $p=0.0003$ ,  $\eta^2=0.63$ ) in the 92-110 min period.

For low-gamma in M1, post-hoc Tukey-Kramer-corrected multiple comparisons revealed injection 1 in naïve animals were significantly greater than the 1<sup>st</sup> ( $p=0.003$ ,  $d=4.54$ ) and 5<sup>th</sup> injections ( $p=0.005$ ,  $d=1.80$ ) of the 6-OHDA group.

For high-gamma in M1, post-hoc Tukey-Kramer-corrected t-tests show that ketamine injection 1 in naïve animals had significantly greater high-gamma than the 1<sup>st</sup> ( $p=0.0006$ ,  $d=4.26$ ) and 5<sup>th</sup> injections ( $p=0.002$   $d=2.09$ ) of the 6-OHDA group. Furthermore, high-gamma from the 5<sup>th</sup> injection in naïve animals were also greater than the 1<sup>st</sup> ( $p=0.002$ ,  $d=3.90$ ) and 5<sup>th</sup> injections ( $p=0.007$ ,  $d=1.83$ ) of 6-OHDA animals.

For HFOs in M1, post-hoc Tukey-Kramer-corrected t-tests revealed that ketamine injection 1 in naïve animals had significantly greater HFOs than the 1<sup>st</sup> ( $p=0.0008$ ,  $d=2.63$ ) and 5<sup>th</sup> injections ( $p=0.02$ ,  $d=1.66$ ) of the 6-OHDA group. Ketamine injection 5 in naïve animals had significantly greater HFOs than the 1<sup>st</sup> ( $p=0.002$ ,  $d=3.31$ ) but not 5<sup>th</sup> injection ( $p=0.05$ ,  $d=1.89$ ) of 6-OHDA animals. Taken together, these results indicate that suppression of low-, high-gamma, and HFOs occur only in 6-OHDA-lesioned animals, suggesting a role for DA in the initial increase (injection 1) and suppression (injection 5) of ketamine-induced oscillations after its metabolically active period.

## **7.4 Ketamine Initially Triggers a Weaker Low-Gamma and HFO Response in 6-OHDA-Lesioned Animals**

In the DLS, a statistically significant difference was observed for low-gamma (ANOVA,  $F(3,21)=4.51$ ,  $p=0.02$ ,  $\eta^2=0.43$ ) and HFOs (ANOVA,  $F(3,21)=4.06$ ,  $p=0.02$ ,  $\eta^2=0.40$ ) in the 2-90 min period. Post-hoc multiple comparisons revealed low-gamma after ketamine injection 1 in the 6-OHDA group was significantly lower than the 5<sup>th</sup> injection in naïve animals ( $p=0.01$ ,  $d=1.79$ ). A similar effect was observed for HFOs ( $p=0.02$ ,  $d=1.84$ ). This suggests that ketamine initially triggers a weaker low-gamma and HFO response in 6-OHDA animals compared to naïves. However, by the 5<sup>th</sup> ketamine injection, the magnitude of response is similar to naïve animals.

## **7.5 Ketamine-Induced HFO Power Was Not Statistically Different in the DMS Between Naïve and 6-OHDA Animals in the 2-90 Min Period**

In the DMS, ketamine-triggered HFO power was statistically significant when comparing injections 1 vs 5 within each group (ANOVA,  $F(3,21)=12.6$  (ANOVA,  $F(3,21)=9.89$ ,  $p=0.0004$ ,  $\eta^2=0.62$ ). Post-hoc multiple comparisons revealed that ketamine injection 5 for both 6-OHDA ( $p=0.03$ ,  $d=1.74$ ) and naïve groups ( $p=0.001$ ,  $d=2.80$ ) triggered significantly greater HFO power than the 1<sup>st</sup> injection within each group, suggesting greater HFO power after repeated ketamine. However, comparing the 1<sup>st</sup> ( $p=0.99$ ) and 5<sup>th</sup> injection ( $p=0.69$ ) between groups was not statistically different. This suggests that ketamine equally induces HFO power in the DMS of naïve and 6-OHDA animals.

## 7.6 Suppression of Low- and High-Gamma, and HFOs in the 6-OHDA DMS (92-110 Min)

In the 92-110 min period, significant differences were observed for theta (ANOVA,  $F(3,21)=3.66$ ,  $p=0.03$ ,  $\eta^2=0.37$ ), low-gamma (ANOVA,  $F(3,21)=12.38$ ,  $p=0.0001$ ,  $\eta^2=0.67$ ), high-gamma (ANOVA,  $F(3,21)=4.27$ ,  $p=0.01$ ,  $\eta^2=0.41$ ), and HFOs (ANOVA,  $F(3,21)=26.88$ ,  $p=0.0000007$ ,  $\eta^2=0.81$ ) in the DMS. Post-hoc t-tests revealed theta oscillations after injection 5 in the naïve group were significantly greater than the 1<sup>st</sup> injection of the 6-OHDA group ( $p=0.02$ ,  $d=1.55$ ).

For low-gamma oscillations in the 92-110 min period, injection 1 in naïve animals were significantly greater than the 1<sup>st</sup> ( $p=0.04$ ,  $d=1.71$ ) and 5<sup>th</sup> injection ( $p=0.01$ ,  $d=2.09$ ) of the 6-OHDA group. Similarly, injection 5 in naïve animals were also greater than the 1<sup>st</sup> ( $p=0.0008$ ,  $d=2.83$ ) and 5<sup>th</sup> injection ( $p=0.002$ ,  $d=3.27$ ) of the 6-OHDA group.

For high-gamma in the 92-110 min period, naïve injection 5 was significantly greater than the 1<sup>st</sup> injection ( $p=0.03$ ,  $d=1.57$ ) of 6-OHDA animals.

For HFOs, injection 1 in naïve animals were significantly greater than the 1<sup>st</sup> ( $p=0.00005$ ,  $d=3.59$ ) and 5<sup>th</sup> injection ( $p=0.0003$ ,  $d=2.78$ ) of the 6-OHDA group. Similarly, injection 5 in naïve animals were also greater than the 1<sup>st</sup> ( $p=0.00004$ ,  $d=5.22$ ) and 5<sup>th</sup> injection ( $p=0.00002$ ,  $d=3.98$ ) of the 6-OHDA group. Taken together, these findings suggests a suppression of gamma and HFOs in DA-depleted animals after ketamine's metabolically active period.

## **7.7 Ketamine Triggers Stronger HFOs in the NAc of the Naïve Group Compared to 6-OHDA Animals in the 2-90 Min Period**

In the NAc, a statistically significant difference was found for ketamine-induced HFOs in the 2-90 min period (ANOVA,  $F(3,21)=11.24$   $p=0.0002$ ,  $\eta^2=0.65$ ). Post-hoc t-tests revealed that HFOs in naïve injection 5 was significantly greater than the 1<sup>st</sup> ( $p=0.0003$ ,  $d=3.09$ ) and 5<sup>th</sup> injection ( $p=0.001$ ,  $d=2.38$ ) of 6-OHDA animals. This suggests that repeated injections of ketamine in naïve animals has a greater effect on HFO power than in the DA-depleted brain.

## **7.8 Suppression of Low- and High-Gamma, and HFOs in the 6-OHDA NAc (92-110 Min)**

In the 92-110 min period, significant differences were observed for theta (ANOVA,  $F(3,21)=3.73$ ,  $p=0.03$ ,  $\eta^2=0.38$ ), low-gamma (ANOVA,  $F(3,21)=24.11$ ,  $p=0.000001$ ,  $\eta^2=0.80$ ), high-gamma (ANOVA,  $F(3,21)=10.87$ ,  $p=0.0002$ ,  $\eta^2=0.64$ ), and HFOs (ANOVA,  $F(3,21)=12.80$ ,  $p=0.0001$ ,  $\eta^2=0.68$ ) in the NAc. Post-hoc t-tests revealed theta oscillations after injection 5 in the naïve group were significantly greater than the 1<sup>st</sup> injection of the 6-OHDA group ( $p=0.03$ ,  $d=1.74$ ).

For low-gamma oscillations in the 92-110 min period, injection 1 in naïve animals were significantly greater than the 1<sup>st</sup> ( $p=0.0005$ ,  $d=3.28$ ) and 5<sup>th</sup> injection ( $p=0.00006$ ,  $d=4.74$ ) of the 6-OHDA group. Similarly, injection 5 in naïve animals were also greater than the 1<sup>st</sup> ( $p=0.00007$ ,  $d=2.98$ ) and 5<sup>th</sup> injection ( $p=0.000009$ ,  $d=3.87$ ) of the 6-OHDA group.

For high-gamma oscillations, injection 1 in naïve animals were significantly greater than the 1<sup>st</sup> ( $p=0.003$ ,  $d=2.26$ ) and 5<sup>th</sup> injection ( $p=0.002$ ,  $d=3.02$ ) of the 6-OHDA group. Similarly,

injection 5 in naïve animals were also greater than the 1<sup>st</sup> ( $p=0.006$ ,  $d=2.04$ ) and 5<sup>th</sup> injection ( $p=0.004$ ,  $d=2.70$ ) of the 6-OHDA group.

For HFOs, injection 1 in naïve animals were significantly greater than the 1<sup>st</sup> ( $p=0.003$ ,  $d=2.55$ ) and 5<sup>th</sup> injection ( $p=0.005$ ,  $d=2.42$ ) of the 6-OHDA group. Similarly, injection 5 in naïve animals were also greater than the 1<sup>st</sup> ( $p=0.0006$ ,  $d=2.82$ ) and 5<sup>th</sup> injection ( $p=0.001$ ,  $d=2.70$ ) of the 6-OHDA group. These results taken together, similar to the DMS suggests a suppression of gamma and HFOs after ketamine in 6-OHDA-lesioned animals.

## **7.9 Ketamine-Induced Locomotor Activity is Significantly Lower in 6-OHDA-Lesioned Animals**

Average locomotor activity was significantly different between naïve and 6-OHDA groups in the 2-90 min period (ANOVA,  $F(3,21)=5.60$ ,  $p=0.009$ ,  $\eta^2=0.55$ ). Post-hoc multiple comparisons revealed ketamine injection 5 in naïve animals triggered significantly greater locomotor activity compared to the 6-OHDA group ( $p=0.005$ ,  $d=1.48$ ) (**Figure 12D**).

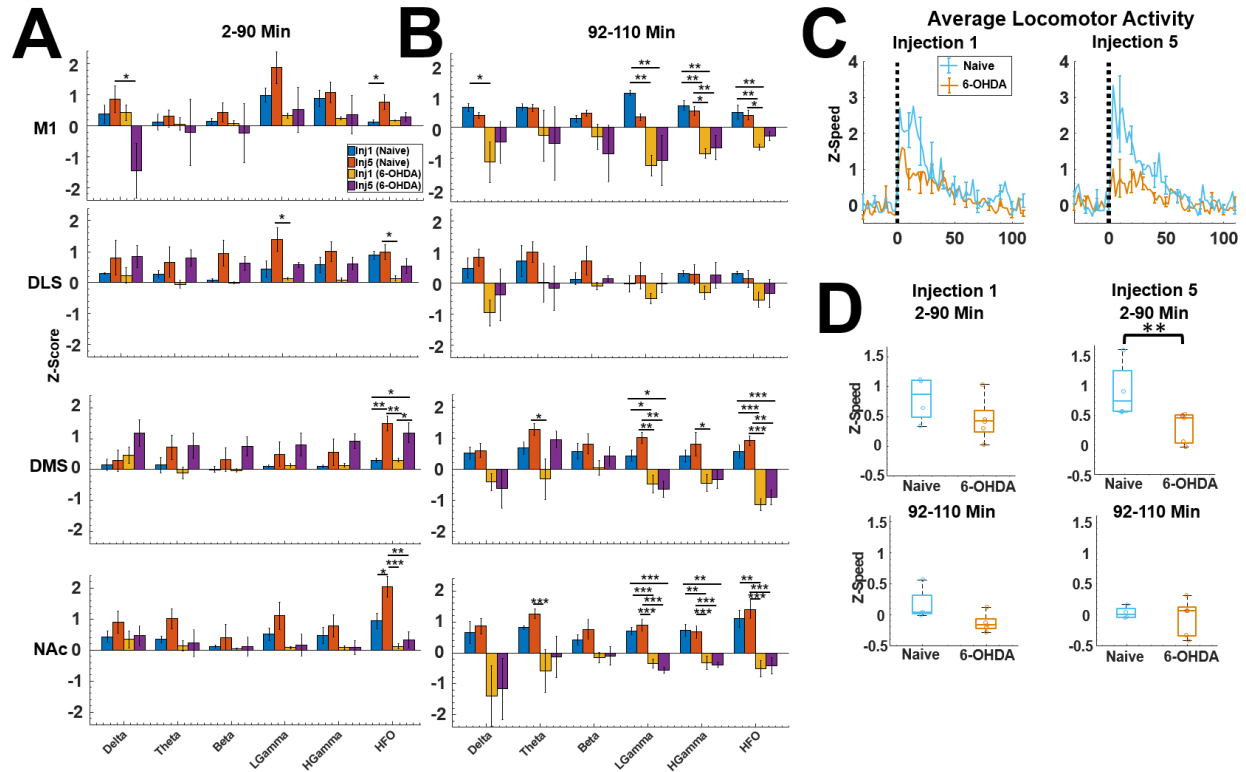


**Figure 12. Comparison of ketamine-induced oscillations in 6-OHDA-lesioned vs. naïve animals.** (A) Average spectral response of ketamine injections 1 and 5 for 6-OHDA lesioned animals (see Figure 11) and Naïve controls (see Figure 2) in the M1, DLS, DMS, and NAc. All activity were normalized to the pre-injection 1 (-32 to -2 min) baseline period of the respective groups in units of standard deviation. (B) As in A, but for the 92-110 min post-injection period. (C) Average locomotor activity ketamine injections 1 and 5 for 6-OHDA-lesioned animals and Naïve controls. All Activity were normalized to the pre-injection 1 (-32 to -2 min) baseline period, units in standard deviation. (D) Average locomotion from C separated into 2-90 min and 92-110 min post-injection period. Naïve controls had significantly greater average locomotion after ketamine injection 5 compared to 6-OHDA group in the 2-90 min period ( $p=0.005$ ,  $d=1.48$ ).

## **7.10 Prior History of Ketamine Exposure Does Not Alter Resting Oscillatory Activity in 6-OHDA-Lesioned Animals.**

Given that we did not observe any statistically different changes in beta oscillations after ketamine in 6-OHDA-lesioned animals, we explored the hypothesis repeated exposure to ketamine may produce changes in resting state oscillatory power. This was assessed by comparing raw oscillatory power during the pre-injection 1 baseline period (-32 to -2 min) for sessions in which rats had either no prior ketamine exposure vs. after at least one previous ketamine exposure. A within-subjects analysis identified no significant relationships between the number of previous ketamine exposure and oscillatory power in any frequency band (paired t-test,  $p > 0.05$ ,  $n = 7$ ) (**Figure 13**).

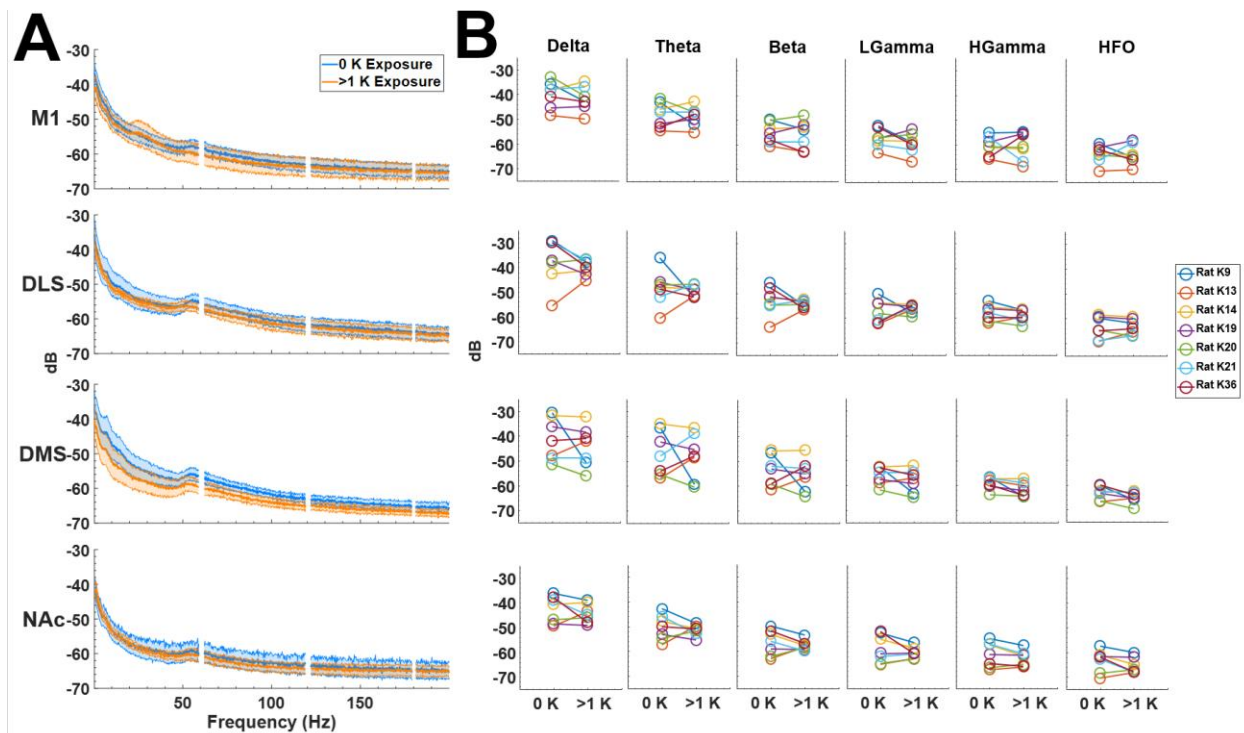


**Figure 13. Prior history of extended ketamine exposure does not alter resting oscillatory activity in 6-OHDA-lesioned animals.** (A) Average power spectra (dB) of baseline activity prior to any ketamine exposure (blue) compared to after one or more ketamine exposures (orange) for each region. (B) Within-subjects comparison of each frequency range before and after ketamine exposure for each animal in the 6-OHDA-lesioned group ( $n=7$ ). No significant difference was observed for any frequency band in any region. These results indicate that repeated exposure to ketamine does not reduce resting state oscillatory activity in 6-OHDA-lesioned animals.

## 7.11 Ketamine Does Not Trigger Cross-Frequency Interactions in M1 of 6-OHDA Animals

Phase-amplitude CFC (PAC) measures the degree to which the phase of a low-frequency oscillation coordinates with the amplitude of a higher frequency oscillation. Alterations in coupling (i.e., coordination) of multiple frequency bands are believed to impact a variety of functions such as information processing and plasticity (Canolty and Knight, 2010; Lisman and Jensen, 2013a). We investigated the effects of ketamine on within-region CFC in 6-OHDA animals. Given that we observed increased delta- and theta-HFO coupling in naïve animals (see **Figure 7**), we explored whether these effects were present in the DA-depleted hemisphere of 6-OHDA-lesioned animals. Analysis was performed on CFC units that were normalized to the pre-injection 1 baseline (-32 to -2 min), shown as PAC-Z on the y-axis while the x-axis displays time in minutes with injections aligned to time=0. Time course of PAC for injections 1 (left column) and 5 (right column) for all regions (row) is presented in **Figure 14A**.

In M1, significant differences were observed in delta-HFO in the 2-90 min period (ANOVA,  $F(3,23)=36.51$ ,  $p=0.00000002$ ,  $\eta^2=0.84$ ). Post-hoc multiple comparisons revealed increased delta-HFO CFC during ketamine injection 1 in naïve animals compared to the 1<sup>st</sup> ( $p=0.001$ ,  $d=3.46$ ) and 5<sup>th</sup> injections ( $p=0.0002$ ,  $d=3.91$ ) of 6-OHDA animals. Similarly, injection 5 of naïve animals was also significantly greater compared to the 1<sup>st</sup> ( $p=0.0000007$ ,  $d=4.58$ ) and 5<sup>th</sup> injections ( $p=0.00006$ ,  $d=4.05$ ). There was no increased delta-HFO CFC for either injection in the 6-OHDA group ( $p>0.05$ ).

Similar observations were made with theta-HFO CFC in M1 (ANOVA,  $F(3,23)=41.63$ ,  $p=0.000000009$ ,  $\eta^2=0.86$ ). Post-hoc multiple comparisons revealed increased theta-HFO CFC during ketamine injection 1 in naïve animals compared to the 1<sup>st</sup> ( $p=0.00001$ ,  $d=3.46$ ) and 5<sup>th</sup>

injections ( $p=0.00002$ ,  $d=3.91$ ) of 6-OHDA animals. Similarly, injection 5 of naïve animals was also significantly greater compared to the 1<sup>st</sup> ( $p=0.00000007$ ,  $d=4.58$ ) and 5<sup>th</sup> injections ( $p=0.000006$ ,  $d=5.32$ ). There was no increased theta-HFO CFC for either injection in the 6-OHDA group ( $p>0.05$ ) and no other significant CFC effects were observed ( $p>0.05$ ). Taken together, these results indicate that the lack of delta- and theta-HFO CFC in 6-OHDA animals suggests DA contributes to the interaction between lower and HFO frequencies.

## **7.12 Ketamine Does Not Trigger Cross-Frequency Interactions in DLS of 6-OHDA Animals**

In the DLS, significant differences were observed for delta-HFO CFC between groups (ANOVA,  $F(3,23)=42.65$ ,  $p=0.00000002$ ,  $\eta^2=0.87$ ). Post-hoc multiple comparisons revealed increased delta-HFO CFC during ketamine injection 1 in naïve animals compared to the 1<sup>st</sup> ( $p=0.0001$ ,  $d=4.05$ ) and 5<sup>th</sup> injections ( $p=0.00002$ ,  $d=3.68$ ) of 6-OHDA animals. Similarly, injection 5 of naïve animals was also significantly greater compared to the 1<sup>st</sup> ( $p=0.0000001$ ,  $d=5.84$ ) and 5<sup>th</sup> injections ( $p=0.0000002$ ,  $d=5.35$ ). There was no increased delta-HFO CFC for either injection in the 6-OHDA group ( $p>0.05$ ).

Increased theta-HFO CFC was also observed (ANOVA,  $F(3,23)=30.56$ ,  $p=0.0000002$ ,  $\eta^2=0.83$ ). Post-hoc multiple comparisons revealed increased theta-HFO CFC during ketamine injection 1 in naïve animals compared to the 1<sup>st</sup> ( $p=0.0001$ ,  $d=3.40$ ) and 5<sup>th</sup> injections ( $p=0.00007$ ,  $d=3.37$ ) of 6-OHDA animals. Similarly, injection 5 of naïve animals was also significantly greater compared to the 1<sup>st</sup> ( $p=0.0000004$ ,  $d=4.77$ ) and 5<sup>th</sup> injections ( $p=0.000002$ ,  $d=4.66$ ). There was no increased theta-HFO CFC for either injection in the 6-OHDA group

( $p > 0.05$ ) and no other significant CFC effects were observed ( $p > 0.05$ ). Taken together, these results indicate that the lack of delta- and theta-HFO CFC in both M1 and DLS of 6-OHDA animals suggests DA contributes to the interaction between lower and HFO frequencies.

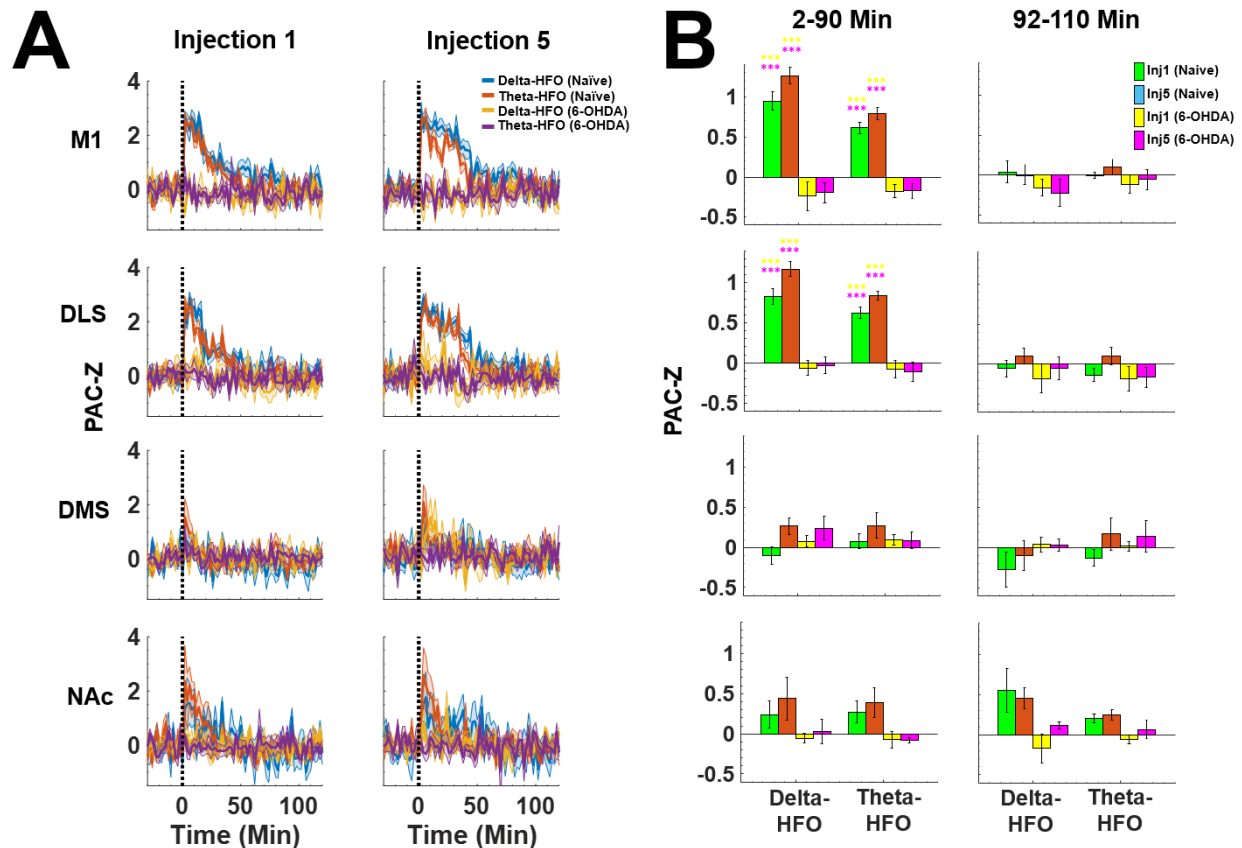


**Figure 14. Ketamine-induced cross-frequency coupling in 6-OHDA-lesioned animals. (A)** Time course of baseline normalized phase-amplitude coupling (PAC) after the 1<sup>st</sup> (left column) and 5<sup>th</sup> (right column) injections of ketamine in naïve ( $n=8$ ) and 6-OHDA-lesioned animals ( $n=7$ ). Given the enhanced delta- and theta-HFO CFC found in naïve animals, these frequencies were used for comparison to 6-OHDA group to assess whether these effects were also present in the DA-depleted brain. **(B)** Comparison of CFC for injections 1 and 5 between both groups during the 2-90 min (left column) and 92-110 min period (right column). In both M1 and DLS, naïve animals receiving ketamine significantly increased delta- and theta-HFO CFC for during the 2-90 min period following both injections 1 and 5 compared to 6-OHDA-lesioned animals (all  $p < 0.001$ ). The color of asterisk corresponds to the group that is significantly different. No other significant observations were found.

## Chapter 8: AIM 2a: L-DOPA Injections in LID Animals Triggers Wide-Band Gamma

In contrast to 6-OHDA animals, the oscillatory signature of LID is thought to be a strong and focal 80 Hz high-gamma response in M1 as well as the DLS to a lesser degree (Dupre et al., 2016; Halje et al., 2012a). This frequency is associated with the onset and duration of abnormal involuntary movements and is only observable after an injection of L-DOPA (i.e., on-state), otherwise this response is not present. The LID animals of this experiment underwent 21 days of priming with daily injections of L-DOPA (7mg/kg). Animals were scored after the priming period and received two maintenance injections of L-DOPA (7mg/kg) spaced 2-3 days apart to preserve dyskinesia. Average composite LAO (i.e., limb, axial, orolingual) dyskinesia scores for the LID group ( $n=7$ ) is presented in **Table 1**. The average composite score of  $33.6 \pm 6.6$  (Mean  $\pm$  S.D.) is classified as mild to moderate dyskinesia (Bartlett et al., 2016), validating that all animals in the LID group expressed dyskinesia.

Average spectral responses of LID animals after an injection of L-DOPA (7 mg/kg) + SAL for all regions are presented in **Figure 15A**. In these SAL recording sessions, an injection of SAL is administered every two hours. The 5<sup>th</sup>/last injection is paired with L-DOPA to serve as a control for the ketamine recording sessions (e.g., the 5<sup>th</sup> injection of ketamine sessions are ketamine + L-DOPA). Average spectra is normalized to the pre-injection 1 baseline period (-32 to -2 min). Unexpectedly, L-DOPA injections in our LID animals did not trigger a focal 80 Hz gamma response in any of the 4 observed regions. Rather, L-DOPA induced region-dependent gamma oscillations ranging from low to wideband. **Figure 15B** (left column) shows the power spectral density between a L-DOPA + SAL vs. SAL only injection in the LID animals (data from **Figure 15A**). The time period chosen for analysis here was 22-90 min post-injection, as

maximum striatal DA concentration is reached approximately 20-30 min after i.p. administration of L-DOPA (Shen et al., 2003). Results of these comparisons for all regions are presented in **Figure 15B** (right column), L-DOPA triggered significant low-gamma (35 – 58 Hz) in M1 compared to a SAL injection (t-test,  $p=0.03$ ,  $d=1.14$ ). This L-DOPA-triggered low-gamma was only observed in M1, while the DLS (t-test,  $p=0.03$ ,  $d=1.06$ ), DMS (t-test,  $p=0.04$ ,  $d=1.53$ ), and NAc (t-test,  $p=0.04$ ,  $d=1.08$ ) had a significant wideband gamma response (40 – 85 Hz) compared to SAL. Average locomotion also increased significantly compared to SAL injection (t-test,  $p<0.0001$ ,  $d=5.95$ ) (**Figure 15C**).

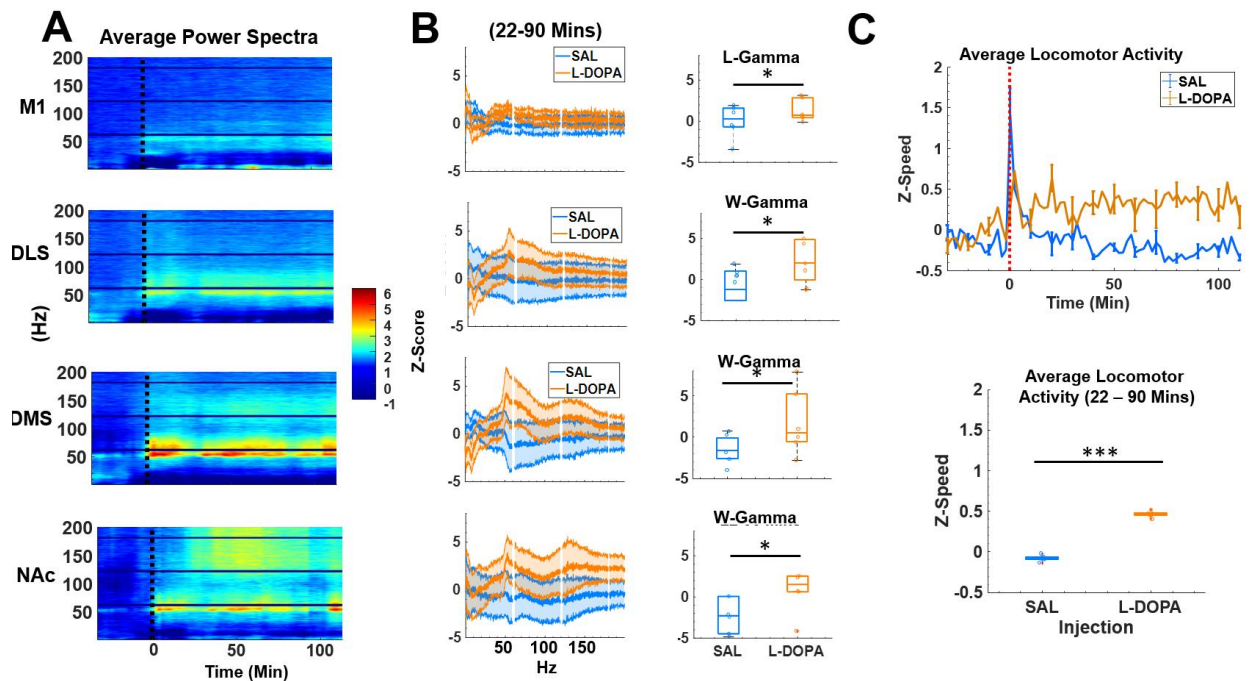


**Figure 15. L-DOPA triggers region-specific low-to-wide-band gamma in LID animals. (A)** Average spectral response after L-DOPA + SAL (7 mg/kg) vs SAL-only for each region in LID animals ( $n=7$ ). Spectral responses were normalized to the pre-injection 1 (-32 to -2 mins) baseline period. **(B) LEFT COLUMN:** Power spectral density 22-90 mins after L-DOPA exposure vs SAL-only injections in LID animals. **RIGHT COLUMN:** Comparison of the 22-90 min period after L-DOPA vs SAL-only. For the M1, L-DOPA triggered significant increases in low-gamma (35-58 Hz). Unlike other regions, wide-band gamma was not statistically different (boxplot not shown). For the DLS, DMS, and NAc, L-DOPA injections triggered significant increases in wide-band gamma (40 – 85 Hz) (all  $p<0.05$ ). **(C)** L-DOPA significantly increased locomotor activity compared to SAL-only condition ( $p<0.0001$ ).

## 8.1 Baseline AIMs Scores Are Not Correlated to L-DOPA-Induced Gamma

Although LID animals were not scored for AIMs during neural recordings, we explored the question of whether the established AIMs prior to the recordings are related to the L-DOPA-induced wide-band gamma. Each LID animal's baseline composite AIMs score (i.e., prior to electrode implantation) was correlated to their average low- and wide-band gamma response in M1 and striatal regions, respectively (**Figure 16**). Although correlations of AIMs to low-gamma in M1 ( $r=0.73$ ,  $p=0.06$ ) (**16A**) and wide-band gamma in the DLS ( $r=0.60$ ,  $p=0.15$ ) (**16B**), DMS ( $r=0.71$ ,  $p=0.07$ ) (**16C**), and NAc ( $r=0.74$ ,  $p=0.05$ ) (**16D**) were high, these were all non-significant. This suggests no relationship between baseline AIMs and L-DOPA-induced gamma. However, this may also be due to the lack of statistical power.

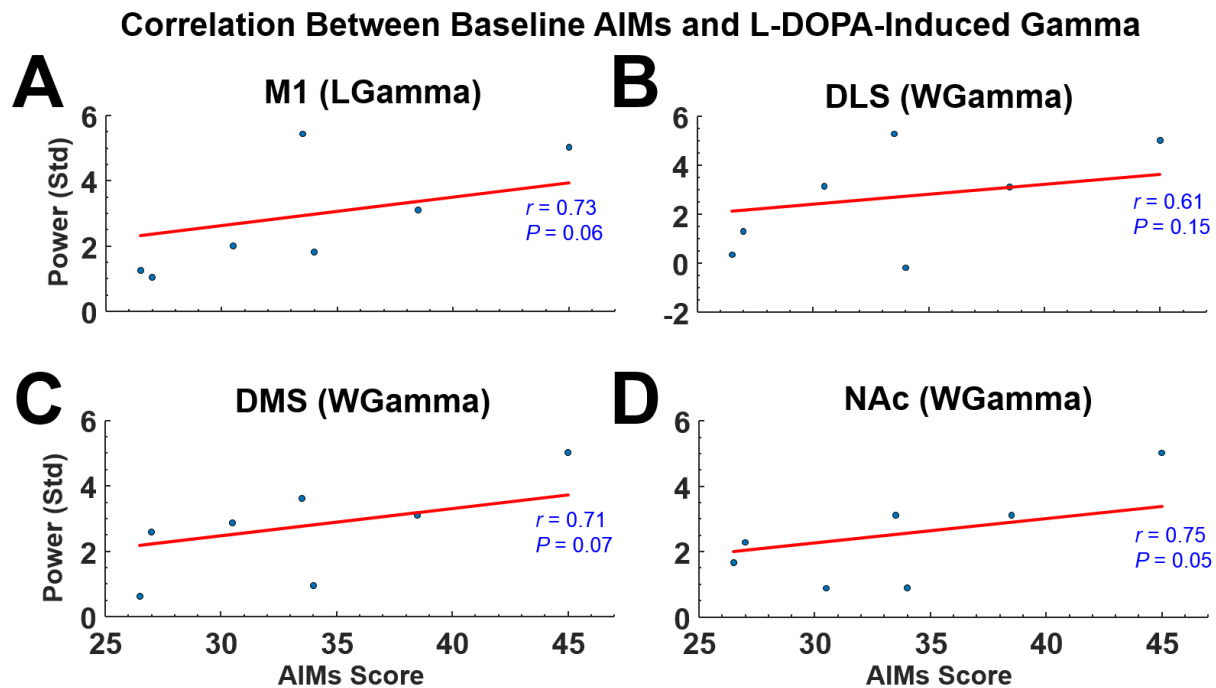


**Figure 16. Correlation between LID animals' baseline AIMs scores to average L-DOPA-induced gamma response during neural recordings.** (A) Average L-DOPA-induced low-gamma activity in M1 of LID animals. Time period chosen for gamma average was 22-90 min post-injection period (see Figure 15). Baseline AIMs scores were taken after L-DOPA priming and prior to electrode implantation. Each animal's average composite score was correlated to 22-90 min post-L-DOPA-injection during neural recordings. Baseline AIMs was highly correlated with L-DOPA-induced low-gamma in M1 but was not statistically significant ( $r=0.73$ ,  $p=0.06$ ). Baseline AIMs scores were highly correlated with L-DOPA-induced wide-band gamma in the DLS (B;  $r=0.61$ ,  $p=0.15$ ), DMS (C;  $r=0.71$ ,  $p=0.07$ ), and NAc (D;  $r=0.75$ ,  $p=0.05$ ) but were all not statistically significant.

## 8.2 Increased Low-to-Wide-Band Gamma Immediately After L-DOPA Injection

Another novel observation in our LID animals was the immediate onset of region-dependent gamma immediately after the L-DOPA injection. Maximum striatal DA concentrations are reached approximately 20-30 min after L-DOPA exposure in the 6-OHDA-lesioned rat (Shen et al., 2003), others have shown that L-DOPA-induced gamma occurs within this time frame (Dupre et al., 2016; Halje et al., 2013). Yet we observed a gamma response prior to this 20-30 min period. Note in **Figure 15A**, region-dependent low-to-wideband gamma increases immediately after injection, with an abrupt decrease at approximately 20-25 min, then gamma activity resumes at the point in which L-DOPA becomes metabolically active. This led to the question of whether this immediate gamma response was movement-related.

To test this, we compared LID animals receiving an injection of L-DOPA + SAL vs naïve animals receiving SAL only during the 2-20 min post-injection period. Average spectral responses are presented in **Figure 17A**. For M1, low-gamma was compared between LID and naïve animals as L-DOPA triggered significant low-gamma in this region, while the other 3 regions were compared against wide-band gamma. There was no significant difference in post-injection low-gamma in M1 ( $t$ -test,  $p=0.27$ ,  $d=0.71$ ), and no significant difference in wideband gamma in the DLS ( $t$ -test,  $p=0.20$ ,  $d=0.85$ ) or DMS ( $t$ -test,  $p=0.47$ ,  $d=0.43$ ). However, LID animals did have significantly greater wide-band gamma compared to naïve animals during the 2-20 min post-injection period ( $t$ -test,  $p=0.03$ ,  $d=1.95$ ). This difference may reflect the NAc's increased sensitivity to DA influx via L-DOPA to significantly higher wide-band gamma compared to a naïve animal. Furthermore, movement speed was not statistically different between the two groups of animals during 2-18 min post-injection period ( $t$ -test,  $p=0.17$ ,  $d=0.93$ )

(**Figure 17C**). The lack of difference in movement speed and in gamma in M1, DMS, and DLS between LID and naïve animals suggests that the immediate increase in post-injection gamma of LID animals may be movement-related. However, we cannot draw firm conclusions as to the cause of this immediate gamma response in LID animals. Movement speed was significantly different in the 22-90 min period between groups (*t*-test,  $p=0.02$ ,  $d=1.67$ ) (**Figure 17C**), suggesting that once L-DOPA becomes metabolically active in the LID animals, movement is at a sustained increase while naïve animals receiving SAL decreased movement.

## L-DOPA-Induced Region-Dependent Gamma

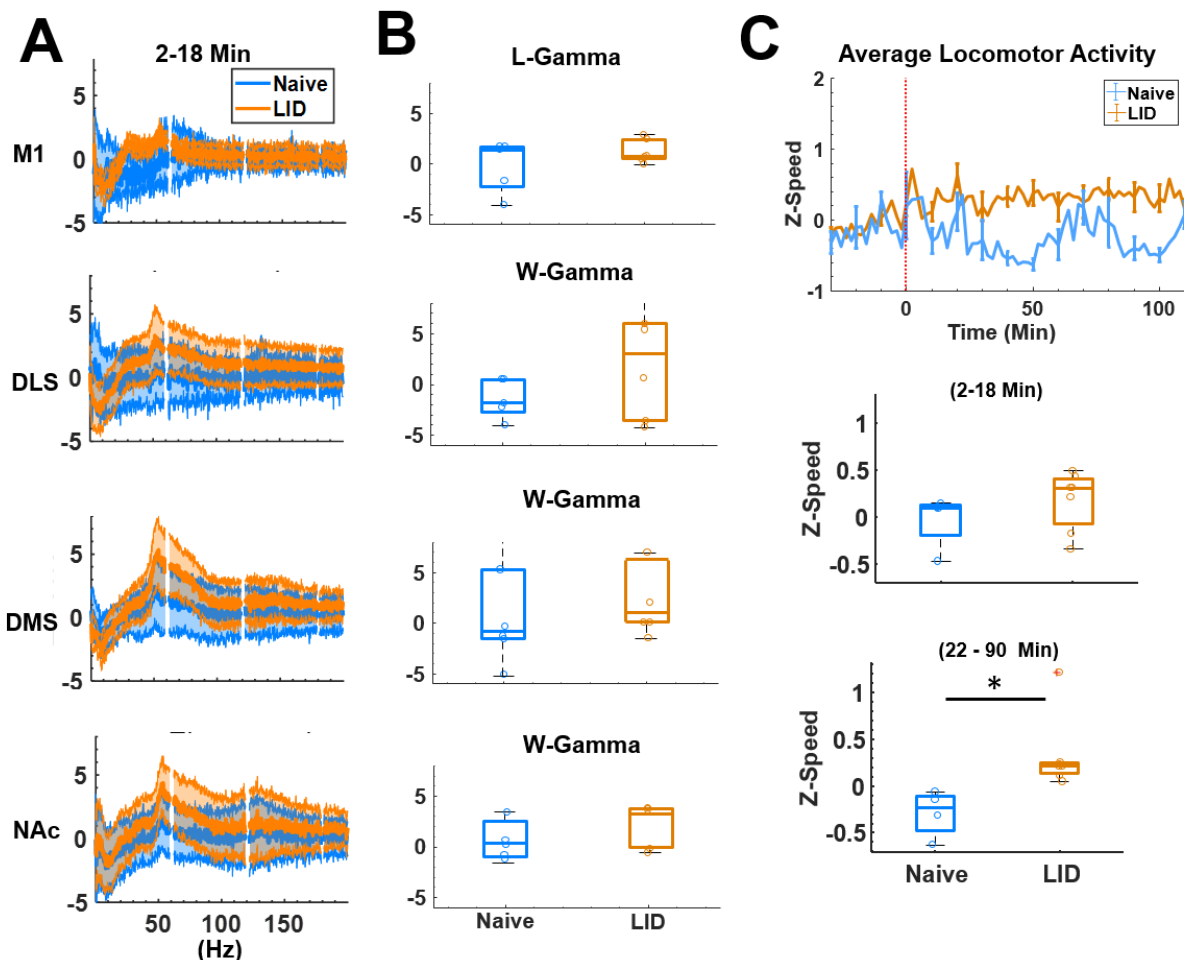


**Figure 17. Increased low-to-wide-band gamma in LID animals immediately after L-DOPA injection.** (A) Average spectral responses of LID animals receiving L-DOPA (7 mg/kg) + SAL vs naïve animals receiving an injection of SAL-only in the first 2-18 mins post-injection. (B) T-test comparisons reveal non-significant differences for low-gamma in the M1 (top) between LID vs Naïve animals. For the other regions, wide-band gamma was also not statistically different. (C) Average locomotor activity of LID animals after L-DOPA + SAL injection was not statistically different compared to naïve animals receiving SAL-only in the first 2-20 mins (middle). However, the locomotor activity of LID animals was significantly greater than naïves for the 22-90 min period. Taken together, these findings suggest that the immediate gamma increase in LID animals may be movement-induced rather than L-DOPA induced as L-DOPA becomes metabolically active approximately 20 mins post-injection. LID animals may be more sensitive to stimuli.

## Chapter 9: AIM 2b: Repeated Ketamine Exposure Does Not Reduce L-DOPA-Triggered Gamma in LID Animals

Repeated exposure to low-dose ketamine has been shown to have therapeutic effects on LID both in human patients and animals (Bartlett et al., 2016; Sherman et al., 2016b), yet the mechanisms are still unknown. Using the exact L-DOPA priming and ketamine injection protocol as Bartlett et al. (2016), we have thus far observed that L-DOPA triggers a low-to-wide-band region dependent gamma response in LID animals. Given that repeated injections of ketamine (20 mg/kg) reduces AIMs of LID (Bartlett et al., 2016), it is conceivable that this dose of ketamine may alter LID wide-band gamma that underlies the reduction of LID. To test this hypothesis, we first compared LID animals receiving an injection of L-DOPA vs. ketamine + L-DOPA. Average spectral response for each successive ketamine injection is presented in **Figure 18**. The 5<sup>th</sup> injection from the SAL and ketamine sessions (i.e., L-DOPA + SAL vs L-DOPA + ketamine) along with the 4<sup>th</sup> injection from ketamine sessions (i.e., ketamine alone) were used and average power spectra is presented in **Figure 19A** for each region. The period chosen for this comparison was 22-90 min post-injection as ketamine and L-DOPA are simultaneously metabolically active. Black lines represent L-DOPA + SAL, blue lines represent injections of ketamine alone, and orange lines represent ketamine + L-DOPA. For M1, low-gamma was chosen for this comparison as L-DOPA triggered significant increases in this frequency band (**Figure 15**), wide-band gamma was chosen for all other regions.

A significant difference was observed in the M1 (ANOVA,  $F(3,23)=3.87$ ,  $p=0.02$ ,  $\eta^2=0.36$ ). Post-hoc multiple comparisons revealed low-gamma in LID was significantly higher when ketamine was paired with L-DOPA compared to L-DOPA alone ( $p=0.01$ ,  $d=2.46$ ) (**19B**).

Contrary to our original hypothesis, this result indicates that ketamine does not reduce L-DOPA-triggered low-gamma in M1, rather, ketamine increases low-gamma.

A significant difference was observed in wide-band gamma in the DLS (ANOVA,  $F(3,23)=5.42, p=0.006, \eta^2=0.43$ ). Post-hoc multiple comparisons revealed greater wide-band gamma in LID animals receiving ketamine alone ( $p=0.03, d=3.59$ ) and ketamine + L-DOPA ( $p=0.005, d=4.27$ ) compared to naïve animals receiving ketamine. The result that ketamine alone enhances the wide-band gamma response in LID animals compared to naïve suggest that ketamine may have a greater effect on the hypersensitive DA receptors in the DLS of LID animals. L-DOPA-triggered wide-band gamma (black) was not statistically different from ketamine alone (blue) or ketamine + L-DOPA (orange) in LID animals (all  $p>0.05$ ). Furthermore, no significant difference was observed in wide-band gamma in the DMS or NAc (all  $p>0.05$ ).

Average locomotor activity was statistically different among these conditions (ANOVA,  $F(3,23)=5.08, p=0.008, \eta^2=0.42$ ) (**19C**). LID animals receiving ketamine alone (blue) had significantly lower average locomotion compared to naïve animals receiving ketamine alone ( $p=0.04, d=1.49$ ) (magenta). Locomotion was significantly greater in LID animals receiving ketamine + L-DOPA (orange) compared to L-DOPA alone ( $p=0.04, d=1.58$ ) (black) and ketamine alone ( $p=0.01, d=2.63$ ). This suggests that the combination of ketamine + L-DOPA in LID animals enhances locomotor activity.

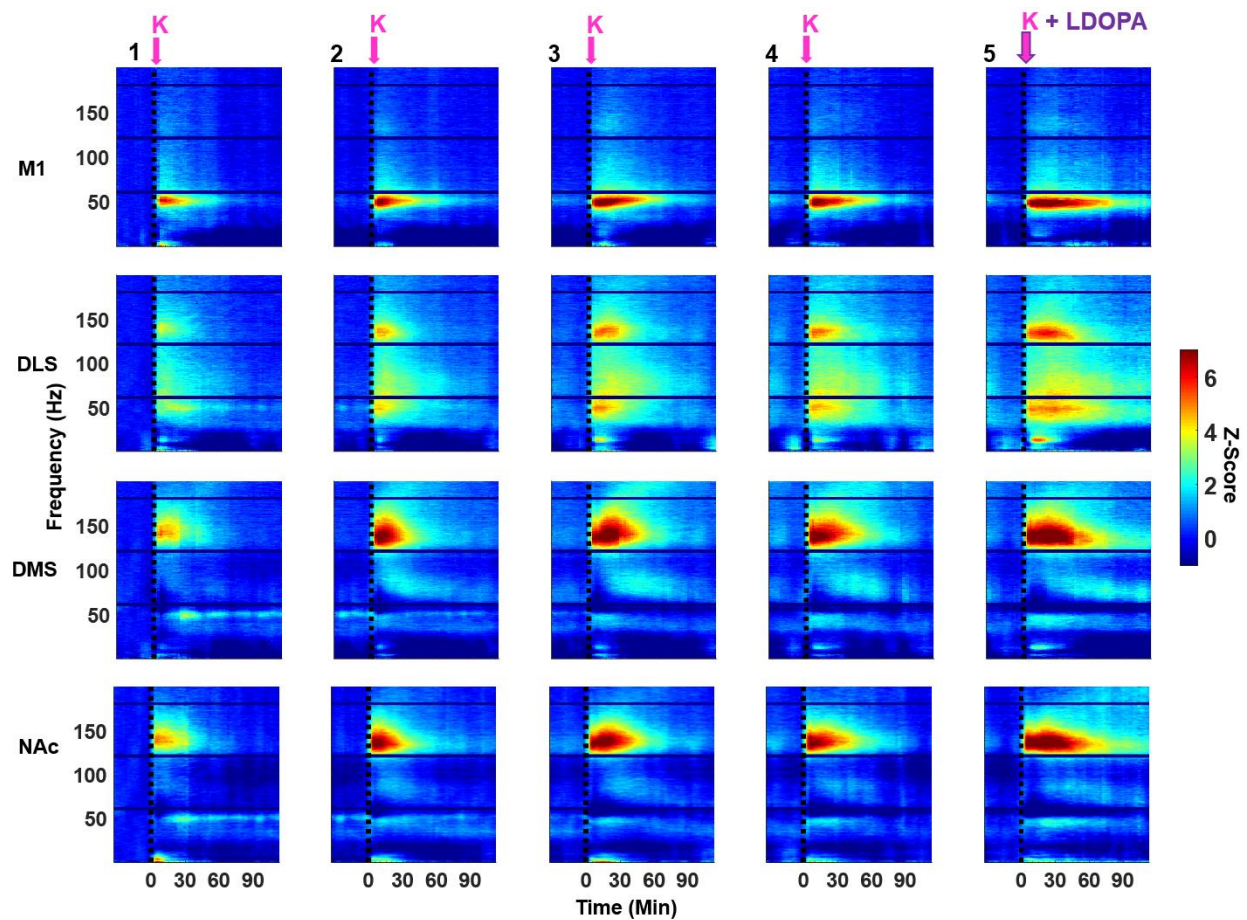


**Figure 18. Average spectral responses for each successive ketamine injection in LID animals for each region.** Spectral responses were normalized to the pre-injection 1 baseline (-32 to -2 mins) period. In these ketamine sessions for LID animals, single injections of ketamine (20 mg/kg) were administered every two hours. The 5th/final injection was co-administration of ketamine + L-DOPA (7 mg/kg) to trigger the L-DOPA on-state.

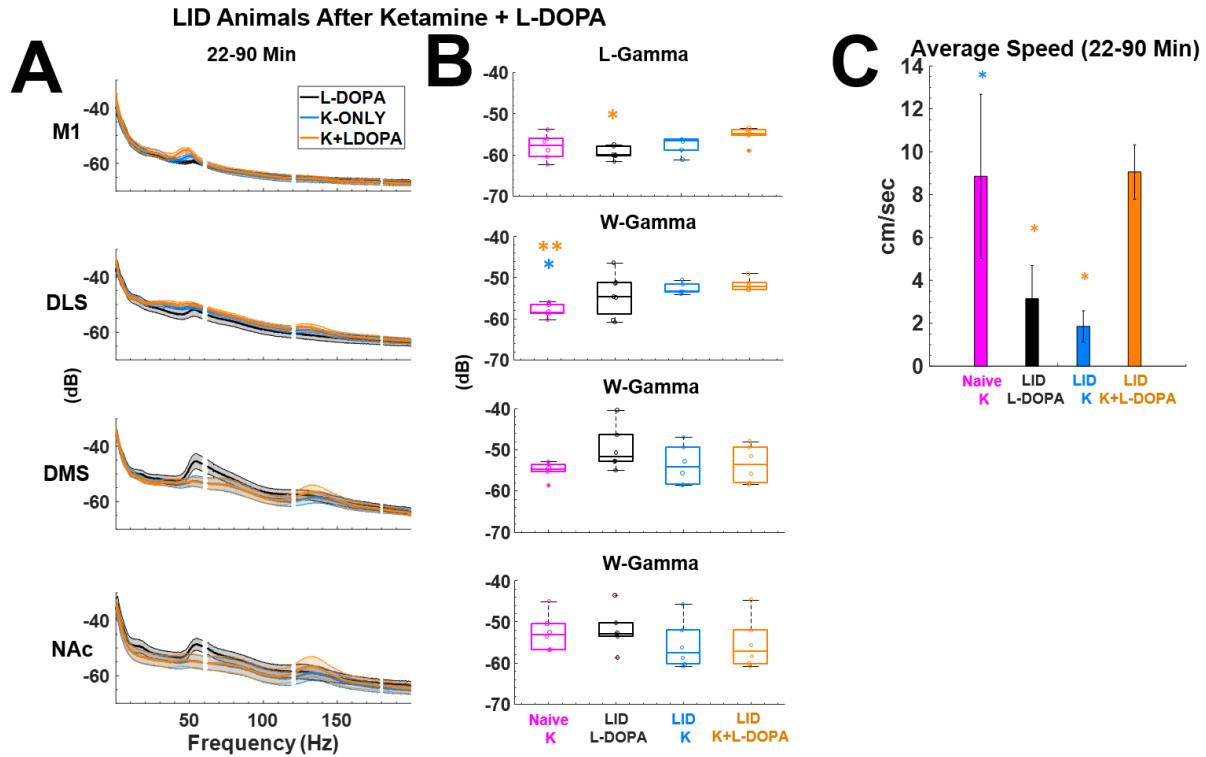


**Figure 19. Repeated ketamine exposure does not reduce L-DOPA-triggered Gamma in LID Animals.** (A) Average power spectra of 22-90 min following an injection of L-DOPA, ketamine alone, and ketamine + L-DOPA in LID animals for each region. (B) The 5<sup>th</sup> injection from the SAL and ketamine sessions (i.e., L-DOPA + SAL vs L-DOPA + ketamine) along with the 4<sup>th</sup> injection from ketamine sessions (i.e., ketamine alone) were used for comparison. The period chosen for this comparison was 22-90 min post-injection as ketamine and L-DOPA are simultaneously metabolically active. The color of asterisk corresponds with the group that is significantly different. For M1, low-gamma was chosen for this comparison as L-DOPA triggered significant increases in this frequency band (Figure 15), wide-band gamma was chosen for all other regions. Post-hoc multiple comparisons revealed low-gamma in LID was significantly higher when ketamine was paired with L-DOPA compared to L-DOPA alone ( $p=0.01$ ,  $d=2.46$ ) in M1 and greater wide-band gamma in LID animals receiving ketamine alone ( $p=0.03$ ,  $d=3.59$ ) and ketamine + L-DOPA ( $p=0.005$ ,  $d=4.27$ ) compared to naïve animals receiving ketamine. (C) Average locomotor activity for conditions in B, units in cm/sec. Post-hoc comparisons revealed LID animals receiving ketamine alone (blue) had significantly lower average locomotion compared to naïve animals receiving ketamine alone ( $p=0.04$ ,  $d=1.49$ ) (magenta). Locomotion was significantly greater in LID animals receiving ketamine + L-DOPA (orange) compared to L-DOPA alone ( $p=0.04$ ,  $d=1.58$ ) (black) and ketamine alone ( $p=0.01$ ,  $d=2.63$ ). This suggests that the combination of ketamine + L-DOPA in LID animals enhances locomotor activity.

## 9.1 Cross-Frequency Coupling in LID Animals

Electrophysiological recordings in awake and behaving LID animals is a largely unexplored field, and cross-frequency interactions in this animal model is no exception. To our knowledge, only one report has been published that explores CFC in any LID animal model supporting a decrease in theta (10 Hz)-focal 80 Hz gamma coupling in corticostriatal regions (Belić et al., 2016). Despite the lack of acute changes in L-DOPA-induced gamma during metabolically active ketamine, it is possible that changes in cross-frequency interactions may manifest during exposure that may not be apparent when observing overall changes in power. Given the previous reports of LID gamma decoupling with theta (Belić et al., 2016), along with our previous observation of ketamine-induced delta- and theta-HFO coupling in naïve but not 6-OHDA-lesioned animals (see **Figure 14**), we hypothesized that theta oscillations will also decouple with the LID gamma observed here.

To test this hypothesis, we compared LID animals receiving an injection of L-DOPA vs. ketamine + L-DOPA. The 5<sup>th</sup> injection from the SAL and ketamine sessions were used (i.e., L-DOPA + SAL vs L-DOPA + ketamine) and averaged PAC-Z over time is presented in **Figure 20A** for each region. The period chosen for this comparison was 22-90 min post-injection as ketamine and L-DOPA are simultaneously metabolically active. The groups chosen for comparison were naïve animals receiving ketamine alone (magenta), LID animals receiving L-DOPA alone (black), ketamine alone (blue), and ketamine + L-DOPA (orange). Theta (5-10 Hz) oscillations were chosen due to a previous report of theta-gamma decoupling (Belić et al., 2016), wide-band gamma was divided into low- (35 – 58 Hz) and high- (70 – 85 Hz) gamma to increase frequency specificity, HFOs (120 – 160 Hz) were chosen given that a previous report from our

group showing ketamine-induced HFOs preferentially couples with lower frequencies in naïve animals (Ye et al., 2018). Boxplots of these comparisons are presented in **Figure 20B**.

## **9.2 Delta- and Theta-HFO CFC Was Not Present in M1 LID**

### **Animals**

In M1, a significant difference was observed in delta-HFO CFC (ANOVA,  $F(3,23)=88.58$ ,  $p=0.000000000011$ ,  $\eta^2=0.93$ ). Post-hoc multiple comparisons revealed naïve animals had significantly greater delta-HFO coupling compared to LID animals receiving L-DOPA alone ( $p=0.000000004$ ,  $d=6.25$ ), ketamine alone ( $p=0.000000009$ ,  $d=7.04$ ), and ketamine + L-DOPA ( $p=0.000000003$ ,  $d=6.57$ ) (**20B, 1<sup>st</sup> row**). Theta-HFO CFC was also significantly different  $F(3,23)=28.79$ ,  $p=0.000000009$ ,  $\eta^2=0.81$ ). Post-hoc multiple comparisons revealed naïve animals had greater theta-HFO CFC compared to LID animals receiving L-DOPA alone ( $p=0.000008$ ,  $d=4.45$ ), ketamine alone ( $p=0.000002$ ,  $d=4.49$ ), and ketamine + L-DOPA ( $p=0.0000007$ ,  $d=4.28$ ) (**20B, 1<sup>st</sup> row**). We did not observe any increased CFC in LID animals (all  $p>0.05$ ). These results suggest that ketamine-induced delta- and theta-HFO CFC in M1 are only present in the naïve animal.

## **9.3 Delta- and Theta-HFO CFC Was Not Present in DLS of LID**

### **Animals**

Similar to M1, the DLS a significant difference was observed in delta-HFO CFC (ANOVA,  $F(3,23)=18.40$ ,  $p=0.000002$ ,  $\eta^2=0.70$ ). Post-hoc multiple comparisons revealed naïve animals had significantly greater delta-HFO coupling compared to LID animals receiving L-DOPA alone ( $p=0.000001$ ,  $d=4.21$ ), ketamine alone ( $p=0.0003$ ,  $d=2.96$ ), and ketamine + L-

DOPA ( $p=0.0003$ ,  $d=3.96$ ) (**20B, 2<sup>nd</sup> row**). Theta-HFO CFC was also significantly different  $F(3,23)=9.85$ ,  $p=0.0002$ ,  $\eta^2=0.1.91$ ). Post-hoc multiple comparisons revealed naïve animals had greater theta-HFO CFC compared to LID animals receiving L-DOPA alone ( $p=0.0001$ ,  $d=5.60$ ), ketamine alone ( $p=0.02$ ,  $d=1.91$ ), and ketamine + L-DOPA ( $p=0.02$ ,  $d=1.54$ ) (**20B, 2<sup>nd</sup> row**). We did not observe any increased CFC in LID animals (all  $p>0.05$ ). These results suggest that ketamine-induced delta- and theta-HFO CFC in the DLS are only present in naïve animals.

#### **9.4 Ketamine + L-DOPA Enhances Theta-HFO CFC in the DMS and Suppresses Theta-High-Gamma CFC in the NAc**

Despite the lack of theta-HFO CFC in M1 and DLS of LID animals, we observed a significant difference in the DMS (ANOVA,  $F(3,23)=5.9$ ,  $p=0.003$ ,  $\eta^2=0.43$ ). Post-hoc multiple comparisons revealed LID animals receiving and injection of L-DOPA alone significantly decreased theta-HFO coupling compared to ketamine + L-DOPA ( $p=0.002$ ,  $d=1.90$ ). This finding suggests that administration of ketamine + L-DOPA in an LID animal reverses theta-HFO decoupling induced by L-DOPA alone.

Theta-high-gamma CFC was observed in the NAc (ANOVA,  $F(3,23)=4.09$ ,  $p=0.01$ ,  $\eta^2=0.34$ ). Post-hoc  $t$ -tests revealed that ketamine alone ( $p=0.03$ ,  $d=1.60$ ) and ketamine + L-DOPA ( $p=0.02$ ,  $d=1.81$ ) significantly decreased theta-high-gamma CFC compared to L-DOPA alone in LID animals. This finding suggests that enhancement of theta-high-gamma CFC in the NAc of LID animals is facilitated by systemic L-DOPA administration, but was suppressed when co-active with ketamine.

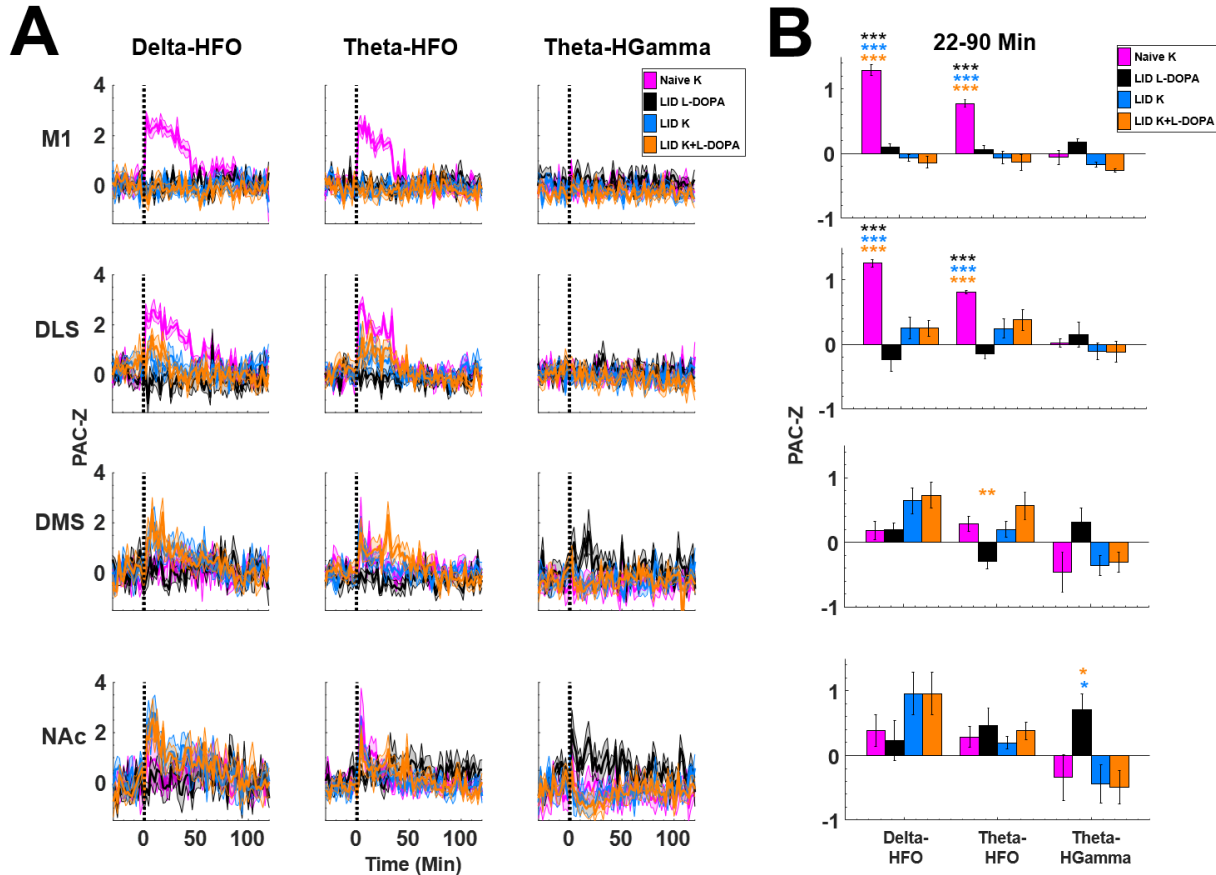


**Figure 20. Differential cross-frequency coupling in LID animals.** (A) Average baseline normalized phase-amplitude coupling for delta- and theta-HFO, and theta-high-gamma. Conditions chosen for comparison were naïve animals receiving ketamine (pink), LID animals receiving L-DOPA (black), ketamine alone (blue), and ketamine + L-DOPA (orange). (B) Post-hoc Tukey-Kramer corrected t-tests show delta- and theta-HFO CFC were significantly higher compared to all LID animal conditions (all  $p > 0.001$ ) in both M1 and DLS. In the DMS, ketamine + L-DOPA in LID animals significantly increased theta-HFO coupling compared to L-DOPA alone ( $p = 0.002$ ,  $d = 1.90$ ). In the NAc, ketamine + L-DOPA ( $p = 0.02$ ,  $d = 1.81$ ) and ketamine alone ( $p = 0.03$ ,  $d = 1.60$ ) in LID animals significantly decreased theta-high-gamma coupling compared to L-DOPA alone. These findings suggest that ketamine-induced delta- and theta-HFO CFC is only present in naïve M1 and DLS, while ketamine in LID animals reverses L-DOPA-induced coupling in DMS and NAc.

## 9.5 Repeated Ketamine Exposure Has No Long-Term Effect on L-DOPA-Induced Gamma

Although we did not observe an instantaneous reduction of L-DOPA-induced gamma, it is conceivable that ketamine's action on oscillatory activity may extend beyond its metabolically active period. Given that Bartlett and colleagues (2016) found long-term therapeutic benefits of ketamine to last up to 3 weeks post-exposure, we examined the neural activity of LID animals during the L-DOPA on-state before and after ketamine exposure as this may show any long-term changes in oscillatory activity. SAL sessions of the LID group ( $n=7$ ) were used. Each animal had a total of 2 SAL recording sessions, one session took place prior to any ketamine exposure (i.e., ketamine sessions) while the other SAL session occurred after 1 or more ketamine sessions. The 5<sup>th</sup> injection of each SAL session (i.e., L-DOPA + SAL) was used to compare oscillatory activity while L-DOPA was metabolically active (20-90 min post-injection). Average spectral response for each region is represented in **Figure 21A**. L-DOPA injections prior to any ketamine exposure (blue) was compared against L-DOPA injections after one or more ketamine exposures (orange). As with previous comparisons, low-gamma was used for M1 while other regions used wide-band gamma.

A within-subjects comparison (*t*-test) revealed significant differences in multiple frequency bands in M1. L-DOPA administration after one or more exposures to ketamine significantly increased delta ( $p=0.04$ ,  $d=1.00$ ), beta ( $p=0.02$ ,  $d=1.19$ ), low-gamma ( $p=0.01$ ,  $d=1.28$ ), high-gamma ( $p=0.01$ ,  $d=1.31$ ), and HFOs ( $p=0.025$ ,  $d=1.15$ ). No other statistically significant differences were observed for other regions in any frequency band (all  $p>0.05$ ). Contrary to our original hypothesis, ketamine does not reduce L-DOPA-triggered gamma.

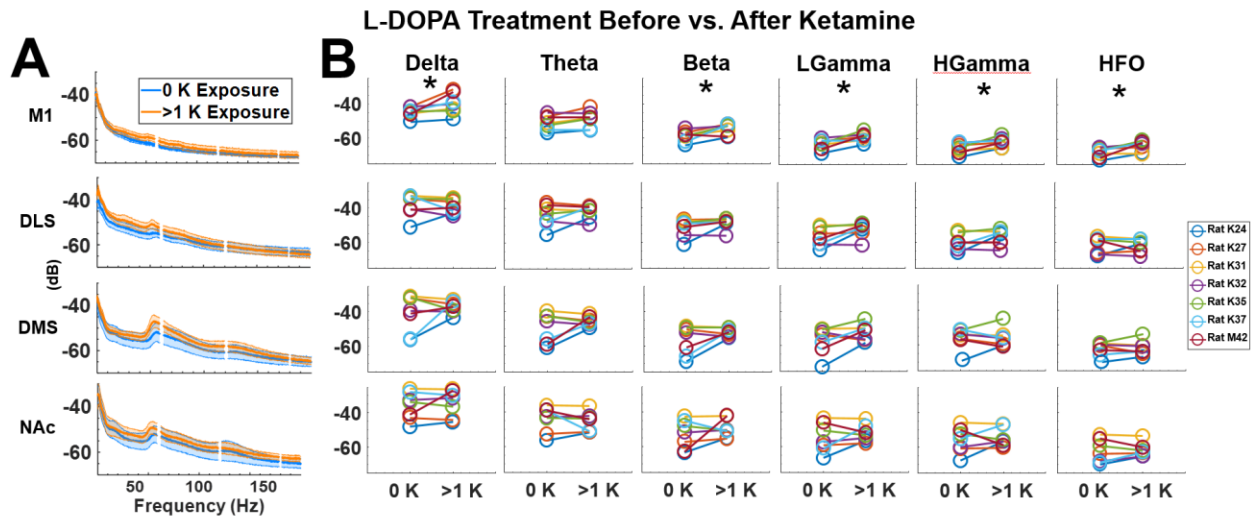


**Figure 21. Repeated ketamine exposure has no lasting effect on L-DOPA-Induced Gamma.** (A) The 5<sup>th</sup> injection (L-DOPA, 22-90 min) of SAL sessions were used for comparison. Average power spectra (dB) for each region is shown. (B) Within-subjects comparisons revealed significant increases in delta, beta, low- and high-gamma, and HFOs only in M1 (all  $p < 0.05$ ). No other significant differences were observed for any frequency band in any region. Contrary to our hypothesis, repeated ketamine does not have lasting reductions on L-DOPA-induced activity.

## **Chapter 10: AIM 2c: Opioid-, D1-, and D2-Receptor Antagonism Does Not Affect Ketamine's Oscillatory Activity During L-DOPA**

LID-induced gamma is thought to be generated by stimulating dopamine D1 and D2 receptors. Ketamine is a partial agonist for D2 receptors, suggesting potential involvement in gamma generation. Other non-dopaminergic systems, such as the opioid system, are also thought to contribute to LID as abnormal increases in opioid signaling have been found in patients with LID (Aubert et al., 2007; Calon et al., 2002). Endogenous opioid receptors act as co-transmitters for striatal MSNs (Gerfen, 1992), it is therefore conceivable that opioid receptors may be involved in regulating gamma oscillations. Given that ketamine serves as an opioid receptor agonist, ketamine-induced stimulation of these receptors on GABA-ergic striatal MSNs may inhibit interneuron activity and decrease L-DOPA-induced gamma. The purpose of Aim 2c was to block specific receptor systems targeted by ketamine during the L-DOPA on-state that may contribute to ketamine's effect on oscillatory activity.

The same group of LID animals ( $n=7$ ) were used in this phase of the experiment 1 week following the completion of the SAL and ketamine sessions. The timeline of these neural recordings is presented in **Figure 22A** (see Methods) with average spectral responses and locomotor activity in **22B-D** for each specific antagonist in each region. The time period chosen was 2-90 min post-injection of ketamine rather than post-injection of antagonist due to the approximate 15 min delay in onset of the drug antagonist. Average 2-90 min spectral response for each region and antagonist is presented in **Figure 23**. The conditions chosen for comparison includes SAL (black), drug antagonist alone (green), ketamine alone (cyan), antagonist +

ketamine (magenta), ketamine + L-DOPA (orange), and antagonist + ketamine + L-DOPA (blue). The color of asterisk corresponds to the condition to which is significantly different.

For the opioid-antagonist Naloxone, we only observed significant differences in M1 (ANOVA,  $F(5,32)=4.13$ ,  $p=0.005$ ,  $\eta^2=0.39$ ) (**Figure 24A, 1<sup>st</sup> row**). Post-hoc multiple comparisons revealed opioid-antagonist + ketamine (magenta) significantly increased low-gamma compared to SAL (black) ( $p=0.01$ ,  $d=2.16$ ). However, opioid-antagonism was not statistically different in the presence of ketamine and/or L-DOPA (all  $p>0.05$ ). This suggests that blocking opioid receptors during ketamine's action on L-DOPA has no effect. No other statistically significant observations were made for opioid-antagonism in the other regions.

For D1-antagonist (SCH-23390), significant differences were observed only in M1 (ANOVA,  $F(5,32)=5.01$ ,  $p=0.001$ ,  $\eta^2=0.36$ ) (**Figure 24A, 2<sup>nd</sup> row**). Post-hoc multiple comparisons revealed low-gamma during D1-antagonist + ketamine (magenta) ( $p=0.01$ ,  $d=2.00$ ), ketamine + L-DOPA (orange) ( $p=0.01$ ,  $d=1.87$ ), and D1-antagonist + ketamine + L-DOPA (blue) ( $p=0.01$ ,  $d=1.69$ ). were all significantly higher compared to SAL (black). However, low-gamma was not statistically different in the presence of D1-antagonist, ketamine and/or L-DOPA (all  $p>0.05$ ), suggesting that blocking D1-receptors during ketamine's action on L-DOPA has no effect on low-gamma.

For D2-antagonist (Eticlopride), significant differences were observed only in M1 (ANOVA,  $F(5,32)=4.32$ ,  $p=0.002$ ,  $\eta^2=0.32$ ) (**Figure 24A, 3<sup>rd</sup> row**). Post-hoc multiple comparisons revealed low-gamma during D2-antagonist + ketamine (magenta) ( $p=0.03$ ,  $d=1.77$ ), ketamine + L-DOPA (orange) ( $p=0.02$ ,  $d=1.87$ ), and D1-antagonist + ketamine + L-DOPA (blue) ( $p=0.009$ ,  $d=1.92$ ). were all significantly higher compared to SAL (black). However, low-gamma was not statistically different in the presence of D2-antagonist, ketamine and/or L-DOPA

(all  $p > 0.05$ ), suggesting that blocking D2-receptors during ketamine's action on L-DOPA has no effect on low-gamma.

Taken together, these findings suggest that blocking opioid-, dopamine D1- and D2-receptors in LID animals does not affect ketamine- or L-DOPA-induced oscillatory activity.

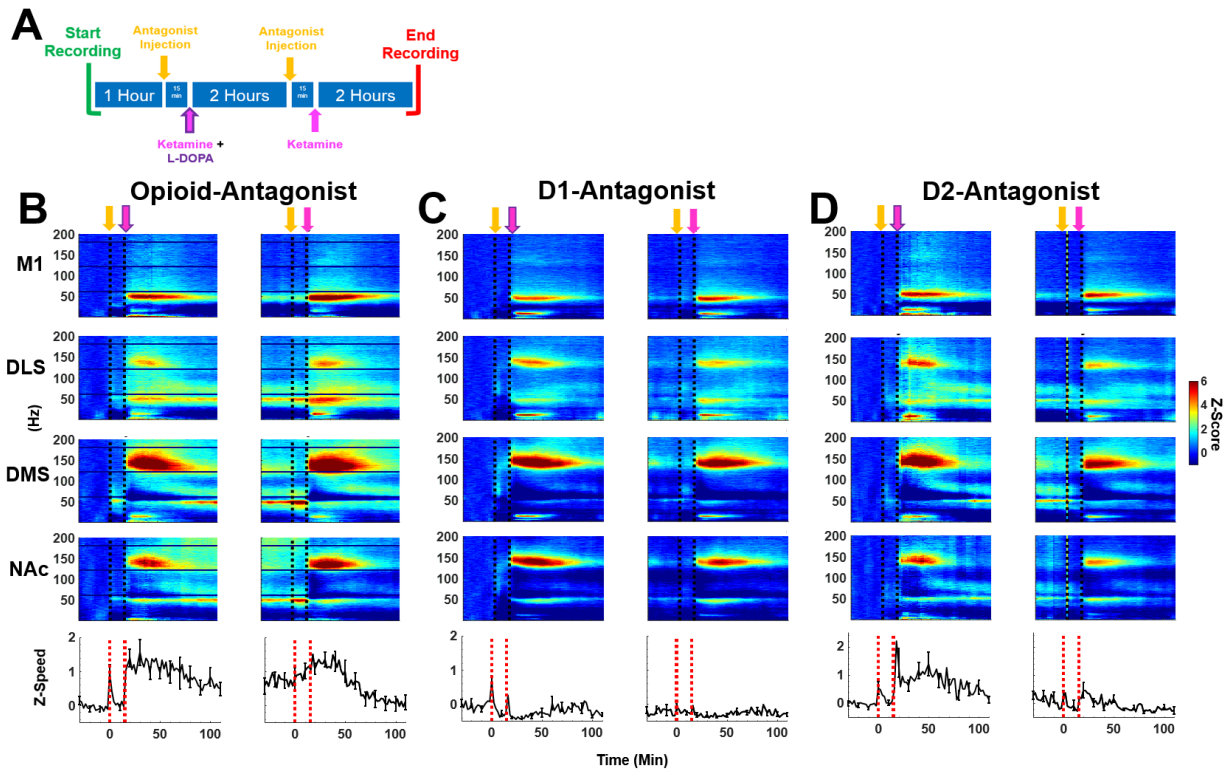


**Figure 22. Experiment 2 receptor antagonism.** (A) Timeline of neural recording session for Experiment 2. Recordings began with a 1-hour baseline. At the 2<sup>nd</sup> hour, a single injection of receptor antagonist was administered followed by a paired injection of ketamine + L-DOPA 15 mins after. This injection scheme was repeated after 2 hours without L-DOPA. (B-C) Average spectral responses ( $n=7$ ) of each receptor antagonist for each region following the timeline in (A). Average locomotor activity is shown on the bottom row.

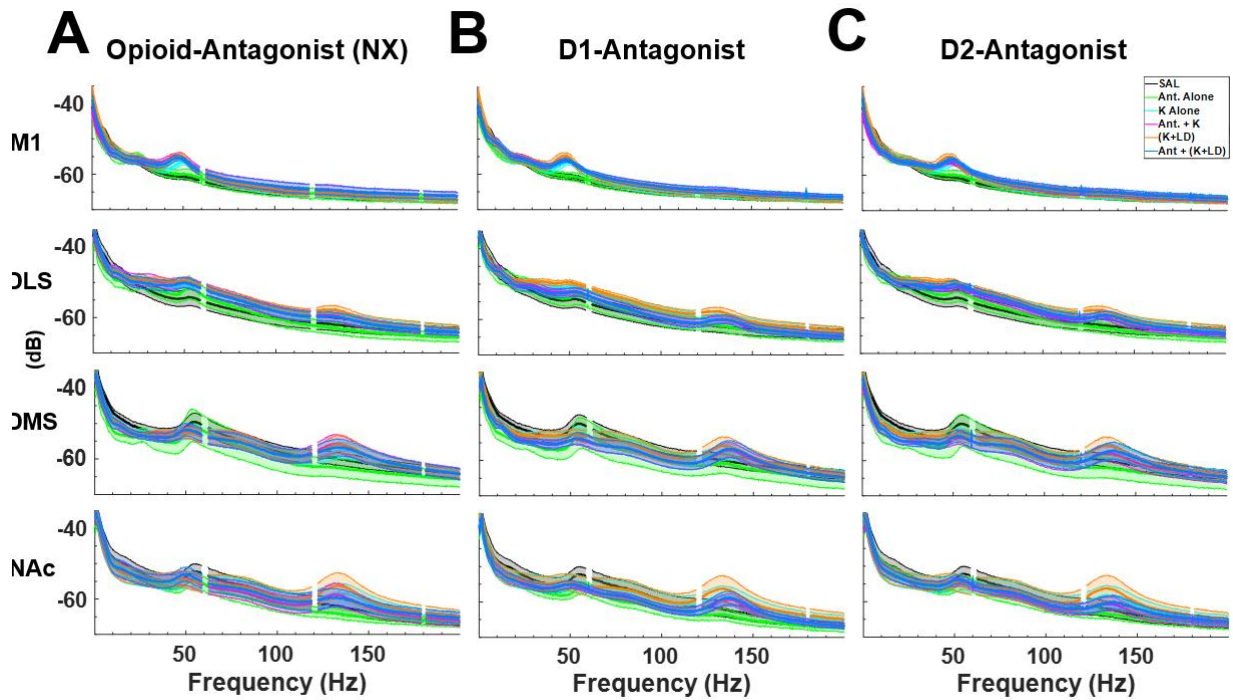


**Figure 23. Average power spectra for each region after drug-antagonist.** (A) Raw spectral responses ( $n=7$ ) for opioid-receptor antagonist Naloxone averaged within the 2-90 min post-injection period, units in power (dB). The conditions chosen for comparison includes SAL (black), drug antagonist alone (green), ketamine alone (cyan), antagonist + ketamine (magenta), ketamine + L-DOPA (orange), and antagonist + ketamine + L-DOPA (blue). (B) As in A but for D1-antagonist. (C) As in A but for D2-antagonist.

## 10.1 Blocking Opioid-Receptors Does Not Affect Ketamine-Induced Locomotion in LID Animals

Significant differences were found for opioid-antagonism on average locomotor activity in LID animals (ANOVA,  $F(5,32)=13.77$ ,  $p=0.007$ ,  $\eta^2=0.66$ ) (**Figure 24B, 1<sup>st</sup> row**). Post-hoc multiple comparisons revealed locomotion was significantly higher when LID animals received opioid-antagonist + ketamine (magenta) ( $p=0.005$ ,  $d=2.09$ ), ketamine + L-DOPA (orange) ( $p=0.0003$ ,  $d=5.31$ ), and opioid-antagonist + ketamine + L-DOPA (blue) ( $p=0.00001$ ,  $d=2.57$ ) compared to SAL (black). Similarly compared to opioid-antagonist alone (green), average locomotion was significantly higher LID animals received opioid-antagonist + ketamine (magenta) ( $p=0.003$ ,  $d=2.13$ ), ketamine + L-DOPA (orange) ( $p=0.000002$ ,  $d=5.2$ ), and opioid-antagonist + ketamine + L-DOPA (blue) ( $p=0.00001$ ,  $d=2.57$ ). Opioid-antagonist + ketamine + L-DOPA (blue) produced significantly higher locomotor activity compared to ketamine alone (cyan) ( $p=0.02$ ,  $d=1.38$ ). Despite these differences compared to SAL and opioid-antagonist alone, blocking opioid-receptors had no effect on locomotion in the presence of ketamine and/or L-DOPA (all  $p>0.05$ ).

## 10.2 Blocking D1-Receptors Suppresses Ketamine and L-DOPA-Induced Locomotion in LID Animals

D1-receptor antagonism produced significant effects in average locomotor activity (ANOVA,  $F(5,32)=64.66$ ,  $p=0.000000000000000006$ ,  $\eta^2=0.87$ ) (**Figure 24B, 2<sup>nd</sup> row**). Post-hoc multiple comparisons revealed administration of D1-antagonist (SCH-23390) with ketamine (magenta) ( $p=0.00000002$ ,  $d=5.28$ ) and with ketamine + L-DOPA (blue) ( $p=0.0000007$ ,  $d=7.22$ ) significantly reduced locomotor activity compared to ketamine alone (cyan) and ketamine + L-DOPA (orange). Similarly, administration of ketamine alone (cyan) produced significantly

greater locomotion than SAL ( $p=0.00002$   $d=3.49$ ) and D1-antagonist alone (green) ( $p=0.00000003$ ,  $d=4.78$ ). Locomotion was also significantly greater with ketamine + L-DOPA (orange) compared to SAL ( $p=0.00000002$   $d=5.31$ ) and D1-antagonist alone (green) ( $p=0.00000002$ ,  $d=6.11$ ). These results suggest that D1-antagonism significantly reduces locomotor activity in all conditions except ketamine + L-DOPA (orange), and ketamine alone (cyan) in LID animals, indicating that low-gamma in M1 is not locomotor-related.

### **10.3 Blocking D2-Receptors Reduces Ketamine-Induced Locomotion But Not in the Presence of L-DOPA**

Antagonism of D2-receptors produced significant differences in locomotor activity in LID animals (ANOVA,  $F(5,32)=64.66$ ,  $p=0.000000003$ ,  $\eta^2=0.63$ ) (**Figure 24B, 3<sup>rd</sup> row**). Post-hoc multiple comparisons revealed that blocking D2-receptors during ketamine (magenta) significantly reduced locomotion compared to ketamine + L-DOPA (orange) ( $p=0.000008$ ,  $d=2.73$ ) and D1-antagonist + ketamine + L-DOPA (blue) ( $p=0.000007$ ,  $d=1.74$ ). However, blocking D1-receptors during ketamine + L-DOPA (blue) did not significantly reduce locomotion compared to ketamine + L-DOPA (orange) ( $p=0.56$ ).

Taken together, D2-antagonism only reduces movement when co-active with ketamine but not during the L-DOPA on-state with ketamine, suggesting ketamine-induced movement relies on both D1-(**24B, 2<sup>nd</sup> row**) and D2-receptors but L-DOPA-induced locomotion does not.

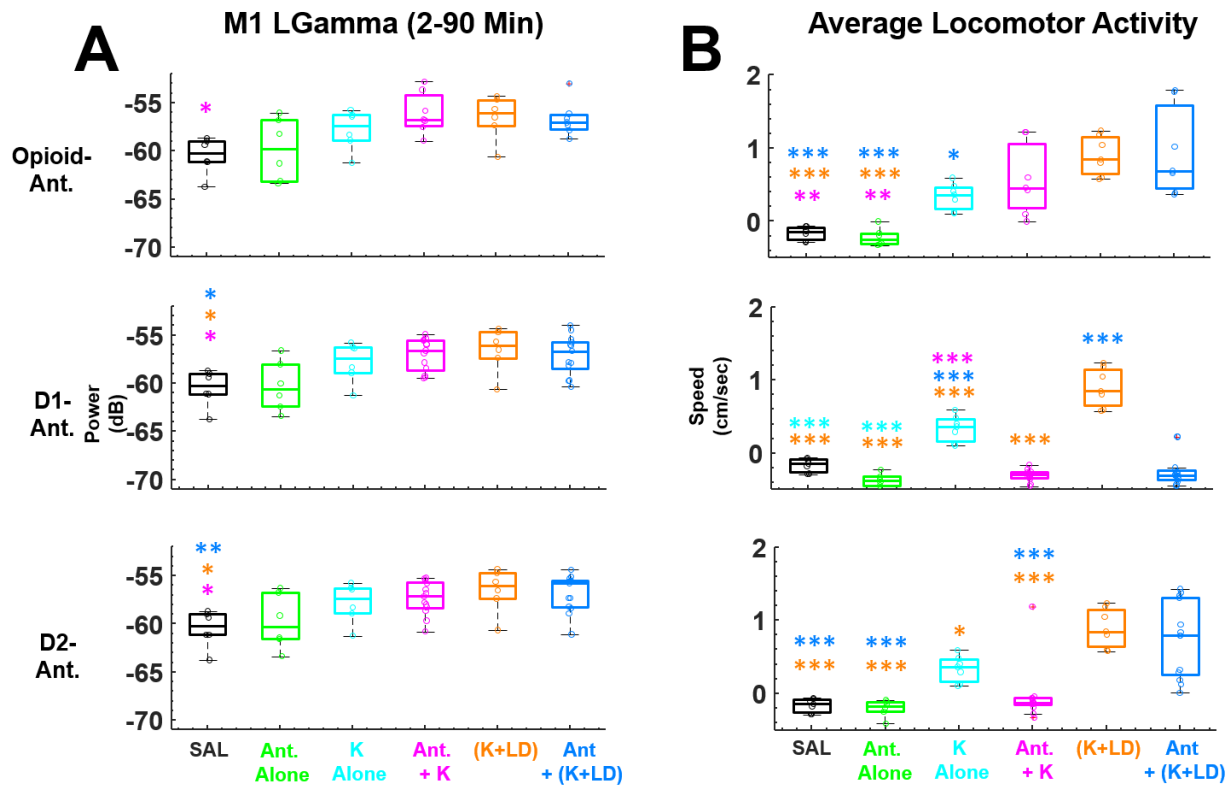


**Figure 24. Opioid-, D1-, and D2-receptor antagonism does not affect ketamine-induced oscillatory activity during L-DOPA in M1.** (A) Average spectral response for each receptor antagonist in M1. The conditions chosen for comparison includes the drug antagonists + ketamine + L-DOPA (blue), ketamine + L-DOPA (orange), drug antagonist + ketamine (magenta), ketamine alone (cyan), drug antagonist alone (green), and SAL (black). The time period chosen was 2-90 min post-injection of ketamine rather than post-injection of antagonist due to the approximate 15 min delay in onset of the drug antagonist. All following statistics are post-hoc tukey-Kramer corrected t-tests. (A, 1<sup>st</sup> row) Antagonism (NX) during ketamine + L-DOPA (blue) was not statistically different compared to ketamine + L-DOPA (orange), NX + ketamine conditions (magenta), or NX alone (green) (all  $p > 0.05$ ). However, opioid-antagonist + ketamine had significantly higher low-gamma compared to SAL ( $p = 0.01$ ,  $d = 2.16$ ). This suggests that opioid-receptor antagonism does not alter low-gamma activity regardless of metabolically active ketamine or L-DOPA. (A, 2<sup>nd</sup> row) Low-gamma activity in the M1 was not altered by D1-receptor antagonism. D1-antagonist + ketamine + L-DOPA (blue), ketamine + L-DOPA (orange) and D1-antagonist + ketamine (magenta) produced low-gamma significantly higher than compared to SAL (all  $p < 0.05$ ). Despite these changes, low-gamma was not statistically different in D1 + ketamine + L-DOPA (blue) vs ketamine + L-DOPA (orange) ( $p = 0.98$ ), suggesting D1 receptors are not involved in ketamine- or L-DOPA-induced gamma. (A, 3<sup>rd</sup> row) low-gamma during D2-antagonist + ketamine (magenta) ( $p = 0.03$ ,  $d = 1.77$ ), ketamine + L-DOPA (orange) ( $p = 0.02$ ,  $d = 1.87$ ), and D1-antagonist + ketamine + L-DOPA (blue) ( $p = 0.009$ ,  $d = 1.92$ ). were all significantly higher compared to SAL (black). However, low-gamma was not statistically different in the presence of D2-antagonist, ketamine and/or L-DOPA (all  $p > 0.05$ ), suggesting that blocking D2-receptors during ketamine's action on L-DOPA has no effect on low-gamma. (B, 1<sup>st</sup> row) Average locomotor activity for conditions in A. Blocking opioid-receptors had no

effect on locomotion in the presence of ketamine and/or L-DOPA (all  $p > 0.05$ ). (**B, 2<sup>nd</sup> row**) D1-antagonism significantly reduces locomotor activity in all conditions except ketamine + L-DOPA (orange), and ketamine alone (cyan) in LID animals, indicating that low-gamma in M1 is not locomotor-related (all  $p < 0.001$ ). (**B, 3<sup>rd</sup> row**) D2-antagonism only reduces movement when co-active with ketamine but not during the L-DOPA on-state with ketamine (all  $p < 0.001$ ), suggesting ketamine-induced movement relies on both D1-(**B, 2<sup>nd</sup> row**) and D2-receptors but L-DOPA-induced locomotion does not.

## **Chapter 11: Beta Oscillations in 6-OHDA-Lesioned Animals Are Unaffected by Ketamine**

Injections of ketamine did not reduce overall beta power or alter beta CFC in any region of 6-OHDA rats. We examined ketamine's effect during its metabolically active period (i.e., 2-90 min post-injection) as well as its non-active periods (i.e., 92-110 min post-injection) along with the acute effects from injection 1 to lasting effects after the 5<sup>th</sup>/final injection. Contrary to our original hypothesis, we did not observe a clear reduction of overall beta power during injections 1 or 5 in either post-injection period after ketamine. Several reasons may account for this null effect. Ketamine's primary affinity is for NMDA ionotropic glutamate receptors, directly antagonizing the function of these receptors (Harris et al., 1968). However, ketamine's mechanism is complicated by multiple functions such as increasing system levels of DA, glutamate, acetylcholine (ACh), among others (Gunduz-Bruce, 2009; Sleight et al., 2014a). It is established that DA depletion results in abnormal beta oscillations, and administering DA replacement therapy (e.g., L-DOPA) restores net DA levels thereby reducing hypersynchronous beta oscillations. Since L-DOPA is a precursor to DA, it is conceivable that increased DA production/release underlies the reduction of beta in a DA-depleted brain. Ketamine also stimulates DA release in both the striatum and cortex, and is a partial agonist for D2 receptors (Kokkinou et al., 2018). Given that ketamine stimulates DA release with some action on DA receptors akin to L-DOPA, it is conceivable that ketamine would also reduce abnormal beta oscillations as well. Since we did not observe this, it is possible that ketamine-induced DA release and receptor stimulation is not enough to reduce beta in a 6-OHDA-lesioned animal. Although ketamine significantly increases DA release in the cortex and striatum (Kokkinou et al., 2018), the magnitude of DA release compared to L-DOPA may not be as comparable. Future

studies should implement real-time measurements of DA release (e.g., fast-scan cyclic voltammetry, fast scan controlled-absorption voltammetry) after acute and repeated injections of ketamine vs. L-DOPA in the cortex and striatum of 6-OHDA-lesioned animals to test this hypothesis.

Beta oscillations are also thought to be related to GABA activity. Increasing GABA either by stimulation of GABA-A receptors or GABA-reuptake inhibitors has been found to increase beta power (Hall et al., 2010; Muthukumaraswamy et al., 2013). Ketamine is also known to be a GABA-A receptor agonist (Sleigh et al., 2014). There is also some evidence suggest that NDMA receptor antagonism (i.e., ketamine's primary mechanism) may also increase global GABA levels (Wood and Hertz, 1980). It is therefore conceivable that ketamine-induced GABA increase and/or GABA-A receptor agonism prevents the reduction of beta power in 6-OHDA-lesioned animals. Future studies can test this hypothesis by blocking GABA-A receptor subtypes  $\alpha 6\beta 3\delta$  and  $\alpha 6\beta 2\delta$  with an injection of ketamine as these receptor subtypes have been found to be directly activated by ketamine (Hevers et al., 2008).

## **11.1 Suppression of Low- and High-Gamma, and HFOs in the 92-110 Min Period of 6-OHDA-Lesioned Animals**

In M1, DMS, and NAc, we observed significant reductions in low- and high-gamma, and HFOs in the 92-110 min post-injection period of 6-OHDA-lesioned animals compared to naïve. This was a surprising finding as we show ketamine produces the opposite effect in the naïve groups. The most evident explanation for this between group difference is the lack of striatal DA in the 6-OHDA animals. The suppression of gamma and HFOs in 6-OHDA animals after ketamine's metabolically active period may suggest that the DAergic system facilitates long-

term ketamine-induced oscillatory activity. Evidence supports this theory as chronic exposure to ketamine in healthy rats increased DA concentrations (Li et al., 2015). Ketamine-induced DA release may be required for the increase in low-, high-gamma, and HFOs in naïve animals for the 92-110 min period. Given the DA-depleted hemisphere of our 6-OHDA animals, it is conceivable that ketamine's effect on the DA system does not last beyond its metabolically active period. Furthermore, suppression of these frequencies in 6-OHDA animals may not be locomotor related as average locomotion was not statistically different in the 92-110 min period compared to naïve animals for either injection 1 or 5 (**Figure 12D**).

## **11.2 Prior History of Extended Ketamine Exposure Does Not Alter Resting-State Oscillatory Activity in 6-OHDA-Lesioned Animals**

Contrary to our original hypothesis, ketamine exposure does not acutely reduce beta oscillations in 6-OHDA-lesioned animals. We therefore explored whether prior history of ketamine exposure would reduce resting-state beta oscillations and compared the pre-injection 1 baseline from neural recordings prior to any ketamine exposure vs. more than one exposure (**Figure 13**). We did not observe any significant within-subject differences for beta or other frequency bands. One explanation for this null result may again be due to the lack of an intact DAergic system in the lesioned hemisphere of our 6-OHDA animals. Ketamine is thought to stimulate DA release in both cortex and striatum (Kokkinou et al., 2018). However, the lack of DA to begin with in these animals may render this mechanism of ketamine ineffective. Furthermore, despite the suppression of gamma and HFOs after ketamine's metabolically active period M1, DMS, and NAc (**Figure 12**), we did not observe any lasting suppression of these frequencies. However, it is conceivable that long-term structural changes after ketamine exposure in the DA-lesioned hemisphere is taking place that is not reflected in overall oscillatory

power (Phoumthippavong et al., 2016a). Future studies can implement real-time DA measurements and examination of spine density to test this theory.

### **11.3 Lack of Ketamine-Induced Cross-Frequency Interactions in 6-OHDA Animals**

In naïve animals, we showed an increase in delta- and theta-HFO CFC in the corticostriatal regions (see **Figure 7**). We explored CFC in 6-OHDA-lesioned animals to answer the question of whether these cross-frequency interactions were also present in the diseased brain. We did not observe any changes in delta- or theta-HFO CFC after ketamine exposure in our 6-OHDA group (**Figure 14**). However, the increased delta- and theta-HFO coupling in naïve animals injections 1 and 5 were significantly greater compared to 6-OHDA-lesioned animals only in M1 and DLS (2-90 min). These changes are in line with the overall power increase after ketamine injections in naïve animals. As such, the lack of DA in 6-OHDA-lesioned animals may also underlie the null effects of ketamine on cross-frequency interactions. CFC is thought to facilitate information transfer across regions (Canolty and Knight, 2010). Aberrant CFC is implicated in disorders such as schizophrenia (Allen et al., 2011) and Parkinson's disease (Belić et al., 2016). The observation of increased CFC between the lower frequencies and HFOs is only present in naïve animals after ketamine. Delta oscillations are thought to be generated by the thalamic and cortical regions, yet striatal origins of delta are not well understood (Lőrincz et al., 2015; Steriade et al., 1994). Our finding that both the lack of increase in delta power and delta CFC in 6-OHDA animals suggest involvement of DA as naïve animals with an intact DAergic system is capable of ketamine-induced changes to the delta frequency.

Another interesting observation was the lack of HFO and HFO coupling in 6-OHDA-lesioned animals. Evidence suggest that HFOs are generated by the NAc as tetrodotoxin

inactivation eliminates HFOs (Olszewski et al., 2013). Our finding in 6-OHDA animals suggest DAergic activation of the NAc is involved in HFO generation.

## **Chapter 12: Results of Aim 2a: L-DOPA Did Not Trigger Focal 80 Hz High-Gamma in LID Animals**

### **12.1 Differences in L-DOPA Priming**

Contrary to the existing literature (Dupre et al., 2016; Halje et al., 2012), we did not observe a focal 80 Hz response after a L-DOPA injection in LID animals. Instead, L-DOPA triggered region-dependent low-to-wide-band gamma oscillations. Several reasons may account for this finding. The L-DOPA priming protocol used here (Bartlett et al., 2016) contained major differences compared to others (Dupre et al., 2016; Halje et al., 2012). The animal model of LID requires a 6-OHDA lesion and subsequent chronic treatment with L-DOPA to produce dyskinesia. In humans, LID will only occur once the patient is diagnosed with Parkinson's disease and undergoes treatment with L-DOPA and animal models of LID are no exception. First, healthy naïve rodents undergo 6-OHDA lesion surgeries to replicate a DA-depleted striatum. After recovery from the surgery, the L-DOPA priming stage begins. The priming protocol used by Halje et al. (2012) and Dupre et al. (2016) is considered an accelerated model of LID such that larger doses of L-DOPA are administered to induce dyskinesia in a short amount of time. The doses used by these groups were approximately twice as large with the total priming period resulting in 1/3 of the time compared to our priming protocol. Dupre et al. (2016) used a dose of 12 mg/kg of L-DOPA daily for 7 days with neural recordings taking place during the 7-day priming period. Halje et al. (2012) used a L-DOPA dose of  $15.6 \pm 4.8$  mg/kg daily

although the exact duration is not specified. We primed our 6-OHDA-lesioned animals with only 7 mg/kg of L-DOPA for 21 days prior to electrode implantation and continued administering maintenance doses of L-DOPA (7 mg/kg) every 2-3 days to maintain dyskinesia (Dekundy et al., 2007). This extended L-DOPA priming protocol used here leads to a dyskinetic state that is steadily established (weeks vs days) and may therefore be more clinically relevant as human PD patients develop LID after several years of L-DOPA treatment (De Jong et al., 1987; Hauser et al., 2007).

Another reason why we couldn't replicate the focal 80 Hz may be due to the severity of dyskinesia. The composite AIMs score of our LID animals  $33.6 \pm 6.6$  (mean  $\pm$  S.D.) (**Table 1**) is classified as mild-to-moderate dyskinesia (Bartlett et al., 2016). Other groups used a L-DOPA dose nearly twice the amount of ours (12 mg/kg vs 7 mg/kg) with a composite AIMs score of  $56 \pm 13$  (mean  $\pm$  S.D.) during the very first injection of L-DOPA (Dupre et al., 2016). Dyskinesia can manifest with a large enough dose of L-DOPA (Iderberg et al., 2012), it is possible that the focal 80 Hz response may only be associated with severe dyskinesia. It is therefore conceivable that the reason why we observed a different gamma response was due to a longer L-DOPA priming process with lower doses. Future experiments can test this question by using the accelerated L-DOPA priming protocol to replicate the focal 80 Hz and use escalating doses of L-DOPA on multiple groups to assess dose-response changes in L-DOPA-induced gamma.

It is also important to note the difference in the time of when neural recordings began. Halje et al. (2012) began L-DOPA priming and neural recordings approximately 1 week after the 6-OHDA lesion surgeries. Dupre et al. (2016) began L-DOPA priming and recording 14 days after 6-OHDA lesions. In our experiment, L-DOPA priming commenced approximately 3 weeks post-6-OHDA lesion with a total priming duration of 21 days. Animals were then subjected to

the electrode array implantation surgery followed by 1 week of recovery before any neural recordings began. Effectively, our LID animals have been dyskinetic for a longer period before neural data collection. It is therefore conceivable that the focal 80 Hz gamma observed by other groups only manifests at the early stages of L-DOPA priming then diffusing into broader gamma frequency ranges. However, there is one study in human PD patients with LID that shows increased 60 – 80 Hz gamma during the L-DOPA ‘on-state’ in the STN (Alonso-Frech et al., 2006). Although the authors report patients’ average PD duration of 10.5 years, the duration of their DA replacement therapy is unclear. Therefore it is not possible to draw firm conclusions between the L-DOPA-induced response between the only existing human study and the present experiment.

## **12.2 L-DOPA-Induced Wide-Band Gamma Mechanism**

Gamma oscillations are involved in many functional roles such as synchronizing the timing of action potentials to support plasticity and inter-region communication (Buzsáki and Wang, 2012; Colgin et al., 2009). The generation of gamma oscillations are still debated, but it is generally thought to be the result of reciprocal interactions between excitatory (glutamatergic) and inhibitory (GABAergic) neurons (Buzsáki and Wang, 2012). The reciprocal interactions between these two types of neurons are regulated by inhibitory post-synaptic potentials (IPSPs) lasting approximately 12-50 ms. This range of delay results in gamma oscillations that are 20–80 Hz and the rapidly varying IPSPs determines the peaks in gamma from narrow to wide-band (Welle and Contreras, 2017). A proper balance between these excitatory and inhibitory neurons are required to generate normal gamma oscillations. Evidence shows that DA acting on D1 receptors increases the excitability of striatal fast-spiking inhibitory interneurons (Towers and Hestrin, 2008; Tseng et al., 2006). Manifestation of LID is thought to be the result of DA

stimulation of the hypersensitive D1 receptors in the DA-depleted striatum. Therefore, it is conceivable that the striatal fast-spiking interneurons expressing D1 receptors have also become hypersensitive after DA depletion and stimulation via L-DOPA DA release enhances interneuron excitability resulting in wide-band gamma observed here.

### **12.3 Baseline AIMs Scores Were Not Significantly Correlated to L-DOPA-Induced Gamma**

Other groups have shown that focal 80 Hz gamma is correlated with the onset and duration of dyskinesia (Dupre et al., 2016; Halje et al., 2012). However, one limitation of the present experiment was the absence of behavioral AIMs scoring during neural recordings. Given the differential gamma response in our experiment, we asked whether the degree of baseline dyskinesia is correlated to post-baseline L-DOPA-induced gamma. To supplement this limitation, composite AIMs scores prior to electrode implantation for each LID animal was correlated to the L-DOPA-induced gamma for each region (**Figure 16**). We observed large correlation coefficients for the L-DOPA-induced gamma in each region to baseline AIMs scores, however these were not statistical significant. This may be due to the lack of statistical power, and therefore cannot firmly conclude that baseline severity of dyskinesia is associated with L-DOPA-induced gamma response. Future experiments can answer this question by increasing the sample size and conduct behavioral scoring during neural recordings.

## **12.4 Gamma Response Immediately After L-DOPA Administration in LID Animals**

The onset of L-DOPA occurs approximately 20 min post-injection (Bastide et al., 2015) with maximum striatal DA concentrations at 20-30 min (Shen et al., 2003). Others have observed the onset of L-DOPA-induced gamma to coincide with this time frame (Dupre et al., 2016; Halje et al., 2012). It is therefore a surprising and novel finding that gamma in the same frequency as that after L-DOPA exposure to occur immediately after the injection of L-DOPA. We compared gamma-band activity of our LID animals receiving an injection of L-DOPA + SAL to naïve animals receiving an injection of SAL and found that gamma and locomotor activity was not statistically different (**Figure 17**). Although we cannot firmly conclude the cause of the immediate gamma response, this comparison suggests that the immediate gamma response in our LID animals may be locomotor related.

## **12.5 Repeated Ketamine Exposure Does Not Acutely or Chronically Reduce L-DOPA-Induced Gamma**

Recent reports have shown the therapeutic benefits of repeated low-dose ketamine in LID using both patients and animal models (Bartlett et al., 2016; Sherman et al., 2016), however the mechanisms underlying ketamine's efficacy is unknown. Using the identical experimental protocol of Bartlett and colleagues (2016) with the addition of electrophysiological recordings, we assessed the acute and long-term oscillatory changes in LID animals after repeated ketamine exposure. We found that L-DOPA-induced gamma varied depending on the region such that a low-gamma response (35 – 58 Hz) was observed in M1 while the DLS, DMS, and NAc produced a wide-band gamma response (40 – 85 Hz). Therefore, different gamma bands were chosen for

analysis depending on the region. We compared the 5<sup>th</sup> injection of ketamine vs SAL sessions as the 5<sup>th</sup> injection was always paired with L-DOPA to induce the AIMs (i.e., on-state).

Contrary to our original hypothesis, repeated ketamine does not reduce overall L-DOPA-induced gamma power in M1, DLS, DMS, or NAc (**Figure 19**). The mechanism of ketamine-induced gamma is not well understood. As mentioned in the previous section, it is believed that gamma oscillations are dependent on the interaction between excitatory pyramidal neurons and inhibitory interneurons. The dichotomy between low- and high-gamma are likely generated by distinct local circuits (e.g., interneuron-interneuron (high-gamma) vs. pyramidal-interneuron networks (low-gamma)). Our initial hypothesis (AIM 2a) that simultaneous activation of ketamine-induced low-gamma and L-DOPA-induced high-gamma would cause a disruption in the two competing gamma-generating circuits that ultimately reduces pathological high-gamma. However, given that we observed L-DOPA to trigger wide-band gamma that overlaps with and is not reduced by ketamine-induced low-gamma, this would suggest that ketamine and L-DOPA operate on the same gamma networks. As mentioned in the previous section, DA and D1 receptors are implicated in the balance of excitatory and inhibitory neurons for gamma generation (Towers and Hestrin, 2008; Tseng et al., 2006). DA release via L-DOPA may stimulate the hypersensitive D1-expression GABAergic neurons and shift the balance to increase gamma oscillations. NMDA receptor-activation is also critical for the balance of interneuron circuits. NMDA antagonists such as ketamine may inhibit GABAergic NDMA-expressing interneurons. In turn, this disinhibits excitatory glutamatergic neurons to result in increased gamma oscillations (Hakami et al., 2009). If both ketamine and L-DOPA are working equally to disrupt the same interneuron gamma networks, this may also explain why we did not observe any long-term reductions in gamma oscillations after ketamine exposure (**Figure 21**).

## 12.6 Differential Effects on Cross-Frequency Coupling During Ketamine + L-DOPA

Cross-frequency coupling is thought to serve functional roles in the brain by facilitating information transfer over local and large-scale networks. The high-frequency activity likely reflects coordinated local populations of neurons whereas low-frequency activity is entrained across brain region (Canolty and Knight, 2010). Although CFC has been widely investigated in the domains of learning and memory (Lisman and Jensen, 2013a), interactions between frequencies in LID remains relatively unexplored. To our knowledge, only one report exists that inspects CFC in LID and found decoupling between theta (10 Hz) and L-DOPA-induced focal high-gamma (80 Hz) in the striatum and cortex (Belić et al., 2016). It is important to note that this report used the accelerated L-DOPA priming protocol as Halje et al. (2012).

Given that we found increased delta- and theta-HFO coupling in naïve animals, we asked whether this effect was also present in LID animals. We did not observe significant changes in delta- or theta-HFO coupling in LID animals given L-DOPA and/or ketamine (**Figure 20**). Naïve animals given ketamine alone did produce significant delta- and theta-HFO CFC in the M1 and DLS compared to LID animals. Given that this effect was also not present in 6-OHDA-lesioned animals, we can conclude that ketamine-induced delta- and theta-HFO CFC is only present in the DLS and M1 of a healthy brain with a functioning DAergic system.

We did observe differential effects of L-DOPA vs L-DOPA + ketamine on CFC in the DMS and NAc of LID animals. In the DMS, administration of ketamine + L-DOPA significantly enhanced theta-HFO coupling compared to an injection of L-DOPA alone. The neighboring

striatal region such as the NAc poses as a likely candidate as a generator for HFOs after ketamine exposure (Hunt et al., 2006a, 2015) as inactivation of the NAc with tetrodotoxin eliminates ketamine-induced HFOs (Olszewski et al., 2013). HFOs in the NAc are believed to be dependent on NMDA receptors as non-competitive NMDA receptor antagonists such as ketamine and MK-801 triggers these oscillations (Hunt et al., 2006a). It is conceivable that the NAc's HFOs entrain other striatal regions as observed here. Naturally-occurring theta-HFO coupling in the striatum has also been found in healthy naïve animals traversing a goal-directed maze (Tort et al., 2008). While ketamine-induced theta-HFO coupling in the striatum is thought to drive hyperlocomotion (Cordon et al., 2015). This would suggest that theta-HFO coupling is locomotor-related.

In the NAc of LID animals, we observed significant decoupling in theta-high-gamma CFC during ketamine alone and ketamine + L-DOPA compared to L-DOPA alone. This is somewhat consistent with the existing report on LID CFC such that theta frequencies were decoupled with high-gamma. However, the notable difference is that we did not observe any focal 80 Hz high gamma (Belić et al., 2016). Gamma oscillations in M1 are associated with movement execution (Muthukumaraswamy, 2010), and the gamma-theta frequencies are often co-generated during exploration (Hsiao et al., 2016). Others have shown that theta-gamma coupling in the sensorimotor areas may reflect different movement and behavioral states (Igarashi et al., 2013), Theta-high-gamma coupling in the NAc is also an interesting observation as evidence in humans have shown that this is correlated with cognitive control in monitoring movement programs (Dürschmid, 2013). This suggests that coupling of theta and gamma oscillations is involved in structuring motor-related activity. Given that we observed decoupling of theta-gamma, this would indicate that LID rats during ketamine + L-DOPA exposure have a

decreased capacity to regulate controlled movement. Given the evidence that LID animals eventually regain voluntary movement (i.e., reduction of LID) after repeated ketamine (Bartlett et al., 2016), this decreased control of movement suggested by theta-high-gamma decoupling may only be a short-term effect during ketamine + L-DOPA treatment.

# Chapter 13: AIM 2c: Opioid-, D1-, D2-Receptor Antagonism Did Not Alter Ketamine-Induced Oscillations During L- DOPA, But Differential Effects on Locomotion Were Observed

## 13.1 Blocking Opioid Receptors Did Not Alter Ketamine-Induced Oscillatory Activity During L-DOPA

We tested the hypothesis of whether blocking ketamine's specific receptor targets during the L-DOPA on-state will reduce L-DOPA-associated gamma. We compared conditions during which a receptor antagonist (e.g., opioid, D1, D2) was co-administered with ketamine + L-DOPA with ketamine + L-DOPA alone and control conditions (e.g., SAL, antagonist alone, antagonist + ketamine). In M1 (**Figure 24**), blocking opioid receptors during ketamine + L-DOPA (blue) did not significantly alter low-gamma compared to ketamine + L-DOPA (orange). Given that ketamine is an opioid receptor agonist, blocking its action on opioid receptors has no effect on low-gamma oscillations in during the L-DOPA on-state. The only significant effect we observed in M1 with naloxone was that low-gamma significantly increased in conditions involving co-administration of naloxone with ketamine (**Figure 24A, top row**) compared to SAL (black, magenta). Conditions involving any combination of opioid-antagonist, ketamine, and/or L-DOPA had significantly greater locomotor activity than the control conditions (**Figure 24B, top row**). Given that locomotor activity for the injection of naloxone alone (green) was not statistically different than SAL (black), this suggests that the increased locomotion observed in the other conditions were likely the result of ketamine- or L-DOPA-induced movement. Contrary to our original hypothesis, opioid receptors do not play a role in regulating gamma oscillations

despite ketamine's high affinity for this system (Fink and Ngai, 1982; Gupta et al., 2011). However, it is important to note that specific opioid receptors with a higher affinity may prove to be a better target especially for the striatal regions as we did not observe significant differences in these regions. Naloxone is non-selective opioid receptor antagonist that blocks multiple opioid receptors at varying degrees of affinity ( $\mu$ -,  $\delta$ -, then  $\kappa$ -opioid receptors) (Nestler et al., 2002). The striatum is in abundance with  $\mu$ - and  $\delta$ -opioid receptors (Hadjiconstantinou and Neff, 2011), therefore, using selective opioid receptor antagonists (e.g.,  $\delta$ -selective antagonist naltrindole,  $\mu$ -selective antagonist CTAP,  $\kappa$ -selective antagonist binaltorphimine) may better determine ketamine's effect on L-DOPA-associated oscillatory activity. Future studies can test this question by co-administration of ketamine with selective blockade of opioid receptors. Specific  $\mu$ -opioid receptor targets are currently being studied for their potential anti-dyskinetic properties (Koprach et al., 2011).

### **13.2 Differential Effects of D1- And D2-Receptor Antagonism on Locomotor Activity Despite Lack of Impact On Ketamine-Induced Oscillatory Activity**

We observed that blocking D1 receptors during ketamine + L-DOPA administration does not alter ketamine-induced oscillatory activity during the L-DOPA on-state in M1 (**Figure 24A, 2<sup>nd</sup> row**, blue vs orange). These two conditions were also not statistically different compared to D1-antagonist + ketamine (magenta). This would suggest that blocking D1-receptors does not alter ketamine-induced low-gamma oscillations when co-administered with L-DOPA. We also observed that any condition involving D1-antagonist obliterated all locomotor activity (**Figure 24B, 2<sup>nd</sup> row**), despite the null effect on low-gamma. We previously found that D1-antagonist

reduces both low-gamma in M1 and locomotor activity in naïve rats (Ye et al., 2018). This would suggest that D1 receptors are crucial for ketamine-induced low-gamma in healthy naïve animals but not LID animals.

D2 receptor antagonist also had no effect on ketamine + L-DOPA administration (**Figure 24A, 3<sup>rd</sup> row**, blue vs orange) similar to the naloxone conditions. The most interesting observations were made on the locomotor activity. In LID animals, blocking D2 receptors during ketamine + L-DOPA (blue) administration does not alter locomotor activity compared to ketamine + L-DOPA (orange) (**Figure 24B, 3<sup>rd</sup> row**). However, co-administration of D2-antagonist with ketamine (magenta) significantly reduced locomotor activity compared to D2-antagonism with ketamine + L-DOPA (blue). D2 receptor blockade only reduces ketamine-induced locomotion but not when L-DOPA is involved. This suggests that ketamine-induced movement is dependent on both D1 (**Figure 24B, 2<sup>nd</sup> row**; magenta) and D2 receptors (**Figure 24B, 3<sup>rd</sup> row**; magenta), but L-DOPA-induced movement even co-administered with ketamine only relies on D1 receptors. This consistent with other groups reporting D1 antagonism reduces locomotor activity in LID (Halje et al., 2012a). These results indicate that blocking ketamine's action on D2 receptors eliminates movement only if L-DOPA is not simultaneously co-active. The increased locomotor activity in the D2-antag + ketamine + L-DOPA (**24B, 3<sup>rd</sup> row**; blue) compared to D2-antag + ketamine (**24B, 3<sup>rd</sup> row**; magenta) is likely due to the overstimulation of D1 receptors by L-DOPA to create movement.

## Chapter 14: Conclusions

Low-dose extended ketamine exposure is increasingly being used to successfully treat disorders such as chronic pain, treatment-resistant depression, and movement disorders. Despite its therapeutic efficacy, extended exposure to low-dose ketamine has never been investigated and thus not well understood. The goal of this dissertation was to fill this wide gap of knowledge regarding repeated exposure to low-dose ketamine in the healthy and diseased brain states. Using a validated infusion protocol combined with in-vivo neurophysiological recordings, we targeted multiple regions in the corticostriatal circuit of healthy naïve animals as well as the DA-depleted hemisphere of 6-OHDA-lesioned animals and found results that were contrary to our hypotheses.

In naïve animals, prolonged exposure to low-dose ketamine does not enhance gamma or HFOs in corticostriatal circuits, but rather enhances the coordination between low and high frequencies in the striatum. Conversely, ketamine reduced coordination in the hippocampus. These results suggest differential restructuring of corticostriatal and limbic circuits that may contribute to ketamine's therapeutic efficacy.

We discovered that the overall power of pathological beta oscillations were not affected by repeated exposure to ketamine. This null effect was not exclusive to 6-OHDA-lesioned animals as we observed the same results compared to naïve controls. Repeated low-dose ketamine exposure did not reduce L-DOPA-associated gamma activity in M1, DLS, DMS, or NAc during treatment. We then assessed any lasting (e.g., weeks) changes in L-DOPA-induced oscillatory activity examining the L-DOPA on-state prior to any ketamine exposure vs. more than 1 exposure and did not reveal significant reductions in pathological oscillations. Subsequently, we asked whether the lack of change in oscillatory power was due to ketamine's action on multiple receptor systems. To test this question, co-administration of ketamine with

opioid-, D1-, or D2-receptor antagonists was given to LID animals and observed no change in oscillatory activity.

Despite the lack of change in overall oscillatory power, we discovered that ketamine has differential effects on cross-frequency coupling during ketamine exposure. For example, the absence of ketamine-induced delta- and theta-HFO CFC in LID M1 and DLS but highly prevalent in naïve animals. Ketamine + L-DOPA administration in the DMS of LID animals significantly increased theta-HFO coupling compared to L-DOPA alone, while ketamine + L-DOPA significantly decoupled theta-high-gamma in the NAc compared to L-DOPA alone. This indicates that L-DOPA administration in LID animals have differential and region-dependent effects on cross-frequency interactions and co-administration of ketamine successfully reverses L-DOPA-induced CFC. These findings suggest that ketamine-induced cross-frequency interactions in LID may contribute to its therapeutic benefits, however we cannot firmly conclude this relationship given the limitation that behavior AIMs scoring was not conducted during neural recordings.

Another interesting finding of this set of experiments is the region-dependent L-DOPA-induced low-to-wide-band gamma. Previous reports have established a focal 80 Hz high-gamma response in M1 and DLS after L-DOPA injection in LID animals (Dupre et al., 2016; Halje et al., 2012). Here, we are the first to report that L-DOPA triggers low-gamma (35 – 58 Hz) in M1 and wide-band gamma (40 – 85 Hz) in the striatum (**Figure 15**). Our findings are likely due to methodological differences in L-DOPA priming. The accelerated model used by other groups primed 6-OHDA-lesioned animals with L-DOPA (12 – 16 mg/kg) for 7 days, whereas we primed our animals with half the dose (7 mg/kg) for 21 days followed by maintenance injections every 2-3 days for the duration of the experiments. This extended priming protocol ensures a

steady development of AIMS and may be more clinically relevant as LID takes several years to develop in human patients with Parkinson's disease.

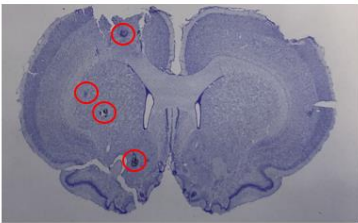
Overall, our findings suggest that ketamine produces differential effects on overall oscillatory power and cross-frequency interactions across the naïve and diseased brain states. The acute oscillatory responses during repeated ketamine exposure may not contribute to its therapeutic effects but may trigger the initiation of gradual synaptic reorganization that is not reflected in overall oscillatory power. This further highlights the complexity of ketamine's mechanism of action and calls for future experiments to utilize multiple complimentary techniques (e.g., in-vivo electrophysiology, real-time neurotransmitter detection, ex-vivo examination of spine density) to draw firm conclusions of ketamine's therapeutic efficacy in treating multiple disorders. Furthermore, using these methods to investigate ketamine's metabolites (e.g., hydroxynorketamine (HNK)) will open new avenues for therapeutic applications to other disorders as recent evidence suggests an enhanced anti-depressant effect without the abuse potential and side effects of racemic ketamine (Zanos et al., 2016). Currently, no one has explored the effects of ketamine's metabolites on oscillatory activity. Future experiments should implement the infusion protocol used here to investigate HNK-induced oscillations in both healthy and disease brains.

# Appendices

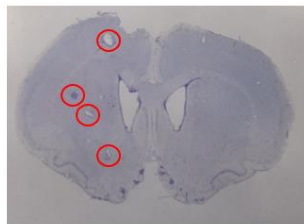
## Appendix A: Nissl-Stained Tissue of Naïve Animals ( $n=8$ )

### Electrolytic Lesions

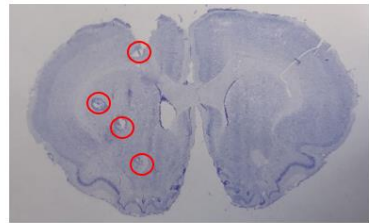
**Rat 89**



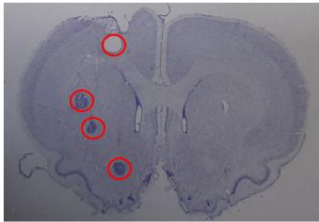
**Rat 90**



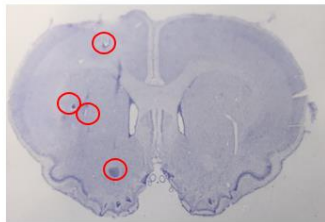
**Rat 91**



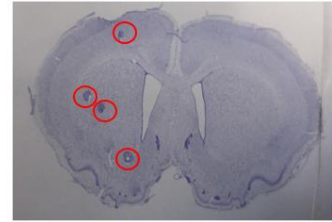
**Rat 168**



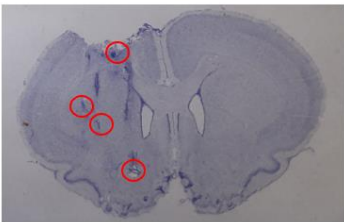
**Rat 169**



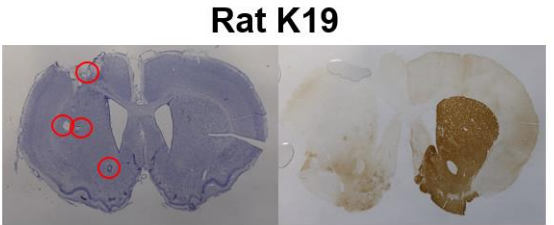
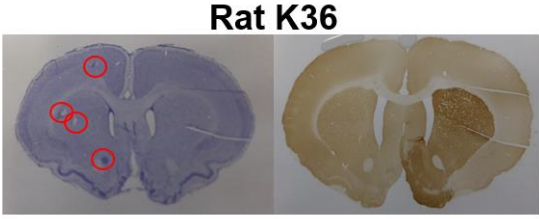
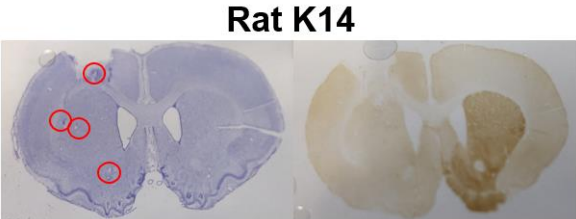
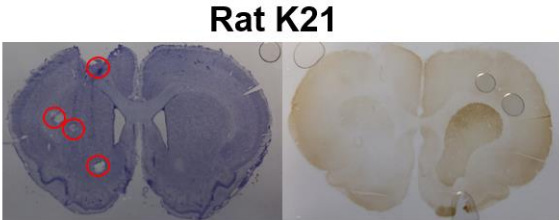
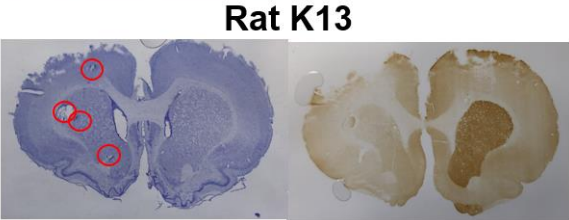
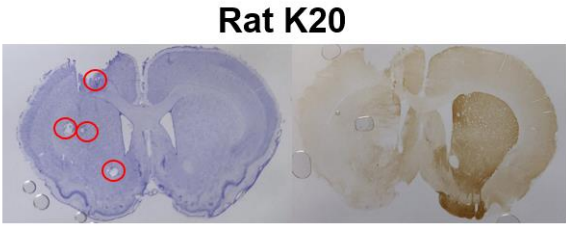
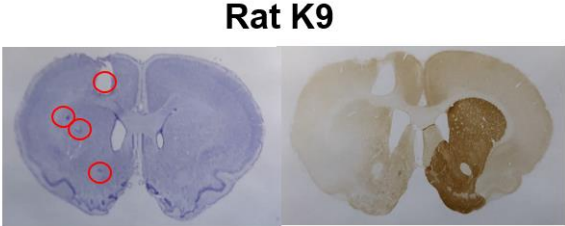
**Rat 194**



**Rat 205**



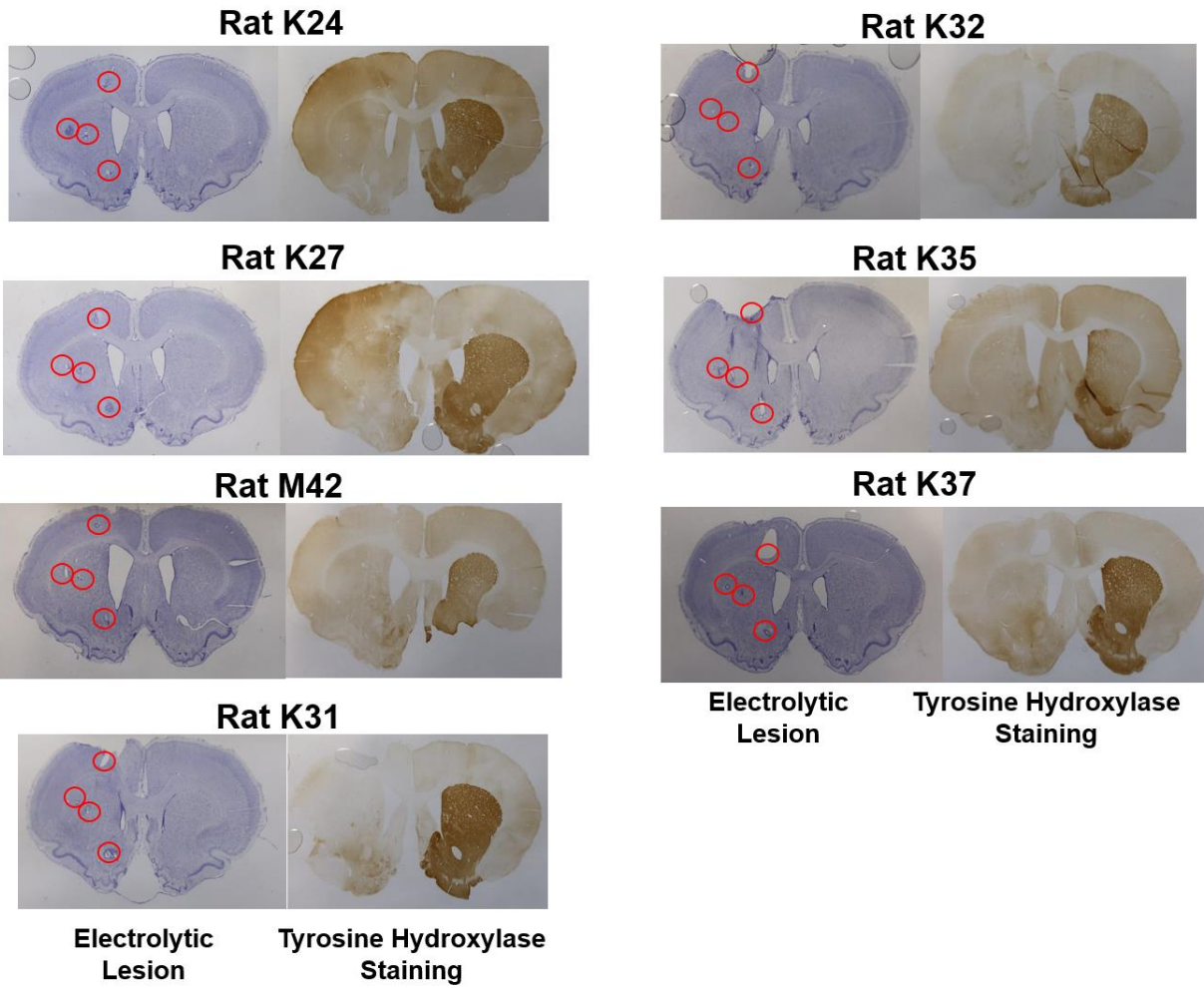
**Appendix B: Nissl- and TH-Stained Tissue of 6-OHDA-Lesioned Animals (*n*=7)**



**Electrolytic Lesion      Tyrosine Hydroxylase Staining**

**Electrolytic Lesion      Tyrosine Hydroxylase Staining**

## Appendix C: Nissl- and TH-Stained Tissue of LID Animals ( $n=7$ )



## References

- Abdallah, C. G., Adams, T. G., Kelmendi, B., Esterlis, I., Sanacora, G., and Krystal, J. H. (2016). Ketamine's mechanism of action: A path to rapid-acting antidepressants. *Depress. Anxiety* 33, 689–697. doi:10.1002/da.22501.
- Allen, E. A., Liu, J., Kiehl, K. A., Gelernter, J., Pearlson, G. D., Perrone-Bizzozero, N. I., et al. (2011). Components of cross-frequency modulation in health and disease. *Front. Syst. Neurosci.* 5, 59. doi:10.3389/fnsys.2011.00059.
- Alonso-Frech, F., Zamarbide, I., Alegre, M., Rodríguez-Oroz, M. C., Guridi, J., Manrique, M., et al. (2006). Slow oscillatory activity and levodopa-induced dyskinesias in Parkinson's disease. *Brain* 129, 1748–1757. doi:10.1093/brain/awl103.
- Amzica, F., and Steriade, M. (1995). Short- and long-range neuronal synchronization of the slow (< 1 Hz) cortical oscillation. *J. Neurophysiol.* 73, 20–38. doi:10.1152/jn.1995.73.1.20.
- Andersen, P. H., and Gronvald, F. C. (1986). Specific binding of 3H-SCH 23390 to dopamine D1 receptors in vivo. *Life Sci.* 38, 1507–1514. doi:10.1016/0024-3205(86)90564-3.
- Andrade, C. (2017). Ketamine for depression, 4: In what dose, at what rate, by what route, for how long, and at what frequency? *J. Clin. Psychiatry* 78, e852–e857. doi:10.4088/JCP.17f11738.
- Aubert, I., Guigoni, C., Li, Q., Dovero, S., Bioulac, B. H., Gross, C. E., et al. (2007). Enhanced Preproenkephalin-B-Derived Opioid Transmission in Striatum and Subthalamic Nucleus Converges Upon Globus Pallidus Internalis in L-3,4-dihydroxyphenylalanine-Induced Dyskinesia. *Biol. Psychiatry* 61, 836–844. doi:10.1016/j.biopsych.2006.06.038.
- Backonja, M., Arndt, G., Gombar, K. a, Check, B., and Zimmermann, M. (1994). Response of chronic neuropathic pain syndromes to ketamine: a preliminary study. *Pain* 56, 51–7. doi:0304-3959(94)90149-X [pii].
- Baradaran, N., Tan, S. N., Liu, A., Ashoori, A., Palmer, S. J., Wang, Z. J., et al. (2013). Parkinson's disease rigidity: Relation to brain connectivity and motor performance. *Front. Neurol.* 4 JUN. doi:10.3389/fneur.2013.00067.
- Barbe, M. T., Liebhart, L., Runge, M., Deyng, J., Florin, E., Wojtecki, L., et al. (2011). Deep brain stimulation of the ventral intermediate nucleus in patients with essential tremor: Stimulation below intercommissural line is more efficient but equally effective as stimulation above. *Exp. Neurol.* 230, 131–137. doi:10.1016/j.expneurol.2011.04.005.
- Bartlett, M. J., Joseph, R. M., LePoidevin, L. M., Parent, K. L., Laude, N. D., Lazarus, L. B., et al. (2016). Long-term effect of sub-anesthetic ketamine in reducing L-DOPA-induced dyskinesias in a preclinical model. *Neurosci. Lett.* 612, 121–125. doi:10.1016/j.neulet.2015.11.047.
- Bartos, M., Vida, I., and Jonas, P. (2007). Synaptic mechanisms of synchronized gamma oscillations in inhibitory interneuron networks. *Nat. Rev. Neurosci.* 8, 45–56. doi:10.1038/nrn2044.

- Bastide, M. F., Meissner, W. G., Picconi, B., Fasano, S., Fernagut, P. O., Feyder, M., et al. (2015). Pathophysiology of L-dopa-induced motor and non-motor complications in Parkinson's disease. *Prog. Neurobiol.* 132, 96–168. doi:10.1016/j.pneurobio.2015.07.002.
- Belić, J. J., Halje, P., Richter, U., Petersson, P., and Hellgren Kotaleski, J. (2016). Untangling Cortico-Striatal Connectivity and Cross-Frequency Coupling in L-DOPA-Induced Dyskinesia. *Front. Syst. Neurosci.* 10, 1–12. doi:10.3389/fnsys.2016.00026.
- Bell, R. F. (2009). Ketamine for chronic non-cancer pain. *Pain* 141, 210–214. doi:10.1016/j.pain.2008.12.003.
- Berman, R. M., Cappiello, A., Anand, A., Oren, D. A., Heninger, G. R., Charney, D. S., et al. (2000). Antidepressant effects of ketamine in depressed patients. *Biol. Psychiatry* 47, 351–354. doi:10.1016/S0006-3223(99)00230-9.
- Bezard, E., and Przedborski, S. (2011). A tale on animal models of Parkinson's Disease. *Mov. Disord.* 26, 993–1002. doi:10.1002/mds.23696.
- Bhatia, K. P., and Joao, M. (2012). Clinical Approach to Parkinson's Disease: *Cold Spring Harb. Perspect. Med.*, 1–16.
- Bi, G. Q., and Poo, M. M. (1998). Synaptic modifications in cultured hippocampal neurons: dependence on spike timing, synaptic strength, and postsynaptic cell type. *J. Neurosci.* 18, 10464–10472.
- Blain-Moraes, S., Lee, U., Ku, S., Noh, G., and Mashour, G. A. (2014). Electroencephalographic effects of ketamine on power, cross-frequency coupling, and connectivity in the alpha bandwidth. *Front. Syst. Neurosci.* 8, 1–9. doi:10.3389/fnsys.2014.00114.
- Blum, D., Torch, S., Lambeng, N., Nissou, M. F., Benabid, A. L., Sadoul, R., et al. (2001). Molecular pathways involved in the neurotoxicity of 6-OHDA, dopamine and MPTP: Contribution to the apoptotic theory in Parkinson's disease. *Prog. Neurobiol.* 65, 135–172. doi:10.1016/S0301-0082(01)00003-X.
- Boraud, T., Bezard, E., Bioulac, B., and Gross, C. E. (2001). Dopamine agonist-induced dyskinesias are correlated to both firing pattern and frequency alterations of pallidal neurones in the MPTP-treated monkey. *Brain* 124, 546–557. doi:10.1093/brain/124.3.546.
- Bosch-Bouju, C., Hyland, B. I., and Parr-Brownlie, L. C. (2013). Motor thalamus integration of cortical, cerebellar and basal ganglia information: implications for normal and parkinsonian conditions. *Front. Comput. Neurosci.* 7, 1–21. doi:10.3389/fncom.2013.00163.
- Bose, A., and Beal, M. F. (2016). Mitochondrial dysfunction in Parkinson's disease. *J. Neurochem.* 139, 216–231. doi:10.1111/jnc.13731.
- Branchi, I., D'Andrea, I., Armida, M., Cassano, T., Pèzzola, A., Potenza, R. L., et al. (2008). Nonmotor symptoms in Parkinson's disease: Investigating early-phase onset of behavioral dysfunction in the 6-hydroxydopamine-lesioned rat model. *J. Neurosci. Res.* 86, 2050–2061. doi:10.1002/jnr.21642.
- Brittain, J. S., and Brown, P. (2014). Oscillations and the basal ganglia: Motor control and beyond. *Neuroimage* 85, 637–647. doi:10.1016/j.neuroimage.2013.05.084.

- Brown, P. (2003). Oscillatory nature of human basal ganglia activity: relationship to the pathophysiology of Parkinson's disease. *Mov. Disord.* 18, 357–363. doi:10.1002/mds.10358.
- Brown, P. (2006). Bad oscillations in Parkinson's disease. *J. Neural Transm.* 70, 27–30.
- Brunel, N., and Wang, X.-J. (2003). What Determines the Frequency of Fast Network Oscillations With Irregular Neural Discharges? I. Synaptic Dynamics and Excitation-Inhibition Balance. *J. Neurophysiol.* 90, 415–430. doi:10.1152/jn.01095.2002.
- Buhusi, C. V., and Meck, W. H. (2005). What makes us tick? Functional and neural mechanisms of interval timing. *Nat. Rev. Neurosci.* 6, 755–765. doi:10.1038/nrn1764.
- Burianova, H., McIntosh, A. R., and Grady, C. L. (2010). A common functional brain network for autobiographical, episodic, and semantic memory retrieval. *Neuroimage* 49, 865–874. doi:10.1016/j.neuroimage.2009.08.066.
- Burns, R., Peter, A., Ebert, MH Pakkenberg, H., and Kopin, I. (1984). The clinical syndrome of striatal dopamine deficiency. Parkinsonism induced by 1-methyl-4-phenyl-1,2,3,6-tetrahydropyridine (MPTP). *N. Engl. J. Med.* 310, 1368–1373.
- Buzsáki, G., and Wang, X.-J. (2012). Mechanisms of Gamma Oscillations. *Annu. Rev. Neurosci.* 35, 203–225. doi:10.1146/annurev-neuro-062111-150444.
- Caixeta, F. V., Cornélio, A. M., Scheffer-Teixeira, R., Ribeiro, S., and Tort, A. B. L. (2013). Ketamine alters oscillatory coupling in the hippocampus. *Sci. Rep.* 3, 2348. doi:10.1038/srep02348.
- Calon, F., Birdi, S., Rajput, A. H., Hornykiewicz, O., Bédard, P. J., and Di Paolo, T. (2002). Increase of preproenkephalin mRNA levels in the putamen of Parkinson disease patients with levodopa-induced dyskinesias. *J. Neuropathol. Exp. Neurol.* 61, 186–196. doi:10.1093/jnen/61.2.186.
- Canolty, R. T., and Knight, R. T. (2010). The functional role of cross-frequency coupling. *Trends Cogn. Sci.* 14, 506–515. doi:10.1016/j.tics.2010.09.001.
- Cantello, R., Gianelli, M., Civardi, C., and Mutani, R. (1996). Pathophysiology of Parkinson's disease rigidity. Role of corticospinal motor projections. *Adv. Neurol.* 69, 129–133. Available at: <http://europepmc.org/abstract/MED/8615120>.
- Carlé N, M., Meletis, K., Siegle, J., Cardin, J., Futai, K., Vierling-Claassen, D., et al. (2011). A critical role for NMDA receptors in parvalbumin interneurons for gamma rhythm induction and behavior. *Mol. Psychiatry* 17, 537–548. doi:10.1038/mp.2011.31.
- Cenci, M. A., and Konradi, C. (2010). *Maladaptive striatal plasticity in l-DOPA-induced dyskinesia*. Elsevier B.V. doi:10.1016/S0079-6123(10)83011-0.
- Cenci, M. A., Lee, C. S., and Björklund, A. (1998). L-DOPA-induced dyskinesia in the rat is associated with striatal overexpression of prodynorphin- and glutamic acid decarboxylase mRNA. *Eur. J. Neurosci.* 10, 2694–2706. doi:10.1046/j.1460-9568.1998.00285.x.
- Cenci, M. A., Whishaw, I. Q., and Schallert, T. (2002). Animal models of neurological deficits:

how relevant is the rat? 574–579.

- Chan, P., Delanney, L. E., Irwin, I., Langston, J. W., and Monte, D. Di (1991). Rapid ATP loss caused by 1-methyl-4-phenyl,1,2,3,6-tetrahydropyridine in the mouse brain. *J. Neurochem.*, 348–351.
- Chaturvedi, R. K., and Beal, M. F. (2008). Mitochondrial approaches for neuroprotection. *Ann. N. Y. Acad. Sci.* 1147, 395–412. doi:10.1196/annals.1427.027.
- Chen, G., Zhang, Y., Li, X., Zhao, X., Ye, Q., Lin, Y., et al. (2017). Distinct Inhibitory Circuits Orchestrate Cortical beta and gamma Band Oscillations. *Neuron* 96, 1403–1418.e6. doi:10.1016/j.neuron.2017.11.033.
- Chrobak, J. J., Hinman, J. R., and Sabolek, H. R. (2008). Revealing Past Memories: Proactive Interference and Ketamine-Induced Memory Deficits. *J. Neurosci.* 28, 4512–4520. doi:10.1523/JNEUROSCI.0742-07.2008.
- Clements, J. A., Nimmo, W. S., and Grant, I. S. (1982). Bioavailability, pharmacokinetics, and analgesic activity of ketamine in humans. *J. Pharm. Sci.* 71, 539–542. doi:10.1002/jps.2600710516.
- Cohen, M. X. (2014). *Fundamentals of Time-Frequency Analyses in Matlab/Octave*. 1st ed. sinc(x) Press.
- Colgin, L. L., Denninger, T., Fyhn, M., Hafting, T., Bonnevie, T., Jensen, O., et al. (2009). Frequency of gamma oscillations routes flow of information in the hippocampus. *Nature* 462, 353–7. doi:10.1038/nature08573.
- Cooper, M. D., Rosenblat, J. D., Cha, D. S., Lee, Y., Kakar, R., and McIntyre, R. S. (2017). Strategies to mitigate dissociative and psychotomimetic effects of ketamine in the treatment of major depressive episodes: a narrative review. *World J. Biol. Psychiatry* 18, 410–423. doi:10.3109/15622975.2016.1139747.
- Cordon, I., Nicolás, M. J., Arrieta, S., Lopetegui, E., López-Azcárate, J., Alegre, M., et al. (2015). Coupling in the cortico-basal ganglia circuit is aberrant in the ketamine model of schizophrenia. *Eur. Neuropsychopharmacol.* 25, 1375–87. doi:10.1016/j.euroneuro.2015.04.004.
- Crone, N. E., Sinai, A., and Korzeniewska, A. (2006). Chapter 19 High-frequency gamma oscillations and human brain mapping with electrocorticography. *Prog. Brain Res.* 159, 275–295. doi:10.1016/S0079-6123(06)59019-3.
- Da Fonseca Pacheco, D., Klein, A., De Castro Perez, A., Da Fonseca Pacheco, C. M., De Francischi, J. N., and Duarte, I. D. G. (2008). The  $\mu$ -opioid receptor agonist morphine, but not agonists at  $\delta$ - Or  $\kappa$ -opioid receptors, induces peripheral antinociception mediated by cannabinoid receptors. *Br. J. Pharmacol.* 154, 1143–1149. doi:10.1038/bjp.2008.175.
- Damier, P., Hirsch, E. C., Agid, Y., and Graybiel, A. M. (1999). The substantia nigra of the human brain: II. Patterns of loss of dopamine-containing neurons in Parkinson's disease. *Brain* 122, 1437–1448. doi:10.1093/brain/122.8.1437.
- Dauer, W., and Przedborski, S. (2003). Parkinson's disease: Mechanisms and models. *Neuron*

39, 889–909. doi:10.1016/S0896-6273(03)00568-3.

- Dawson, T. M., Ko, H. S., and Dawson, V. L. (2010). Genetic Animal Models of Parkinson's Disease. *Neuron* 66, 646–661. doi:10.1016/j.neuron.2010.04.034.
- de Hemptinne, C., Swann, N. C., Ostrem, J. L., Ryapolova-Webb, E. S., San Luciano, M., Galifianakis, N. B., et al. (2015a). Therapeutic deep brain stimulation reduces cortical phase-amplitude coupling in Parkinson's disease. *Nat. Neurosci.* 18, 779–786. doi:10.1038/nn.3997.
- de Hemptinne, C., Swann, N. C., Ostrem, J. L., Ryapolova-Webb, E. S., San Luciano, M., Galifianakis, N. B., et al. (2015b). Therapeutic deep brain stimulation reduces cortical phase-amplitude coupling in Parkinson's disease. *Nat. Neurosci.* 18, 779–786. doi:10.1038/nn.3997.
- De Jong, G. J., Meerwaldt, J. D., and Schmitz, P. I. M. (1987). Factors that influence the occurrence of response variations in Parkinson's disease. *Ann. Neurol.* 22, 4–7. doi:10.1002/ana.410220104.
- de la Salle, S., Choueiry, J., Shah, D., Bowers, H., McIntosh, J., Ilivitsky, V., et al. (2016). Effects of ketamine on resting-state EEG activity and their relationship to perceptual/dissociative symptoms in healthy humans. *Front. Pharmacol.* 7, 1–14. doi:10.3389/fphar.2016.00348.
- Dejean, C., Gross, C. E., Bioulac, B., and Boraud, T. (2008). Dynamic Changes in the Cortex-Basal Ganglia Network After Dopamine Depletion in the Rat. *J. Neurophysiol.* 100, 385–396. doi:10.1152/jn.90466.2008.
- Dekundy, A., Lundblad, M., Danysz, W., and Cenci, M. A. (2007). Modulation of l-DOPA-induced abnormal involuntary movements by clinically tested compounds: Further validation of the rat dyskinesia model. *Behav. Brain Res.* 179, 76–89. doi:10.1016/j.bbr.2007.01.013.
- Delaville, C., Deurwaerdère, P. De, and Benazzouz, A. (2011). Noradrenaline and Parkinson's Disease. *Front. Syst. Neurosci.* 5, 1–12. doi:10.3389/fnsys.2011.00031.
- Delwaide, P. J., Pepin, J. L., and De Noordhout, A. M. (1991). Short-latency autogenic inhibition in patients with parkinsonian rigidity. *Ann. Neurol.* 30, 83–89. doi:10.1002/ana.410300115.
- Diamond, P. R., Farmery, A. D., Atkinson, S., Haldar, J., Williams, N., Cowen, P. J., et al. (2014). Ketamine infusions for treatment resistant depression: a series of 28 patients treated weekly or twice weekly in an ECT clinic. *J. Psychopharmacol.* 28, 536–544. doi:10.1177/0269881114527361.
- Dias, V., Junn, E., and Mouradian, M. M. (2013). The role of oxidative stress in parkinson's disease. *J. Parkinsons. Dis.* 3, 461–491. doi:10.3233/JPD-130230.
- Domino, E. F., Chodoff, P., and Corssen, G. (1965). Pharmacologic effects of CI-581, a new dissociative anesthetic, in man. *Clin. Pharmacol. Ther.* 6, 279–291. doi:10.1002/cpt196563279.
- Dorsey, E. R., Constantinescu, R., Thompson, J. P., Biglan, K. M., Holloway, R. G., Kieburtz,

- K., et al. (2007). Projected number of people with Parkinson disease in the most populous nations, 2005 through 2030. *Neurology* 68, 384 LP-386. Available at: <http://n.neurology.org/content/68/5/384.abstract>.
- Duman, R. S., Li, N., Liu, R. J., Duric, V., and Aghajanian, G. (2012). Signaling pathways underlying the rapid antidepressant actions of ketamine. *Neuropharmacology* 62, 35–41. doi:10.1016/j.neuropharm.2011.08.044.
- Dunkley, B. T., Doesburg, S. M., Sedge, P. A., Grodecki, R. J., Shek, P. N., Pang, E. W., et al. (2014). Resting-state hippocampal connectivity correlates with symptom severity in post-traumatic stress disorder. *NeuroImage Clin.* 5, 377–384. doi:10.1016/j.nicl.2014.07.017.
- Dupre, K. B., Cruz, A. V., McCoy, A. J., Delaville, C., Gerber, C. M., Eyring, K. W., et al. (2016). Effects of L-dopa priming on cortical high beta and high gamma oscillatory activity in a rodent model of Parkinson's disease. *Neurobiol. Dis.* 86, 1–15. doi:10.1016/j.nbd.2015.11.009.
- Dupre, K. B., Ostock, C. Y., Eskow Jaunarajs, K. L., Button, T., Savage, L. M., Wolf, W., et al. (2011). Local modulation of striatal glutamate efflux by serotonin 1A receptor stimulation in dyskinetic, hemiparkinsonian rats. *Exp. Neurol.* 229, 288–299. doi:10.1016/j.expneurol.2011.02.012.
- Dürschmid, S. (2013). Phase-amplitude cross-frequency coupling in the human nucleus accumbens tracks action monitoring during cognitive control. *Front. Hum. Neurosci.* 7, 1–17. doi:10.3389/fnhum.2013.00635.
- Ehlers, C. L., Kaneko, W. M., Wall, T. L., and Chaplin, R. I. (1992). Effects of dizocilpine (MK-801) and ethanol on the eeg and event-related potentials (erps) in rats. *Neuropharmacology* 31, 369–378. doi:10.1016/0028-3908(92)90069-2.
- Espay, A. J., Beaton, D. E., Morgante, F., Gunraj, C. A., Lang, A. E., and Chen, R. (2009). Impairments of speed and amplitude of movement in Parkinson's disease: A pilot study. *Mov. Disord.* 24, 1001–1008. doi:10.1002/mds.22480.
- Feder, A., Parides, M. K., Murrough, J. W., Perez, A. M., Morgan, J. E., Saxena, S., et al. (2014). Efficacy of intravenous ketamine for treatment of chronic posttraumatic stress disorder: a randomized clinical trial. *JAMA Psychiatry* 71, 681–688. doi:10.1001/jamapsychiatry.2014.62.
- Finck, A., and Ngai, S. H. (1982). Opiate receptor mediation of ketamine analgesia. *Anesthesiology* 56, 291–297. doi:10.1167/8.5.1.
- Fink, A., and Ngai, S. (1982). Opiate receptor mediation of ketamine analgesia. *Anesthesiology* 56, 291–297. doi:10.1167/8.5.1.
- Fisahn, A., Pike, F. G., Buhl, E. H., and Paulsen, O. (1998). Cholinergic induction of network oscillations at 40 Hz in the hippocampus in vitro. *Nature* 394, 186–189. doi:10.1038/28179.
- Fries, P., Nikolić, D., and Singer, W. (2007). The gamma cycle. *Trends Neurosci.* 30, 309–16. doi:10.1016/j.tins.2007.05.005.
- Fu, Y., Guo, L., Zhang, J., Chen, Y., Wang, X., Zeng, T., et al. (2008). Differential effects of

- ageing on the EEG during pentobarbital and ketamine anaesthesia. *Eur. J. Anaesthesiol.* 25, 826–833. doi:DOI: 10.1017/S0265021508004687.
- Fujisawa, S., and Buzsáki, G. (2011). A 4 Hz oscillation adaptively synchronizes prefrontal, VTA, and hippocampal activities. *Neuron* 72, 153–65. doi:10.1016/j.neuron.2011.08.018.
- Garcia, L. S. B., Comim, C. M., Valvassori, S. S., Réus, G. Z., Barbosa, L. M., Andreazza, A. C., et al. (2008). Acute administration of ketamine induces antidepressant-like effects in the forced swimming test and increases BDNF levels in the rat hippocampus. *Prog. Neuropsychopharmacol. Biol. Psychiatry* 32, 140–4. doi:10.1016/j.pnpbp.2007.07.027.
- Gerfen, C. R. (1992). The neostriatal mosaic: multiple levels of compartmental organization. *Trends Neurosci.* 15, 133–139. doi:10.1016/0166-2236(92)90355-C.
- Goebel, D. J., and Poosch, M. S. (1999). NMDA receptor subunit gene expression in the rat brain: A quantitative analysis of endogenous mRNA levels of NR1(Com), NR2A, NR2B, NR2C, NR2D and NR3A. *Mol. Brain Res.* 69, 164–170. doi:10.1016/S0169-328X(99)00100-X.
- Goldberg, J. a, Boraud, T., Maraton, S., Haber, S. N., Vaadia, E., and Bergman, H. (2002). Enhanced synchrony among primary motor cortex neurons in the 1-methyl-4-phenyl-1,2,3,6-tetrahydropyridine primate model of Parkinson's disease. *J. Neurosci.* 22, 4639–4653. doi:20026424.
- Gopalakrishna, A., and Alexander, S. A. (2015). Understanding Parkinson disease: A complex and multifaceted illness. *J. Neurosci. Nurs.* 47, 320–326. doi:10.1097/JNN.000000000000162.
- Gradinaru, V., Mogri, M., Thompson, K. R., Henderson, J. M., and Deisseroth, K. (2009). Optical deconstruction of parkinsonian neural circuitry. *Science* (80-. ). 324, 354–359. doi:10.1126/science.1167093.
- Graham, D. (1978). Oxidative pathways for cawtcholamines in the genesis of neuromelanin and cytotoxic quinones. *Mol. Pharmacol.* 14, 633–643.
- Graveland, G. A., Williams, R. S., and Difiglia, M. (1985). A Golgi study of the human neostriatum: Neurons and afferent fibers. *J. Comp. Neurol.* 234, 317–333. doi:10.1002/cne.902340304.
- Gunduz-Bruce, H. (2009). The acute effects of NMDA antagonism: From the rodent to the human brain. *Brain Res. Rev.* 60, 279–286. doi:10.1016/j.brainresrev.2008.07.006.
- Gupta, A., Devi, L. A., and Gomes, I. (2011). Potentiation of mu-opioid receptor-mediated signaling by ketamine. *J. Neurochem.* 119, 294–302. doi:10.1111/j.1471-4159.2011.07361.x.
- Hadjiconstantinou, M., and Neff, N. H. (2011). Nicotine and endogenous opioids: Neurochemical and pharmacological evidence. *Neuropharmacology* 60, 1209–1220. doi:10.1016/j.neuropharm.2010.11.010.
- Hakami, T., Jones, N. C., Tolmacheva, E. A., Gaudias, J., Chaumont, J., Salzberg, M., et al. (2009). NMDA receptor hypofunction leads to generalized and persistent aberrant  $\gamma$

- oscillations independent of hyperlocomotion and the state of consciousness. *PLoS One* 4, e6755. doi:10.1371/journal.pone.0006755.
- Halje, P., Tamte, M., Richter, U., Mohammed, M., Cenci, M. A., and Petersson, P. (2012a). Levodopa-induced dyskinesia is strongly associated with resonant cortical oscillations. *J. Neurosci.* 32, 16541–16551. doi:10.1523/JNEUROSCI.3047-12.2012.
- Halje, P., Tamte, M., Richter, U., Mohammed, M., Cenci, M. A., and Petersson, P. (2012b). Levodopa-Induced Dyskinesia Is Strongly Associated with Resonant Cortical Oscillations. *J. Neurosci.* 32, 16541–16551. doi:10.1523/JNEUROSCI.3047-12.2012.
- Hall, S. D., Barnes, G. R., Furlong, P. L., Seri, S., and Hillebrand, A. (2010). Neuronal network pharmacodynamics of GABAergic modulation in the human cortex determined using pharmaco-magnetoencephalography. *Hum. Brain Mapp.* 31, 581–594. doi:10.1002/hbm.20889.
- Hammond, C., Bergman, H., and Brown, P. (2007). Pathological synchronization in Parkinson's disease: networks, models and treatments. *Trends Neurosci.* 30, 357–364. doi:10.1016/j.tins.2007.05.004.
- Harris, J. E., Letson, R. D., and Buckley, J. J. (1968). The use of CI-581, a new parenteral anesthetic, in ophthalmic practice. *Trans. Am. Ophthalmol. Soc.* 66, 206–213. Available at: [http://eutils.ncbi.nlm.nih.gov/entrez/eutils/elink.fcgi?dbfrom=pubmed&id=5720838&retmode=ref&cmd=prlinks%5Cnfile:///Users/alexandershaw/Library/Application Support/Papers2/Articles/1968/Harris/Trans Am Ophthalmol Soc 1968 Harris.pdf%5Cnpapers2://publicati](http://eutils.ncbi.nlm.nih.gov/entrez/eutils/elink.fcgi?dbfrom=pubmed&id=5720838&retmode=ref&cmd=prlinks%5Cnfile:///Users/alexandershaw/Library/Application%20Support/Papers2/Articles/1968/Harris/Trans%20Am%20Ophthalmol%20Soc%201968/Harris.pdf%5Cnpapers2://publicati).
- Hasenstaub, A., Otte, S., and Callaway, E. (2016). Cell Type-Specific Control of Spike Timing by Gamma-Band Oscillatory Inhibition. *Cereb. Cortex* 26, 797–806. doi:10.1093/cercor/bhv044.
- Hauser, R. A., Rascol, O., Korczyn, A. D., Stoessl, A. J., Watts, R. L., Poewe, W., et al. (2007). Ten-year follow-up of Parkinson's disease patients randomized to initial therapy with ropinirole or levodopa. *Mov. Disord.* 22, 2409–2417. doi:10.1002/mds.21743.
- Heimer, G., Bar-Gad, I., Goldberg, J. A., and Bergman, H. (2002). Dopamine replacement therapy reverses abnormal synchronization of pallidal neurons in the 1-methyl-4-phenyl-1,2,3,6-tetrahydropyridine primate model of parkinsonism. *J. Neurosci.* 22, 7850–5. doi:22/18/7850 [pii].
- Hevers, W., Hadley, S. H., Luddens, H., and Amin, J. (2008). Ketamine, But Not Phencyclidine, Selectively Modulates Cerebellar GABAA Receptors Containing  $\alpha 6$  and  $\beta 2$  Subunits. *J. Neurosci.* 28, 5383–5393. doi:10.1523/JNEUROSCI.5443-07.2008.
- Hirai, T., Miyazaki, M., Nakajima, H., Shibasaki, T., and Ohye, C. (1983). the Correlation Between Tremor Characteristics and the Predicted Volume of Effective Lesions in Stereotaxic Nucleus Ventralis. 1001–1018.
- Hirsch, E. C., and Faucheux, B. A. (1998). Iron metabolism and Parkinson's disease. *Mov. Disord.* 13 Suppl 1, 39–45. Available at: <http://europepmc.org/abstract/MED/9613717>.
- Hiyoshi, T., Hikichi, H., Karasawa, J. ichi, and Chaki, S. (2014a). Metabotropic glutamate

- receptors regulate cortical gamma hyperactivities elicited by ketamine in rats. *Neurosci. Lett.* 567, 30–34. doi:10.1016/j.neulet.2014.03.025.
- Hiyoshi, T., Kambe, D., Karasawa, J., and Chaki, S. (2014b). Differential effects of NMDA receptor antagonists at lower and higher doses on basal gamma band oscillation power in rat cortical electroencephalograms. *Neuropharmacology* 85, 384–96. doi:10.1016/j.neuropharm.2014.05.037.
- Hocking, G., and Cousins, M. (2003). Ketamine in chronic pain management: an evidence-based review. *Anesth. Analg.* 97, 1730–1739. doi:10.1213/01.ANE.0000086618.28845.9B.
- Homayoun, H., and Moghaddam, B. (2007). NMDA Receptor Hypofunction Produces Opposite Effects on Prefrontal Cortex Interneurons and Pyramidal Neurons. *J. Neurosci.* 27, 11496–11500. doi:10.1523/JNEUROSCI.2213-07.2007.
- Hong, L. E., Summerfelt, A., Buchanan, R. W., O'Donnell, P., Thaker, G. K., Weiler, M. A., et al. (2010). Gamma and delta neural oscillations and association with clinical symptoms under subanesthetic ketamine. *Neuropsychopharmacology* 35, 632–640. doi:10.1038/npp.2009.168.
- Hornykiewicz, O. (1966). Dopamine (3-Hydroxytyramine) and Brain Function. *Pharmacol. Rev.* 18, 925–964. Available at: <http://pharmrev.aspetjournals.org/content/18/2/925.abstract%5Cnhttp://pharmrev.aspetjournals.org/content/18/2/925.full.pdf>.
- Hsiao, Y.-T., Zheng, C., and Colgin, L. L. (2016). Slow gamma rhythms in CA3 are entrained by slow gamma activity in the dentate gyrus. *J. Neurophysiol.*, jn.00499.2016. doi:10.1152/jn.00499.2016.
- Hunt, M. J., Falinska, M., Łeski, S., Wójcik, D. K., and Kasicki, S. (2011). Differential effects produced by ketamine on oscillatory activity recorded in the rat hippocampus, dorsal striatum and nucleus accumbens. *J. Psychopharmacol.* 25, 808–821. doi:10.1177/0269881110362126.
- Hunt, M. J., and Kasicki, S. (2013). A systematic review of the effects of NMDA receptor antagonists on oscillatory activity recorded in vivo. *J. Psychopharmacol.* 27, 972–86. doi:10.1177/0269881113495117.
- Hunt, M. J., Olszewski, M., Piasecka, J., Whittington, M. A., and Kasicki, S. (2015). Effects of NMDA receptor antagonists and antipsychotics on high frequency oscillations recorded in the nucleus accumbens of freely moving mice. *Psychopharmacology (Berl)*. 232, 4525–4535. doi:10.1007/s00213-015-4073-0.
- Hunt, M. J., Raynaud, B., and Garcia, R. (2006a). Ketamine Dose-Dependently Induces High-Frequency Oscillations in the Nucleus Accumbens in Freely Moving Rats. *Biol. Psychiatry* 60, 1206–1214. doi:10.1016/j.biopsych.2006.01.020.
- Hunt, M. J., Raynaud, B., and Garcia, R. (2006b). Ketamine Dose-Dependently Induces High-Frequency Oscillations in the Nucleus Accumbens in Freely Moving Rats. *Biol. Psychiatry* 60, 1206–1214. doi:10.1016/j.biopsych.2006.01.020.
- Iderberg, H., Francardo, V., and Pioli, E. Y. (2012). Animal models of l-DOPA-induced

- dyskinesia: An update on the current options. *Neuroscience* 211, 13–27.  
doi:10.1016/j.neuroscience.2012.03.023.
- Igarashi, J., Isomura, Y., Arai, K., Harukuni, R., and Fukai, T. (2013). A theta-gamma Oscillation Code for Neuronal Coordination during Motor Behavior. *J. Neurosci.* 33, 18515–18530. doi:10.1523/JNEUROSCI.2126-13.2013.
- Jahanshahi, M., Jones, C. R. G., Dirnberger, G., and Frith, C. D. (2006). The Substantia Nigra Pars Compacta and Temporal Processing. *J. Neurosci.* 26, 12266–12273.  
doi:10.1523/JNEUROSCI.2540-06.2006.
- Jankovic, J. (2005). Motor fluctuations and dyskinesias in Parkinson's disease: Clinical manifestations. *Mov. Disord.* 20. doi:10.1002/mds.20458.
- Jenkinson, N., and Brown, P. (2011). New insights into the relationship between dopamine, beta oscillations and motor function. *Trends Neurosci.* 34, 611–618.  
doi:10.1016/j.tins.2011.09.003.
- Jenner, P. (2008). Molecular mechanisms of L-dopa-induced dyskinesia. *Heal. (San Fr.)* 9, 665–677. doi:10.1038/nrn2471.
- Jonsson, G. (1980). Chemical neurotoxins as denervation tools in neurobiology. *Annu. Rev. Neurosci.* 3, 169–187. doi:10.1146/annurev.ne.03.030180.001125.
- Kapur, S., and Seeman, P. (2002). NMDA receptor antagonists ketamine and PCP have direct effects on the dopamine D2 and serotonin 5-HT2 receptors - Implications for models of schizophrenia. *Mol. Psychiatry* 7, 837–844. doi:10.1038/sj.mp.4001093.
- Kiss, T., Hoffmann, W. E., Scott, L., Kawabe, T. T., Milici, A. J., Nilsen, E. A., et al. (2011). Role of thalamic projection in NMDA receptor-induced disruption of cortical slow oscillation and short-term plasticity. *Front. Psychiatry* 2, 1–12.  
doi:10.3389/fpsy.2011.00014.
- Kocsis, B. (2012). Differential role of NR2A and NR2B subunits in N-methyl-D-aspartate receptor antagonist-induced aberrant cortical gamma oscillations. *Biol. Psychiatry* 71, 987–995. doi:10.1016/j.biopsych.2011.10.002.
- Kokkinou, M., Ashok, A. H., and Howes, O. D. (2018). The effects of ketamine on dopaminergic function: Meta-Analysis and review of the implications for neuropsychiatric disorders. *Mol. Psychiatry* 23, 59–69. doi:10.1038/mp.2017.190.
- Kopell, N., Whittington, M. A., and Kramer, M. A. (2011). Neuronal assembly dynamics in the beta1 frequency range permits short-term memory. *Proc. Natl. Acad. Sci.* 108, 3779–3784.  
doi:10.1073/pnas.1019676108.
- Koprach, J. B., Fox, S. H., Johnston, T. H., Goodman, A., Le Bourdonnec, B., Dolle, R. E., et al. (2011). The selective mu-opioid receptor antagonist adl5510 reduces levodopa-induced dyskinesia without affecting antiparkinsonian action in mptp-lesioned macaque model of Parkinson's disease. *Mov. Disord.* 26, 1225–1233. doi:10.1002/mds.23631.
- Korotkova, T., Fuchs, E. C., Ponomarenko, A., von Engelhardt, J., and Monyer, H. (2010). NMDA receptor ablation on parvalbumin-positive interneurons impairs hippocampal

- synchrony, spatial representations, and working memory. *Neuron* 68, 557–69. doi:10.1016/j.neuron.2010.09.017.
- Krystal, J. H., Sanacora, G., and Duman, R. S. (2013). Rapid-acting glutamatergic antidepressants: The path to ketamine and beyond. *Biol. Psychiatry* 73, 1133–1141. doi:10.1016/j.biopsych.2013.03.026.
- Kudrimoti, H. S., Barnes, C. a, and McNaughton, B. L. (1999). Reactivation of hippocampal cell assemblies: effects of behavioral state, experience, and EEG dynamics. *J. Neurosci. Off. J. Soc. Neurosci.* 19, 4090–4101. Available at: <http://www.jneurosci.org/content/19/10/4090.full.pdf>.
- Kühn, A. A., Trottenberg, T., Kivi, A., Kupsch, A., Schneider, G. H., and Brown, P. (2005). The relationship between local field potential and neuronal discharge in the subthalamic nucleus of patients with Parkinson’s disease. *Exp. Neurol.* 194, 212–220. doi:10.1016/j.expneurol.2005.02.010.
- Kulikova, S. P., Tolmacheva, E. A., Anderson, P., Gaudias, J., Adams, B. E., Zheng, T., et al. (2012). Opposite effects of ketamine and deep brain stimulation on rat thalamocortical information processing. *Eur. J. Neurosci.* 36, 3407–3419. doi:10.1111/j.1460-9568.2012.08263.x.
- Kurdi, M., Theerth, K., and Deva, R. (2014). Ketamine: Current applications in anesthesia, pain, and critical care. *Anesth. Essays Res.* 8, 283. doi:10.4103/0259-1162.143110.
- Lang, A. E., and Lozano (1998). Parkinson’s disease: First of two parts. *N. Engl. J. Med.* 339, 1044–1053.
- Langston, J., Ballard, P., Tetrud, J., and Irwin, I. (1983). Chronic Parkinsonism in humans due to a product of meperidine-analog synthesis. *Science* (80-. ). 219, 979–980. doi:10.1126/science.6823561.
- Lazarewicz, M. T., Ehrlichman, R. S., Maxwell, C. R., Gandal, M. J., Finkel, L. H., and Siegel, S. J. (2010). Ketamine modulates theta and gamma oscillations. *J. Cogn. Neurosci.* 22, 1452–1464. doi:10.1162/jocn.2009.21305.
- Leblois, A. (2006). Competition between Feedback Loops Underlies Normal and Pathological Dynamics in the Basal Ganglia. *J. Neurosci.* 26, 3567–3583. doi:10.1523/JNEUROSCI.5050-05.2006.
- Lee, K. H., Mosier, E. M., and Blaha, C. D. (2018). “Mechanisms of Action of Deep Brain Stimulation,” in *Neuromodulation*, 193–210. doi:10.1016/B978-0-12-805353-9.00017-6.
- Lefaucheur, J.-P. (2005). Motor cortex dysfunction revealed by cortical excitability studies in Parkinson’s disease: influence of antiparkinsonian treatment and cortical stimulation. *Clin. Neurophysiol.* 116, 244–253. doi:10.1016/j.clinph.2004.11.017.
- Lenze, E. J., Farber, N. B., Kharasch, E., Schweiger, J., Yingling, M., Olney, J., et al. (2016). Ninety-six hour ketamine infusion with co-administered clonidine for treatment-resistant depression: A pilot randomised controlled trial. *World J. Biol. Psychiatry* 17, 230–238. doi:10.3109/15622975.2016.1142607.

- Li, B., Liu, M.-L., Wu, X.-P., Jia, J., Cao, J., Wei, Z.-W., et al. (2015). Effects of ketamine exposure on dopamine concentrations and dopamine type 2 receptor mRNA expression in rat brain tissue. *Int. J. Clin. Exp. Med.* 8, 11181–7. Available at: <http://www.ncbi.nlm.nih.gov/pubmed/26379921> <http://www.pubmedcentral.nih.gov/articlerender.fcgi?artid=PMC4565304>.
- Li, M., Demenescu, L. R., Colic, L., and Metzger, C. D. (2016). Temporal Dynamics of Antidepressant Ketamine Effects on Glutamine Cycling Follow Regional Fingerprints of AMPA and NMDA Receptor Densities. *Nat. Publ. Gr.* 42, 1201–1209. doi:10.1038/npp.2016.184.
- Lindenbach, D., and Bishop, C. (2013). Critical involvement of the motor cortex in the pathophysiology and treatment of Parkinson's disease. *Neurosci. Biobehav. Rev.* 37, 2737–2750. doi:10.1016/j.neubiorev.2013.09.008.
- Lisman, J., and Buzsáki, G. (2008). A neural coding scheme formed by the combined function of gamma and theta oscillations. *Schizophr. Bull.* 34, 974–980. doi:10.1093/schbul/sbn060.
- Lisman, J. E., and Idiart, M. A. (1995). Storage of 7 +/- 2 short-term memories in oscillatory subcycles. *Science (80-. )*. 267, 1512–5.
- Lisman, J. E., and Jensen, O. (2013b). The Theta-Gamma Neural Code. *Neuron* 77, 1002–1016. doi:10.1016/j.neuron.2013.03.007.
- Lisman, J. E., and Jensen, O. (2013a). The Theta-Gamma Neural Code. *Neuron* 77, 1002–1016. doi:10.1016/j.neuron.2013.03.007.
- Little, S., and Brown, P. (2014). Parkinsonism and Related Disorders The functional role of beta oscillations in Parkinson ' s disease. *Park. Realt. Disord.* 20, S44–S48. doi:10.1016/S1353-8020(13)70013-0.
- Litvak, V., Jha, A., Eusebio, A., Oostenveld, R., Foltynie, T., Limousin, P., et al. (2011). Resting oscillatory cortico-subthalamic connectivity in patients with Parkinson's disease. *Brain* 134, 359–374. doi:10.1093/brain/awq332.
- López-Azcárate, J., Nicolás, M. J., Cordon, I., Alegre, M., Valencia, M., and Artieda, J. (2013). Delta-mediated cross-frequency coupling organizes oscillatory activity across the rat cortico-basal ganglia network. *Front. Neural Circuits* 7, 155. doi:10.3389/fncir.2013.00155.
- Lőrincz, M. L., Gunner, D., Bao, Y., Connelly, W. M., Isaac, J. T. R., Hughes, S. W., et al. (2015). A distinct class of slow (~0.2-2 Hz) intrinsically bursting layer 5 pyramidal neurons determines UP/DOWN state dynamics in the neocortex. *J. Neurosci.* 35, 5442–58. doi:10.1523/JNEUROSCI.3603-14.2015.
- Lundblad, M., Andersson, M., Winkler, C., Kirik, D., Wierup, N., and Cenci Nilsson, M. A. (2002). Pharmacological validation of behavioural measures of akinesia and dyskinesia in a rat model of Parkinson's disease. *Eur. J. Neurosci.* 15, 120–132. doi:10.1046/j.0953-816x.2001.01843.x.
- Ma, L., Skoblenick, K., Johnston, K., and Everling, S. (2018). Ketamine alters lateral prefrontal oscillations in a rule-based working memory task. *J. Neurosci.* 38, 2659–17. doi:10.1523/JNEUROSCI.2659-17.2018.

- Mallet, N., Pogosyan, A., Marton, L. F., Bolam, J. P., Brown, P., and Magill, P. J. (2008). Parkinsonian Beta Oscillations in the External Globus Pallidus and Their Relationship with Subthalamic Nucleus Activity. *J. Neurosci.* 28, 14245–14258. doi:10.1523/JNEUROSCI.4199-08.2008.
- Marquis, K., and Paquette, N. (1989). Comparative electroencephalographic and behavioral effects of phencyclidine, (+)-SKF-10,047 and MK-801 in rats. *J. Pharmacol. ...* 251, 1104–1112. Available at: <http://jpet.aspetjournals.org/content/251/3/1104.short>.
- Martelle, J. L., and Nader, M. A. (2008). A review of the discovery, pharmacological characterization, and behavioral effects of the dopamine D2-like receptor antagonist eticlopride. *CNS Neurosci. Ther.* 14, 248–262. doi:10.1111/j.1755-5949.2008.00047.x.
- Masquelier, T., Hugues, E., Deco, G., and Thorpe, S. J. (2009). Oscillations, phase-of-firing coding, and spike timing-dependent plasticity: an efficient learning scheme. *J. Neurosci.* 29, 13484–93. doi:10.1523/JNEUROSCI.2207-09.2009.
- Mattia, A., and Moreton, J. E. (2008). Electroencephalographic (EEG), EEG power spectra, and behavioral correlates in rats given phencyclidine. *Neuropharmacology* 25, 763–769. doi:10.1016/0028-3908(86)90093-6.
- Matulewicz, P., Kasicki, S., and Hunt, M. J. (2010). The effect of dopamine receptor blockade in the rodent nucleus accumbens on local field potential oscillations and motor activity in response to ketamine. *Brain Res.* 1366, 226–232. doi:10.1016/j.brainres.2010.09.088.
- McCarthy, M. M., Moore-Kochlacs, C., Gu, X., Boyden, E. S., Han, X., and Kopell, N. (2011). Striatal origin of the pathologic beta oscillations in Parkinson's disease. *Proc. Natl. Acad. Sci.* 108, 11620–11625. doi:10.1073/pnas.1107748108.
- Meck, W. H. (2006). Frontal cortex lesions eliminate the clock speed effect of dopaminergic drugs on interval timing. *Brain Res.* 1108, 157–167. doi:10.1016/j.brainres.2006.06.046.
- Mela, F., Marti, M., Bido, S., Cenci, M. A., and Morari, M. (2012). In vivo evidence for a differential contribution of striatal and nigral D1 and D2 receptors to l-DOPA induced dyskinesia and the accompanying surge of nigral amino acid levels. *Neurobiol. Dis.* 45, 573–582. doi:10.1016/j.nbd.2011.09.015.
- Mion, G., and Villevieille, T. (2013). Ketamine Pharmacology: An Update (Pharmacodynamics and Molecular Aspects, Recent Findings). *CNS Neurosci. Ther.* 19, 370–380. doi:10.1111/cns.12099.
- Mir, P., Matsunaga, K., Gilio, F., Quinn, N. P., Siebner, H. R., and Rothwell, J. C. (2005). Dopaminergic drugs restore facilitatory premotor-motor interactions in Parkinson disease. *Neurology* 64, 1906 LP-1912. Available at: <http://n.neurology.org/content/64/11/1906.abstract>.
- Moghaddam, B., Adams, B., Verma, a, and Daly, D. (1997). Activation of glutamatergic neurotransmission by ketamine: a novel step in the pathway from NMDA receptor blockade to dopaminergic and cognitive disruptions associated with the prefrontal cortex. *J. Neurosci.* 17, 2921–2927.
- Möller, M., and Born, J. (2011). Slow oscillations orchestrating fast oscillations and memory

- consolidation. *Prog. Brain Res.* 193, 93–110. doi:10.1016/B978-0-444-53839-0.00007-7.
- Moran, R. J., Mallet, N., Litvak, V., Dolan, R. J., Magill, P. J., Friston, K. J., et al. (2011). Alterations in Brain Connectivity Underlying Beta Oscillations in Parkinsonism. *PLoS Comput. Biol.* 7. doi:10.1371/journal.pcbi.1002124.
- Morin, N., Jourdain, V. A., and Di Paolo, T. (2014). Modeling dyskinesia in animal models of Parkinson disease. *Exp. Neurol.* 256, 105–116. doi:10.1016/j.expneurol.2013.01.024.
- Murrough, J. W., Perez, A. M., Pillemer, S., Stern, J., Parides, M. K., Aan Het Rot, M., et al. (2013). Rapid and longer-term antidepressant effects of repeated ketamine infusions in treatment-resistant major depression. *Biol. Psychiatry* 74, 250–256. doi:10.1016/j.biopsych.2012.06.022.
- Mutel, V., Buchy, D., Klingelschmidt, a, Messer, J., Bleuel, Z., Kemp, J. a, et al. (1998). In vitro binding properties in rat brain of [3H]Ro 25-6981, a potent and selective antagonist of NMDA receptors containing NR2B subunits. *J. Neurochem.* 70, 2147–2155. doi:9572302.
- Muthukumaraswamy, S. D. (2010). Functional properties of human primary motor cortex gamma oscillations. *J Neurophysiol* 104, 2873–2885. doi:jn.00607.2010 [pii]r10.1152/jn.00607.2010.
- Muthukumaraswamy, S. D., Myers, J. F. M., Wilson, S. J., Nutt, D. J., Lingford-Hughes, A., Singh, K. D., et al. (2013). The effects of elevated endogenous GABA levels on movement-related network oscillations. *Neuroimage* 66, 36–41. doi:10.1016/j.neuroimage.2012.10.054.
- Muthukumaraswamy, S. D., Shaw, A. D., Jackson, L. E., Hall, J., Moran, R., and Saxena, N. (2015a). Evidence that Subanesthetic Doses of Ketamine Cause Sustained Disruptions of NMDA and AMPA-Mediated Frontoparietal Connectivity in Humans. *J. Neurosci.* 35, 11694–11706. doi:10.1523/JNEUROSCI.0903-15.2015.
- Muthukumaraswamy, S. D., Shaw, A. D., Jackson, L. E., Hall, J., Moran, R., and Saxena, N. (2015b). Evidence that Subanesthetic Doses of Ketamine Cause Sustained Disruptions of NMDA and AMPA-Mediated Frontoparietal Connectivity in Humans. *J. Neurosci.* 35, 11694–11706. doi:10.1523/JNEUROSCI.0903-15.2015.
- Nambu, A., and Tachibana, Y. (2014). Mechanism of parkinsonian neuronal oscillations in the primate basal ganglia: some considerations based on our recent work. *Front. Syst. Neurosci.* 8, 1–6. doi:10.3389/fnsys.2014.00074.
- Nestler, E., Hyman, S., and Malenka, R. (2002). *Molecular neuropharmacology, a foundation for clinical neuroscience*. Available at: <http://jnnp.bmj.com/content/73/2/210.2.abstract>.
- Neymotin, S. a., Lazarewicz, M. T., Sherif, M., Contreras, D., Finkel, L. H., and Lytton, W. W. (2011). Ketamine Disrupts Theta Modulation of Gamma in a Computer Model of Hippocampus. *J. Neurosci.* 31, 11733–11743. doi:10.1523/JNEUROSCI.0501-11.2011.
- Nicolás, M. J., López-Azcárate, J., Valencia, M., Alegre, M., Pérez-Alcázar, M., Iriarte, J., et al. (2011). Ketamine-induced oscillations in the motor circuit of the rat basal ganglia. *PLoS One* 6, 1–13. doi:10.1371/journal.pone.0021814.

- Niedzielska, E., Smaga, I., Gawlik, M., Moniczewski, A., Stankowicz, P., Pera, J., et al. (2016). Oxidative Stress in Neurodegenerative Diseases. *Mol. Neurobiol.* 53, 4094–4125. doi:10.1007/s12035-015-9337-5.
- Niesters, M., Martini, C., and Dahan, A. (2014). Ketamine for chronic pain: Risks and benefits. *Br. J. Clin. Pharmacol.* 77, 357–367. doi:10.1111/bcp.12094.
- Noppers, I., Niesters, M., Aarts, L., Smith, T., Sarton, E., and Dahan, A. (2010). Ketamine for the treatment of chronic non-cancer pain. *Expert Opin. Pharmacother.* 11, 2417–29. doi:10.1517/14656566.2010.515978.
- Oertel, W. H., Wolters, E., Sampaio, C., Gimenez-Roldan, S., Bergamasco, B., Dujardin, M., et al. (2006). Pergolide versus levodopa monotherapy in early Parkinson's disease patients: The PELMOPET study. *Mov. Disord.* 21, 343–353. doi:10.1002/mds.20724.
- Olanow, C. W., Stern, M. B., and Sethi, K. (2009). The scientific and clinical basis for the treatment of Parkinson disease (2009). *Neurology* 72. doi:10.1212/WNL.0b013e3181a1d44c.
- Olney, J. W., Newcomer, J. W., and Farber, N. B. (1999). NMDA receptor hypofunction model of schizophrenia. *J. Psychiatr. Res.* 33, 523–533. doi:10.1016/S0022-3956(99)00029-1.
- Olszewski, M., Dolowa, W., Matulewicz, P., Kasicki, S., and Hunt, M. J. (2013). NMDA receptor antagonist-enhanced high frequency oscillations: Are they generated broadly or regionally specific? *Eur. Neuropsychopharmacol.* 23, 1795–1805. doi:10.1016/j.euroneuro.2013.01.012.
- Páleníček, T., Fujáková, M., Brunovský, M., Balíková, M., Horáček, J., Gorman, I., et al. (2011). Electroencephalographic spectral and coherence analysis of ketamine in rats: Correlation with behavioral effects and pharmacokinetics. *Neuropsychobiology* 63, 202–218. doi:10.1159/000321803.
- Parkinson, J. (1817). “An Essay on the Shaking Palsy.” in (London: Sherwood;).
- Pastor, M. A., ARTIEDA, J., JAHANSHAH, M., and OBESO, J. A. (1992a). Time Estimation and Reproduction Is Abnormal in Parkinson's Disease. *Brain* 115, 211–225. doi:10.1093/brain/115.1.211.
- Pastor, M. A., Jahanshahi, M., Artieda, J., and Obeso, J. A. (1992b). Performance of repetitive wrist movements in parkinson's disease. *Brain* 115, 875–891. doi:10.1093/brain/115.3.875.
- Patel, I. M., and Chapin, J. K. (1990). Ketamine effects on somatosensory cortical single neurons and on behavior in rats. *Anesth. Analg.* 70, 635–44. Available at: <http://www.ncbi.nlm.nih.gov/pubmed/2344058>.
- Paul, R. K., Singh, N. S., Khadeer, M., Moaddel, R., Sanghvi, M., Green, C. E., et al. (2014). (R,S)-Ketamine metabolites (R,S)-norketamine and (2S,6S)-hydroxynorketamine increase the mammalian target of rapamycin function. *Anesthesiology* 121, 149–59. doi:10.1097/ALN.0000000000000285.
- Phillips, K. G., Cotel, M. C., McCarthy, A. P., Edgar, D. M., Tricklebank, M., O'Neill, M. J., et al. (2012). Differential effects of NMDA antagonists on high frequency and gamma EEG

- oscillations in a neurodevelopmental model of schizophrenia. *Neuropharmacology* 62, 1359–1370. doi:10.1016/j.neuropharm.2011.04.006.
- Phoumthippavong, V., Barthas, F., Hassett, S., and Kwan, A. C. (2016a). Longitudinal Effects of Ketamine on Dendritic Architecture In Vivo in the Mouse Medial Frontal Cortex. *eNeuro* 3. doi:10.1523/ENEURO.0133-15.2016.
- Phoumthippavong, V., Barthas, F., Hassett, S., Kwan, A. C., Autry, A., Adachi, M., et al. (2016b). Longitudinal Effects of Ketamine on Dendritic Architecture In Vivo in the Mouse Medial Frontal Cortex. *eneuro* 3, 91–95. doi:10.1523/eneuro.0133-15.2016.
- Picconi, B., Centonze, D., Håkansson, K., Bernardi, G., Greengard, P., Fisone, G., et al. (2003). Loss of bidirectional striatal synaptic plasticity in L-DOPA–induced dyskinesia. *Nat. Neurosci.*, 501–506. doi:10.1038/nn1040.
- Pinault, D. (2008a). N-methyl d-aspartate receptor antagonists ketamine and MK-801 induce wake-related aberrant gamma oscillations in the rat neocortex. *Biol. Psychiatry* 63, 730–5. doi:10.1016/j.biopsych.2007.10.006.
- Pinault, D. (2008b). N-Methyl d-Aspartate Receptor Antagonists Ketamine and MK-801 Induce Wake-Related Aberrant  $\gamma$  Oscillations in the Rat Neocortex. *Biol. Psychiatry* 63, 730–735. doi:10.1016/j.biopsych.2007.10.006.
- Poewe, W., Seppi, K., Tanner, C. M., Halliday, G. M., Brundin, P., Volkman, J., et al. (2017). Parkinson disease. *Nat. Rev. Dis. Prim.* 3, 1–21. doi:10.1038/nrdp.2017.13.
- Porras, G., Li, Q., and Bezard, E. (2012). Modeling Parkinson ’ s Disease in Primates : *Cold Spring Harb. Perspect. Med.*, 1–10. doi:10.1101/cshperspect.a009308.
- Przedbroski, S., Leviver, M., Jiang, H., Ferreira, M., Jackson-Lewis, V., Donaldson, D., et al. (1995). Dose-dependent lesions of the dopaminergic nigrostriatal pathway induced by intrastriatal injection of 6-hydroxydopamine. *Neuroscience* 67, 631–647. doi:10.1016/0306-4522(95)00066-R.
- Rajput, A. H., Fenton, M. E., Birdi, S., and Macaulay, R. (1997). Is levodopa toxic to human substantia nigra? *Mov. Disord.* 12, 634–638. doi:10.1002/mds.870120503.
- Rascol, O., Brooks, D., Korczyn, A., De Deyn, P., Clarke, C., and Lang, A. (2000). A five-year study of the incidence of dyskinesia in patients with early parkinson’s disease who were treated with ropinirole or levodopa. *N. Engl. J. Med.* 342, 1484–1491.
- Rasmussen, K. G., Lineberry, T. W., Galardy, C. W., Kung, S., Lapid, M. I., Palmer, B. A., et al. (2013). Serial infusions of low-dose ketamine for major depression. *J. Psychopharmacol.* 27, 444–50. doi:10.1177/0269881113478283.
- Rivlin-Etzion, M., Marmor, O., Saban, G., Rosin, B., Haber, S. N., Vaadia, E., et al. (2008). Low-Pass Filter Properties of Basal Ganglia Cortical Muscle Loops in the Normal and MPTP Primate Model of Parkinsonism. *J. Neurosci.* 28, 633–649. doi:10.1523/JNEUROSCI.3388-07.2008.
- Rodriguez, M. C., Guridi, O. J., Alvarez, L., Mewes, K., Macias, R., Vitek, J., et al. (1998a). The subthalamic nucleus and tremor in Parkinson’s disease. *Mov. Disord.* 13 Suppl 3, 111–118.

doi:9827606.

- Rodriguez, M. C., Obeso, J. A., and Olanow, C. W. (1998b). Subthalamic nucleus-mediated excitotoxicity in Parkinson's disease: a target for neuroprotection. *Ann. Neurol.* 44, S175-88. Available at: <http://www.ncbi.nlm.nih.gov/pubmed/9749591>.
- Rosso, I. M., Crowley, D. J., Silveri, M. M., Rauch, S. L., and Jensen, J. E. (2017). Hippocampus Glutamate and N-Acetyl Aspartate Markers of Excitotoxic Neuronal Compromise in Posttraumatic Stress Disorder. *Neuropsychopharmacology* 42, 1698–1705. doi:10.1038/npp.2017.32.
- Rothwell, J. C., Obeso, J. A., Traub, M. M., and Marsden, C. D. (1983). The behaviour of the long - latency stretch reflex in patients with Parkinson's Disease. *J. Neurol. Neurosurgery, Psychiatry* 46, 35–44. Available at: <https://pdfs.semanticscholar.org/9729/95133c65dec9e36364a9e4267f7d0e4e9007.pdf>.
- Rowland, L. M. (2005). Subanesthetic ketamine: How it alters physiology and behavior in humans. *Aviat. Sp. Environ. Med.* 76, 52–58.
- Sailer, U., Robinson, S., Fischmeister, F. P. S., König, D., Oppenauer, C., Lueger-Schuster, B., et al. (2008). Altered reward processing in the nucleus accumbens and mesial prefrontal cortex of patients with posttraumatic stress disorder. *Neuropsychologia* 46, 2836–2844. doi:10.1016/j.neuropsychologia.2008.05.022.
- Sarton, E., Teppema, L. J., Olievier, C., and Nieuwenhuijs, D. (2001). The Involvement of the  $\mu$ -Opioid Receptor in Ketamine- Induced Respiratory Depression and Antinociception. 1495–1500.
- Sauer, H., and Oertel, W. H. (1994). Progressive degeneration of nigrostriatal dopamine neurons following intrastriatal terminal lesions with 6-hydroxydopamine: A combined retrograde tracing and immunocytochemical study in the rat. *Neuroscience* 59, 401–415. doi:10.1016/0306-4522(94)90605-X.
- Schmaal, L., Veltman, D. J., van Erp, T. G. M., Sämann, P. G., Frodl, T., Jahanshad, N., et al. (2016). Subcortical brain alterations in major depressive disorder: findings from the ENIGMA Major Depressive Disorder working group. *Mol. Psychiatry* 21, 806–12. doi:10.1038/mp.2015.69.
- Sgambato-Faure, V., and Cenci, M. A. (2012). Glutamatergic mechanisms in the dyskinesias induced by pharmacological dopamine replacement and deep brain stimulation for the treatment of Parkinson's disease. *Prog. Neurobiol.* 96, 69–86. doi:10.1016/j.pneurobio.2011.10.005.
- Sharma, A. V., Wolansky, T., and Dickson, C. T. (2010). A Comparison of Sleeplike Slow Oscillations in the Hippocampus Under Ketamine and Urethane Anesthesia. *J. Neurophysiol.* 104, 932–939. doi:10.1152/jn.01065.2009.
- Shaw, A. D., Saxena, N., Jackson, L. E., Hall, J. E., Singh, K. D., and Muthukumaraswamy, S. D. (2015). Ketamine amplifies induced gamma frequency oscillations in the human cerebral cortex. *Eur. Neuropsychopharmacol.* 25, 1136–1146. doi:10.1016/j.euroneuro.2015.04.012.
- Shen, H., Kannari, K., Yamato, H., Arai, A., and Mtsunaga, M. (2003). Effects of Benserazide

- on L-DOPA-Derived Extracellular Dopamine Levels and Aromatic L-Amino Acid Decarboxylase Activity in the Striatum of 6-Hydroxydopamine-Lesioned Rat. *Tohoku J. Exp. Med.* 199, 149–159.
- Sherman, S. J. (2016). Case Reports Showing a Long-Term Effect of Subanesthetic Ketamine Infusion in Reducing L -DOPA-Induced Dyskinesias. *Case Rep. Neurol.* 5023, 53–58. doi:10.1159/000444278.
- Sherman, S. J., Estevez, M., Magill, A. B., and Falk, T. (2016a). Case Reports Showing a Long-Term Effect of Subanesthetic Ketamine Infusion in Reducing L-DOPA-Induced Dyskinesias. *Case Rep. Neurol.* 8, 53–58. doi:10.1159/000444278.
- Sherman, S. J., Estevez, M., Magill, A. B., and Falk, T. (2016b). Case Reports Showing a Long-Term Effect of Subanesthetic Ketamine Infusion in Reducing L -DOPA-Induced Dyskinesias. *Case Rep. Neurol.* 5023, 53–58. doi:10.1159/000444278.
- Shikanai, H., Hiraide, S., Kamiyama, H., Kiya, T., Oda, K., Goto, Y., et al. (2014). Subanalgesic ketamine enhances morphine-induced antinociceptive activity without cortical dysfunction in rats. *J. Anesth.* 28, 390–398. doi:10.1007/s00540-013-1722-5.
- Shiroma, P. R., Johns, B., Kuskowski, M., Wels, J., Thuras, P., Albott, C. S., et al. (2014). Augmentation of response and remission to serial intravenous subanesthetic ketamine in treatment resistant depression. *J. Affect. Disord.* 155, 123–129. doi:10.1016/j.jad.2013.10.036.
- Sigtermans, M. J., van Hilten, J. J., Bauer, M. C. R., Arbous, M. S., Marinus, J., Sarton, E. Y., et al. (2009). Ketamine produces effective and long-term pain relief in patients with Complex Regional Pain Syndrome Type 1. *Pain* 145, 304–311. doi:10.1016/j.pain.2009.06.023.
- Singh, J. B., Fedgchin, M., Daly, E. J., De Boer, P., Cooper, K., Lim, P., et al. (2016). A double-blind, randomized, placebo-controlled, dose-frequency study of intravenous ketamine in patients with treatment-resistant depression. *Am. J. Psychiatry* 173, 816–826. doi:10.1176/appi.ajp.2016.16010037.
- Sleigh, J., Harvey, M., Voss, L., and Denny, B. (2014a). Ketamine - more mechanisms of action than just NMDA blockade. *Trends Anaesth. Crit. Care* 4, 76–81. doi:10.1016/j.tacc.2014.03.002.
- Sleigh, J., Harvey, M., Voss, L., and Denny, B. (2014b). Ketamine – More mechanisms of action than just NMDA blockade. *Trends Anaesth. Crit. Care* 4, 76–81. doi:10.1016/j.tacc.2014.03.002.
- Smith, L. A., Jackson, M. J., Al-Barghouthy, G., Rose, S., Kuoppamaki, M., Olanow, W., et al. (2005). Multiple small doses of levodopa plus entacapone produce continuous dopaminergic stimulation and reduce dyskinesia induction in MPTP-treated drug-na??ve primates. *Mov. Disord.* 20, 306–314. doi:10.1002/mds.20317.
- Sohal, V. S., Zhang, F., Yizhar, O., and Deisseroth, K. (2009). Parvalbumin neurons and gamma rhythms enhance cortical circuit performance. *Nature* 459, 698–702. doi:10.1038/nature07991.
- Steriade, M., Contreras, D., and Amzica, F. (1994). Synchronised sleep oscillations and their

- paroxysmal developments. *Trends Neurosci.* 17, 113–122.
- Stocchi, F., Vacca, L., Ruggieri, S., and Olanow, W. (2005). Intermittent vs continuous levodopa administration in patients with advanced parkinson disease. *Arch Neurol* 62, 905–910.
- Swann, N. C., de Hemptinne, C., Miocinovic, S., Qasim, S., Wang, S. S., Ziman, N., et al. (2016). Gamma Oscillations in the Hyperkinetic State Detected with Chronic Human Brain Recordings in Parkinson’s Disease. *J. Neurosci.* 36, 6445–58. doi:10.1523/JNEUROSCI.1128-16.2016.
- Taverna, S., Ilijic, E., and Surmeier, D. J. (2008). Recurrent Collateral Connections of Striatal Medium Spiny Neurons Are Disrupted in Models of Parkinson’s Disease. *J. Neurosci.* 28, 5504–5512. doi:10.1523/JNEUROSCI.5493-07.2008.
- Tepper, J. M., Koós, T., and Wilson, C. J. (2004). GABAergic microcircuits in the neostriatum. *Trends Neurosci.* 27, 662–669. doi:10.1016/j.tins.2004.08.007.
- Thanvi, B., Lo, N., and Robinson, T. (2007). Levodopa-induced dyskinesia in Parkinson’s disease: clinical features, pathogenesis, prevention and treatment. *Postgrad. Med. J.* 83, 384–8. doi:10.1136/pgmj.2006.054759.
- Tort, A. B. L., Kramer, M. a, Thorn, C., Gibson, D. J., Kubota, Y., Graybiel, A. M., et al. (2008). Dynamic cross-frequency couplings of local field potential oscillations in rat striatum and hippocampus during performance of a T-maze task. *Proc. Natl. Acad. Sci. U. S. A.* 105, 20517–20522. doi:10.1073/pnas.0810524105.
- Towers, S. K., and Hestrin, S. (2008). D1-Like Dopamine Receptor Activation Modulates GABAergic Inhibition But Not Electrical Coupling between Neocortical Fast-Spiking Interneurons. *J. Neurosci.* 28, 2633–2641. doi:10.1523/JNEUROSCI.5079-07.2008.
- Tseng, K. Y., Mallet, N., Toreson, K. L., Le Moine, C., Gonon, F., and O’Donnell, P. (2006). Excitatory response of prefrontal cortical fast-spiking interneurons to ventral tegmental area stimulation in vivo. *Synapse* 59, 412–417. doi:10.1002/syn.20255.
- Twelves, D., Perkins, K. S. M., Uk, M., and Counsell, C. (2003). Systematic Review of Incidence Studies of Parkinson ’ s Disease. *Mov. Disord.* 18, 19–31. doi:10.1002/mds.10305.
- Ungerstedt, U. (1968). 6-Hydroxy-Dopamine Induced Degeneration of Central Monoamine Neurons. *Eur. J. Pharmacol.* 5, 107–110. doi:10.1016/0014-2999(68)90164-7.
- van der Meer, M. A. A., and Redish, A. D. (2009). Low and High Gamma Oscillations in Rat Ventral Striatum have Distinct Relationships to Behavior, Reward, and Spiking Activity on a Learned Spatial Decision Task. *Front. Integr. Neurosci.* 3, 9. doi:10.3389/neuro.07.009.2009.
- van der Meer, M. a a, and Redish, a D. (2011). Theta phase precession in rat ventral striatum links place and reward information. *J. Neurosci.* 31, 2843–54. doi:10.1523/JNEUROSCI.4869-10.2011.
- van Wijk, B. C. M., Beudel, M., Jha, A., Oswal, A., Foltynie, T., Hariz, M. I., et al. (2016). Subthalamic nucleus phase-amplitude coupling correlates with motor impairment in

- Parkinson's disease. *Clin. Neurophysiol.* 127, 2010–9. doi:10.1016/j.clinph.2016.01.015.
- Vande Voort, J. L., Morgan, R. J., Kung, S., Rasmussen, K. G., Rico, J., Palmer, B. A., et al. (2016). Continuation phase intravenous ketamine in adults with treatment-resistant depression. *J. Affect. Disord.* 206, 300–304. doi:10.1016/j.jad.2016.09.008.
- Veilleux-Lemieux, D., Castel, A., Carrier, D., Beaudry, F., and Vachon, P. (2013). Pharmacokinetics of ketamine and xylazine in young and old Sprague-Dawley rats. *J. Am. Assoc. Lab. Anim. Sci.* 52, 567–70.
- Videbech, P., and Ravnkilde, B. (2004). Hippocampal volume and depression: A meta-analysis of MRI studies. *Am. J. Psychiatry* 161, 1957–1966. doi:10.1176/appi.ajp.161.11.1957.
- Vila, M., Levy, R., Herrero, M. T., Ruberg, M., Faucheux, B., Obeso, J. a, et al. (1997). Consequences of nigrostriatal denervation on the functioning of the basal ganglia in human and nonhuman primates: an in situ hybridization study of cytochrome oxidase subunit I mRNA. *J. Neurosci.* 17, 765–773. doi:10.1523/JNEUROSCI.17-02-00765.1997.
- Weinberger, M., Mahant, N., Hutchison, W. D., Lozano, A. M., Moro, E., Hodaie, M., et al. (2006). Beta Oscillatory Activity in the Subthalamic Nucleus and Its Relation to Dopaminergic Response in Parkinson's Disease. *J. Neurophysiol.* 96, 3248–3256. doi:10.1152/jn.00697.2006.
- Welle, C. G., and Contreras, D. (2017). New Light on Gamma Oscillations. *Neuron* 93, 247–249. doi:10.1016/j.neuron.2017.01.003.
- Whittington, M. a, Cunningham, M. O., LeBeau, F. E. N., Racca, C., and Traub, R. D. (2011). Multiple origins of the cortical  $\gamma$  rhythm. *Dev. Neurobiol.* 71, 92–106. doi:10.1002/dneu.20814.
- Whittington, M. a, Traub, R. D., and Jefferys, J. G. (1995). Synchronized oscillations in interneuron networks driven by metabotropic glutamate receptor activation. *Nature* 373, 612–615. doi:10.1038/373612a0.
- Winkler, C., Kirik, D., Björklund, A., and Cenci, M. A. (2002). L-DOPA-induced dyskinesia in the intrastriatal 6-hydroxydopamine model of Parkinson's disease: Relation to motor and cellular parameters of nigrostriatal function. *Neurobiol. Dis.* 10, 165–186. doi:10.1006/nbdi.2002.0499.
- Womelsdorf, T., Schoffelen, J.-M., Oostenveld, R., Singer, W., Desimone, R., Engel, A. K., et al. (2007). Modulation of neuronal interactions through neuronal synchronization. *Science* 316, 1609–12. doi:10.1126/science.1139597.
- Wood, J. D., and Hertz, L. (1980). Ketamine-induced changes in the gaba system of mouse brain. *Neuropharmacology* 19, 805–808. doi:10.1016/0028-3908(80)90075-1.
- Yang, C., Hu, Y.-M., Zhou, Z.-Q., Zhang, G.-F., and Yang, J.-J. (2013). Acute administration of ketamine in rats increases hippocampal BDNF and mTOR levels during forced swimming test. *Ups. J. Med. Sci.* 118, 3–8. doi:10.3109/03009734.2012.724118.
- Ye, T., Bartlett, M. J., Schmit, M. B., Sherman, S. J., Falk, T., and Cowen, S. L. (2018). Ten-Hour Exposure to Low-Dose Ketamine Enhances Corticostriatal Cross-Frequency Coupling

and Hippocampal Broad-Band Gamma Oscillations. *Front. Neural Circuits* 12, 61. doi:10.3389/FNCIR.2018.00061.

Yelnik, J., François, C., Percheron, G., and Tandé, D. (1991). *Morphological Taxonomy of the Neurons of the Primate Striatum*. doi:10.1002/cne.903130207.

Zanos, P., Moaddel, R., Morris, P. J., Georgiou, P., Fischell, J., Elmer, G. I., et al. (2016a). NMDAR inhibition-independent antidepressant actions of ketamine metabolites. *Nature* 533, 481–486. doi:10.1038/nature17998.

Zanos, P., Moaddel, R., Morris, P. J., Georgiou, P., Fischell, J., Elmer, G. I., et al. (2016b). NMDAR inhibition-independent antidepressant actions of ketamine metabolites. *Nature* 533, 481–486. doi:10.1038/nature17998.

Zarate, C. A., Brutsche, N., Laje, G., Luckenbaugh, D. A., Venkata, S. L. V., Ramamoorthy, A., et al. (2012). Relationship of ketamine's plasma metabolites with response, diagnosis, and side effects in major depression. *Biol. Psychiatry* 72, 331–8. doi:10.1016/j.biopsych.2012.03.004.

Zhao, X., Venkata, S. L. V., Moaddel, R., Luckenbaugh, D. A., Brutsche, N. E., Ibrahim, L., et al. (2012). Simultaneous population pharmacokinetic modelling of ketamine and three major metabolites in patients with treatment-resistant bipolar depression. *Br. J. Clin. Pharmacol.* 74, 304–14. doi:10.1111/j.1365-2125.2012.04198.x.